

**UNIVERSITY OF CALIFORNIA**

**Santa Barbara**

**Ocean Color Remote Sensing of Chlorophyll and Primary Production  
West of the Antarctic Peninsula**

**A dissertation submitted in partial satisfaction  
of the requirements for the degree of**

**Doctor of Philosophy**

**in**

**Geography**

**by**

**Heidi Melita Dierssen**

**Committee in charge:**

**Dr. Raymond C. Smith, Chairperson**

**Dr. David Siegel**

**Dr. Catherine Gautier**

**Dr. Maria Vernet**

**UMI Number: 3003559**

**UMI<sup>®</sup>**

---

**UMI Microform 3003559**

**Copyright 2001 by Bell & Howell Information and Learning Company.**


**All rights reserved. This microform edition is protected against  
unauthorized copying under Title 17, United States Code.**

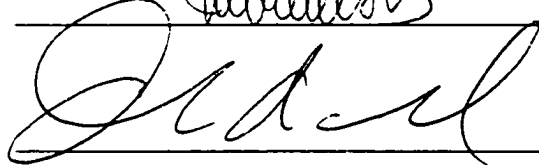
---

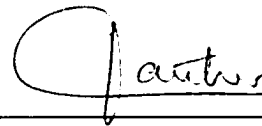
**Bell & Howell Information and Learning Company  
300 North Zeeb Road  
P.O. Box 1346  
Ann Arbor, MI 48106-1346**

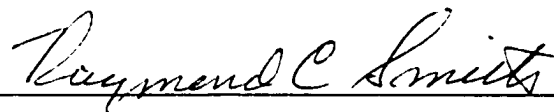
The dissertation of  
Heidi Dierssen

is approved:

  
\_\_\_\_\_

  
\_\_\_\_\_

  
\_\_\_\_\_

  
\_\_\_\_\_

Committee Chairperson

August 2000

## Acknowledgements

I would foremost like to acknowledge the support of my advisor, mentor, and friend Ray Smith. I am grateful that he has shared some of his knowledge and wisdom with me. I would also like to thank my committee, Maria Vernet, Dave Siegel, and Catherine Gautier, for their generous help throughout the PhD process. Acknowledgements also go out to the other members of my group, Sharon Stammerjohn, Charleen Johnson, and Karen Baker for providing technical support and the rest of the folks associated with the Palmer LTER for helping out with the field work.

I wish to thank the funding agencies who supported my graduate studies and this research: NASA, NSF, and CalSpace. Also, I would like to acknowledge the wonderful staff at ICES and the Geography Department who provided administrative support for my studies. I also appreciate the many interesting courses that I took from faculty at UCSB and, of course, all of the fascinating presentations in Colloquia and Geography 264.

I can't help but be thankful for the support and unconditional love from my parents and family. I can't wait to see you at graduation. And, I have to acknowledge all of my wonderful friends who made me laugh throughout this whole process and gave me the opportunity to consume lots of beer. Special thanks to our fearless leader Diana and my fellow yoginis – may you forever chivasena peacefully. I have to especially thank Molly for trekking down to Chile for our wild ride together, for allowing me to drag her to Nova Scotia and Hawaii for Ocean Optics, and generally for her wonderful spirit, energy, and sense of adventure. Special thanks to the crew on the January 1999 cruise, Robin, Andrew, Chris, Terry, Tracy, Wendy, Rich, for keeping my spirits motivated on those many cloud-filled Antarctic days. Of course, I must acknowledge my ICES cohorts: Grace, Eric, Dede, Albright, Painter, and all of the associated Felkner humour. Go Vikings! My dissertation would have been flat (half-flat that is) without the ever amusing antics of Scott Marcus, the Middle Eastern Ensemble, and Um Kulthum (without a doubt, the most influential middle eastern musician of all time). The violin section (Diana, Jeff, Dwight) rules.

Now on to the mushy stuff. This dissertation is dedicated to the love of my life, Brad, and our daughter Melita. Brad has always given me encouragement, love, and support. He is the music that fills my heart and I couldn't imagine my life without him. And, Melita, is the little bundle of joy who came along to make everything richer and more satisfying. Even at 3 months, she is such a happy and wonderful person.



## *Vita*

### **Heidi M. Dierssen**

Institute for Computational Earth System Science  
University of California Santa Barbara  
Santa Barbara, CA 93106

#### **Education**

- 2000 Ph.D., Physical Geography  
Institute for Computational Earth System Science  
University of California Santa Barbara.  
*Title: Remote Sensing of Biomass and Primary Productivity in Antarctic Coastal Waters.*  
*Advisor: Raymond Smith*
- 1989 M.S., Biological Sciences, Stanford University, California.
- 1989 B.S., Biological Sciences, Stanford University, California, with honors.

#### **Awards**

- 1997-2000 NASA Earth System Science Fellowship, Proposal Title: Bio-optical Analysis of Primary Productivity and Glacial Land Cover Change in Antarctic Coastal Waters. NGT5-30063.
- 1997-1998 Merit Fellowship Geography Department. 1998. University of California Santa Barbara.
- 1997-1998 Nominated for GSA Excellence in Teaching Award.
- 1997 Complex Systems Summer School. Sponsored by Santa Fe Institute, New Mexico. Received scholarship through NSF to attend summer school.
- 1995 California Space Grant Fellowship. Proposal Title: Bio-optical Modeling of the Southern Ocean. NGT-40005.
- 1989 Stanford University, Undergraduate Research Fellowship.

#### **Research**

- 6/99-present Visiting Research Scientist. Rosenstiel School of Marine and Atmospheric Research. University of Miami.
- 1/99-2/99 Field Researcher. Antarctic field work aboard *R/V L.M. Gould*.

- 9/93-6/98      Research Assistant. Institute for Computational Earth System Science  
Funded by the Long-term Ecological Research Project, Palmer Station,  
Antarctica to study bio-optics and primary productivity of Antarctic Coastal  
Waters.
- 11/94-2/95      Field Researcher. Palmer Station, Antarctica and R/V *Polar Duke*.
- 11/90-8/93      Associate Scientist - Environ Corporation, Emeryville California.  
Estimated air toxics emissions and dispersion and conducted human health and  
environmental risk assessment.
- 9/88-6/89      Undergraduate Research Assistant. Jasper Ridge Biological Preserve,  
Stanford University, California. Researched differential allocation of resources  
in male and female individuals of a dioecious shrub.
- 6/88-9/88      Undergraduate Research Assistant. Hopkins Marine Station, Monterey,  
California. Analyzed the classification system of calcareous marine sponges.
- 6/87-9/87      Undergraduate Research Assistant. Dept. of Genetics and Cell Biology,  
University of Minnesota. Assisted in experiments designed to elucidate  
general cell behavior from the genetic manipulation of corn.

**Teaching**      (*Evaluations: 1=excellent, 2=very good, 3=good, 4=fair, 5=poor*)

***Instructor:***

- 8/98-12/98      Physical Geography Laboratory. Ventura Community College
- 8/97-12/97      Physical Geography Laboratory. Ventura Community College
- 6/97-8/97      Physical Geography. Univ. California Santa Barbara  
Student evaluations of overall teaching quality: 1.7

***Teaching Assistant:***

- 9/98-12/98      Physical Geography- Univ. California Santa Barbara
- 1/98-3/98      Remote Sensing of the Oceans - Univ. California Santa Barbara  
Student overall evaluation of TA: 1.2
- 9/97-12/97      Introduction to Oceanography - Univ. California Santa Barbara  
Student overall evaluation of TA: 1.5
- 9/95-12/95      Introduction to Oceanography - Univ. California Santa Barbara  
Student overall evaluation of TA: 1.7

**Publications**

Dierssen, H.M., Vernet, M., Smith, R.C. 2000. Optimizing models for remotely estimating  
primary production in Antarctic coastal waters. *Antarctic Science*. 12(1). 20-32.

- Dierssen, H.M., Smith, R.C. In press. Bio-optical properties and remote sensing ocean color algorithms for Antarctic coastal waters. *Journal of Geophysical Research*.
- Dierssen, H.M. and Smith, R.C. 1997. Estimation of irradiance just below the air-water interface. SPIE Volume 2963. Ocean Optics XIII, p. 204-209.
- Smith, R. C., Dierssen, H. M., and Vernet, M., 1996, Phytoplankton biomass and productivity in the Western Antarctic Peninsula Region. Ross, R. M., Hofmann, E. E., and Quetin, L. B., ed., *Foundations for Ecosystem Research West of the Antarctic Peninsula*: AGU Antarctic Research Series.
- Dierssen, H.M., Smith, R.C., Vernet, M. In prep. Validating remotely sensed chlorophyll from the SeaWiFS ocean color sensor for waters west of the Antarctic Peninsula.
- Dierssen, H.M., Smith, R.C. In prep. The bio-optics of glacial meltwater and effects on primary production in Antarctic coastal waters.
- Dierssen, H.M., Smith R.C. In prep. The role of backscattering in the optical characterization of the Southern Ocean.
- Dierssen, H.M., Smith, R.C. In prep. Spatial scaling of phytoplankton and physical parameters in nearshore Antarctic coastal waters.

#### **Presentations**

- Bio-optical properties of Antarctic coastal waters. Dierssen, H.M., Smith, R.C. Baker, Karen S. Poster presented at Ocean Optics XIV. Office of Naval Research and National Aeronautic Space Administration. Kailua-Kona, Hawaii, November 10-13, 1998.
- Modeling primary productivity of the western Antarctic Peninsula region and the Southern Ocean. Dierssen, H.M., Vernet, M., Smith, R.C. Poster presented at AGU/ASLO 1998 Ocean Sciences Meeting, San Diego, February 9-13, 1998. Awarded Gold Star for Student Presentation.
- Temporal and spatial variability of primary productivity in the Western Antarctic Peninsula during 1994/95 and 1995/96 growth seasons. Vernet, M., Baker, K., Dierssen, H.M. and Smith, R.C. Aquatic Sciences Meeting. Santa Fe, New Mexico. February 10-14, 1997.
- Estimation of irradiance just below the air-water interface. Dierssen, H.M., Smith, R.C., Ocean Optics XIII. October 22-25. 1996.
- Modeling of Light-Saturated Photosynthesis in Antarctic Coastal Waters Dierssen, H.M., Smith, R.C., Vernet, M. Poster presented at AGU/ASLO 1996 Ocean Sciences Meeting, San Diego, February 12-16. 1996. Eos, Transactions, American Geophysical Union. Vol 76, No. 3. January 16. 1996. OS41C-06.

Seasonal and Interannual Variability of Phytoplankton Biomass and Primary Production West of the Antarctic Peninsula. R.C. Smith, K.S. Baker, M.L. Byers, H. Dierssen, S.E. Stammerjohn & M. Vernet. Presented at AGU/ASLO 1996 Ocean Sciences Meeting, February 12-16. 1996.

**Invited Lectures**

University of Southern Mississippi, Department of Marine Sciences. April 28, 1999. Bio-optical properties of Antarctic coastal waters.

## Abstract

This dissertation addresses two fundamental questions. First, how do biomass and primary production in Antarctic coastal waters compare to temperate waters? Second, how can we use satellite ocean color observations to accurately estimate biomass and primary production in these Antarctic waters? Satellite technology is critical for understanding the large scale patterns of biomass and primary production in the remote waters of the Southern Ocean. However, considerable uncertainty exists in satellite-derived estimates of biomass and production for this region. As discovered in this dissertation, unique regional algorithms are required for estimating both biomass and primary production in Antarctic waters. Data collected in conjunction with the Palmer Long Term Ecological Research project along the western Antarctic Peninsula are used to address these questions.

From analysis of bio-optical parameters measured at over 1000 stations, the relationship between remotely sensed reflectance and biomass (evaluated as chlorophyll concentrations) is found to be significantly different from other oceanic regions. Remote sensing reflectance is higher in the blue and lower in the green region of the visible spectrum. This is hypothesized to be due to a combination of low backscattering and low absorption per unit chlorophyll. A new empirical algorithm is developed to predict chlorophyll from remotely sensed radiance. If chlorophyll concentrations are accurately retrieved from a satellite, then over 60% of the variability in primary production can be explained. Taking into account the relatively uniform chlorophyll-normalized production profile and low maximum chlorophyll-normalized production ( $P_{opt}^B$ ) characteristic of these cold well-mixed Antarctic waters, an optimized depth-

integrated primary production is presented that explains over 70% of the PAL/LTER data and historic data collected from the region.

Finally, the chlorophyll and primary production models are applied to monthly satellite data obtained from the Sea-viewing Wide Field of View Sensor (SeaWiFS). We find that, as predicted, SeaWiFS generally underestimates chlorophyll concentrations and follows our algorithm. Using the satellite-derived chlorophyll, we are able to model PP both monthly and annually for waters near Palmer Station and for the entire Southern Ocean. Interannual variability is highest in coastal waters near Palmer Station (7-fold variability) and in regional ice shelves containing large polynyas.

## Table of Contents

<b>Chapter 1: Introduction.....</b>	<b>1</b>
<b>Chapter 2: Bio-optical properties and remote sensing ocean color algorithms for Antarctic coastal waters.....</b>	<b>15</b>
<b>Chapter 3: Optimizing models for remotely estimating primary production in Antarctic coastal waters.....</b>	<b>60</b>
<b>Chapter 4: Validating remotely sensed chlorophyll from the SeaWiFS ocean color sensor for waters west of the Antarctic Peninsula.....</b>	<b>104</b>
<b>Chapter 5: Modeling primary production from SeaWiFS-derived chlorophyll for waters west of the Antarctic Peninsula and the Southern Ocean.....</b>	<b>126</b>
<b>Chapter 6: Epilogue.....</b>	<b>158</b>

## Chapter 1

### Introduction

"The waters and the ice of the South Polar Ocean were alike found to abound with microscopic vegetables belonging to the order Diatomaceæ. Though much too small to be discernible by the naked eye, they occurred in such countless myriads as to stain the berg and the pack ice wherever they were washed by the swell of the sea; and, when enclosed in the congealing surface of the water, they imparted to the brash and pancake ice a pale ochreous colour... The universal existence of such an invisible vegetation as that of the Antarctic Ocean, is a truly wonderful fact, and the more from its not being accompanied by plants of a high order. During the years we spent there, I had been accustomed to regard the phenomena of life as differing totally from what obtains throughout all other latitudes, for everything living appeared to be of animal origin. The ocean swarmed with Mollusca, and particularly entomostracous Crustacea, small whales, and porpoises; the sea abounded with penguins and seals, and the air with birds; the animal kingdom was ever present, the larger creatures preying on the smaller and these again on smaller still; all seemed carnivorous. The herbivorous were not recognised, because feeding on a microscopic herbage, of whose true nature I had formed an erroneous impression. It is, therefore with no little satisfaction that I now class the Diatomaceæ with plants, probably maintaining in the south Polar Ocean that balance between the vegetable and the animal kingdom which prevails over the surface of our globe. Nor is the sustenance and nutrition of the animal kingdom the only function these minute productions may perform: they may also be the purifiers of the vitiated atmosphere, and thus execute in the Antarctic latitudes the office of our trees and grass turf in the temperate regions, and the broad leaves of the palm, &c., in the tropics."

--Dr. J.D. Hooker in the "Botany of the Antarctic Voyage," and in a paper which he read before the British Association in 1847



### *Background on Southern Ocean Productivity*

From as far back as the first voyage of Captain James Cook (1772-1775) and the *Erebus* and *Terror* Expeditions under James Clark Ross (1839-1843), a legacy has been put forth concerning the extreme richness of marine life in the Antarctic waters. Not only were the waters filled with plentiful whale and seal populations, the famed botanist J.D. Hooker aboard the *Erebus* and *Terror* Expeditions first reported abundant concentrations of Antarctic diatoms throughout the Antarctic seas. During most of the past century, this initial paradigm of abundantly productive waters has been perpetuated throughout the scientific investigations of the Southern Ocean [El-Sayed, 1970]. However, from the 1960's onward, the paradigm has gradually shifted from a ubiquitously rich Southern Ocean towards one that is extremely variable over space and time. Primary production is strongly influenced by the seasons because of the annual advance and retreat of sea ice and the dramatic shift in daylength over the course of the year. Geographically, striking differences in productivity occur both in the zonal and to a lesser degree in the meridional direction.

The waters of the Southern Ocean have historically been treated as mere extensions of the three major oceans: Atlantic, Pacific and Indian. However, the Southern Ocean contains distinct circulation properties and latitudinal zones that help to define it as its own entity. With reference to the biogeochemistry, the Southern Ocean has been divided into five zones that are continuous around the continent but vary with latitude: the Permanent Ice Zone (PIZ), the Coastal and Continental Shelf Zone (CCSZ), the Seasonal Ice Zone (SIZ), the Permanently Open Ocean Zone (POOZ), and the Polar Front Zone (PFZ) [Treguer and Jacques, 1992]. The area of the PIZ, CCSZ and POOZ remains fairly constant over the seasons, however, the SIZ annually sweeps in and out of the coastal and pelagic zones and the PFZ varies in width and extent over the seasons (Fig. 1).

These zones can be characterized by their physical parameters, nutrient regimes, primary production, and relationship to the upper trophic levels.

This dissertation has been conducted in conjunction with the Palmer Long Term Ecological Research (PAL/LTER) project involving interdisciplinary studies of the ecological systems along the western Antarctic Peninsula. The PAL/LTER study area primarily focuses on the nearshore CCSZ and SIZ, but is also influenced by the more distant POOZ and PFZ. Because of the constriction between the tip of South America and the Antarctic Peninsula, the CCSZ, SIZ, POOZ, and PIZ are all constrained within the Drake Passage, within relatively close proximity to each other and the Antarctic Peninsula. The historic patterns and mechanisms that control biomass and primary production in these Antarctic Peninsula waters are reviewed in a book chapter [Smith *et al.*, 1996]. A brief summary of some of the general mechanisms important in each of the biogeochemical zones is presented below.

The CCSZ is generally considered to be the most highly productive region of the Southern Ocean per unit area. This is the region that J.D. Hooker and other early explorers likely refer to when they discuss the abundance of Antarctic production. While nutrient levels are generally high throughout these waters, massive blooms ( $>30 \text{ mg Chl m}^{-3}$ ) do occur that can cause short-term macronutrient depletion [Smith *et al.*, 1996]. These waters are generally not thought to be limited in the micronutrient iron because of resuspension of iron-rich sediments and terrigenous input from glaciers and runoff. The waters are considered to be generally well mixed with a slight maximum of chlorophyll occurring near the surface [Smith *et al.*, 1996]. In CCSZ waters both near Palmer Station and in the Ross Sea, several large blooms ( $>5 \text{ mg Chl m}^{-3}$ ) occur during the growing season (November-March) [Arrigo and McClain, 1994:

*Dierssen et al.*, 2000]. These blooms last approximately one week and contribute significantly to annual production.

The SIZ, often referred to as the Marginal Ice Zone (MIZ), is the region that is influenced by low salinity meltwater from the receding pack ice and can extend 50-250 km from the ice edge. Studies have shown that the low-density meltwater creates a lens of stable water on the ocean surface that reduces mixing and that allows for the formation of large blooms ( $> 5 \text{ mg Chl m}^{-3}$ ) [*Smith and Nelson*, 1986]. Some contend that the melting sea ice can also “seed” the ocean surface with phytoplankton populations and other nutrients that could be limiting. However, the existence of a stable layer and a resulting bloom is dependent on the strength and frequency of wind mixing event within the SIZ [*Lancelot et al.*, 1993]. In addition, the ice area is a favorable environment for grazers (e.g., euphausiids) which can further control the stock of phytoplankton in this region. When analyzing the ocean color SeaWiFS data discussed in the final chapter of this dissertation, the ice edge area is found to be associated with high biomass only sporadically. Overall, the SIZ region is not as productive as the CCSZ, but has a productivity at least a factor of two higher than the POOZ [*Treguer and Jacques*, 1992].

The POOZ zone is typically defined as a High Nutrient Low Chlorophyll (HNLC) ecosystem and is considered to be an almost “oligotrophic” area [*Treguer and Jacques*, 1992] with chlorophyll concentrations less than  $0.25 \text{ mg m}^{-3}$ . Both light limitation due to high wind mixing and silicate limitation are both given as potential reasons for the low biomass concentrations. In addition, certain sectors of the POOZ could also be limited by low iron or silicate concentrations [*Jeandel et al.*, 1998]. As evident in satellite images from Chapter 5, the area of the oligotrophic POOZ is much smaller than originally defined and is primarily limited to regions within the Drake Passage and South Indian Ocean.

Less than 1% of the Southern Ocean is made up of these low biomass POOZ waters ( $< 1 \times 10^{-6} \text{ km}^2$ ). Salps tend to exploit the oligotrophic waters of the POOZ and appear more efficient at exporting microbial carbon to deep water. Because of the production of highly resistant and fast-sinking faecal pellets, salps may uncouple the opal accumulation in the sediments from primary production [*LeFevre and Treguer, 1998*].

Chlorophyll concentrations again increase when approaching the PFZ northward of the POOZ. The PFZ, filled with mesoscale eddies, is quite productive and an area with very high flux of particulate matter to the sediments. The biogeochemistry of these iron-rich waters is highly influenced by the presence of massive diatom blooms that are exported into the deep ocean [*Bathmann, 1998*]. The most important factor in development of these blooms is thought to be physical stability of the surface waters. In the Indian sector, the flux of organic carbon deposited at the sediment-water interface represents 10-20% of estimated primary production [*Rabouille and al., 1998*]. The lack of degradation of particles in the water column may be attributed to low temperatures and slow bacterial reactions, lack of nutrients fueling bacterial activity, or elevated settling velocities due to aggregate formation. Significant  $\text{CO}_2$  draw-down is associated with these massive diatoms blooms. Grazing of phytoplankton by larger zooplankton is found to be minimal in the PFZ region [*Bathmann, 1998*].

The meridional influences in the Southern Ocean primarily correspond to the proximity of land and ice masses in each sector. The five geographical sectors of the Southern Ocean include [*Zwally et al., 1983*]: the South Indian Ocean (20-90°E), Southwestern Pacific (90-160°E), Ross Sea (160°E-130°W), Bellingshausen-Amundsen (60-130°W), Weddell Sea (130°W-20°E) (Fig. 1). While variation is generally higher zonally, the sectors do display unique features from

one another. Lower production is generally associated with the Indian and Pacific sectors. These regions have minimal terrigenous influences and may be limited by nutrients such as iron and silica. The highest production can occur in polynyas that open up within permanent ice shelves. Depending on the year, the Ross Sea and the Larsen Ice Shelf within the Weddell sector can exhibit large and very productive polynyas. The Bellingshausen-Amundsen sector is influenced by the close proximity of South America and the Antarctic Peninsula. The confluence of the biogeochemical zones in this region can effect distributions of phytoplankton, krill, and nearly all trophic levels.

Much of what is known about the zonal and meridional variations in Southern Ocean phytoplankton biomass comes from remote sensing techniques. Prior to the advent of this technology, the sampling from shipboard operations suggested that the waters were much more homogenous. However, satellite remote sensing has revealed enormous variability of Southern Ocean waters over both space and time. Estimating the amount of carbon dioxide that is absorbed by phytoplankton (i.e., primary production) is a necessary component in understanding the role of the oceans in the global carbon cycle. Covering 70% of the earth's surface, the oceans account for anywhere from 30-50% of the global productivity. However, considerable uncertainty exists in satellite-derived estimates of production, especially in areas like the Southern Ocean where use of regional algorithms may be necessary. The results of this dissertation (Chapter 2) indicate that the Antarctic Peninsula waters are unique with respect to the relationship between chlorophyll and primary production.

### *Background to Ocean Color Remote Sensing*

The basic premise of ocean color remote sensing is that chlorophyll contained within phytoplankton produces systematic variation in the color of the

ocean. As demonstrated in the early work of *Clarke et al.* (1970), the water-leaving radiance backscattered from the ocean surface reflects the concentrations of chlorophyll in near-surface waters and can be observed from aircraft and satellites [*Clarke et al.*, 1970]. However, the remotely sensed radiance is a complex mixture of photons that have been scattered from the atmosphere, sea surface, and ocean. Depending on the wavelength, anywhere from 80-100% of the radiance received by a satellite originates in atmospheric scattering, both from air molecules (Rayleigh) or from aerosol scattering. When the effects of the atmosphere and sea surface are decoupled from the flux received at the satellite, we obtain an estimate of the water-leaving radiance that has been scattered from within the surface layer of the ocean. Improvements to the atmospheric correction schemes are the subject of ongoing research not addressed in this dissertation.

The water-leaving radiance can be adequately simulated by measurements of the radiance reflectance or ratio of upwelling radiance to downwelling irradiance. Theoretically, the radiance reflectance can be related to the inherent optical properties of the water-column, specifically the wavelength-specific absorption coefficient,  $a(\lambda)$ , and the backscattering coefficient,  $b_b(\lambda)$ . By making reasonable assumptions about how  $a(\lambda)$  and  $b_b(\lambda)$  vary with the different components in the water (i.e., phytoplankton, colored dissolved organic matter, suspended solids), then the actual concentrations of phytoplankton can be theoretically estimated. Specifically, total absorption at a particular wavelength is commonly broken into absorption due to water, phytoplankton, and colored dissolved organic matter. Backscattering primarily occurs from water molecules and very small submicron detrital particles. However, the current general processing routines used to derive chlorophyll concentrations from satellite data make use of simple empirical approaches involving relationships between radi-

ance reflectance in particular wavebands and the corresponding concentrations of measured chlorophyll. As described in Chapter 1 of this dissertation, the properties of  $a(\lambda)$  and  $b_b(\lambda)$  must be evaluated to understand why areas like the Southern Ocean have unique empirical relationships from other regions.

The most common empirical ocean color algorithms make use of the fact that phytoplankton pigments (e.g., chlorophyll) absorb light at the blue end of the spectrum. As chlorophyll concentrations increase, the blue radiation is increasingly absorbed causing a decrease in radiance reflectance at this end of the spectrum (400-515 nm). Similarly, a corresponding increase in the green radiance reflectance (515-600 nm) is also commonly found with increasing chlorophyll. As phytoplankton increase, the concentrations of small backscattering particles also tend to increase causing increased reflectance in the green region (the blue and red light being highly absorbed). Using the ratio of blue to green reflectance, a simple log-linear relationship can be used to estimate chlorophyll concentrations. Such approaches only work for waters that are considered to be Case 1, where ocean color is primarily associated with phytoplankton and dissolved organic matter. In highly turbid Case 2 waters, where sediments and terrigenous materials influence the optical properties of the waters, alternative approaches must be used. While most of the Antarctic Peninsula waters are Case 1, the simple algorithms must be adjusted to account for the unique bio-properties of these waters (see Chapter 1).

### *Dissertation Objectives and Organization*

The overall goal of my dissertation is to evaluate and improve the algorithms by which ocean color observations can be used to estimate biomass and primary productivity in Antarctic Peninsula waters. From the bio-optical properties measured *in situ* at over 1000 stations, Chapter 2 develops a robust ocean

color algorithm to estimate chlorophyll for this region. Chapter 3 evaluates measured chlorophyll and primary production profiles and presents an optimized depth-integrated primary production that can be simply applied to estimate primary production from satellite-derived chlorophyll concentrations. Chapter 4 validates the chlorophyll-retrieval model developed in Chapter 1 using radiance and chlorophyll that has been remotely estimated from the Sea-viewing Wide Field of View Sensor (SeaWiFS). Chapter 5 couples the chlorophyll and primary production models with SeaWiFS data to estimate monthly and annual primary production for the Antarctic Peninsula region and the Southern Ocean. One of the overreaching conclusions of this dissertation is that this region of the Southern Ocean is different from temperate waters with respect to both the bio-optical properties and primary production of the water column and must be analyzed using regional algorithms. A summary of the dissertation chapters is presented below.

Chapter 2 presents an analysis of the bio-optical properties and remote sensing ocean color algorithms for Antarctic Peninsula waters. Ratios of remote sensing reflectance measured at over 1000 oceanographic stations are used to evaluate methods for retrieving remotely sensed chlorophyll concentrations. The data collected over the course of seven years (1991-1998) is found to be different from data collected from other regions of the world's oceans. Remote sensing reflectance is found to be significantly higher in the blue and lower in the green region of the spectrum for high chlorophyll concentrations. Therefore, the general processing algorithms used for both the now defunct Coastal Zone Color Scanner, CZCS, and the currently operating Sea-viewing Wide Field of view Sensor (SeaWiFS) underestimate chlorophyll concentrations by roughly a factor of two. We hypothesize that both low chlorophyll-specific absorption and low backscattering contribute to this difference. These Antarctic waters are unique



in that phytoplankton blooms generally consist of large diatoms that can cause low chlorophyll-specific absorption of light. In addition, the Antarctic waters have low backscattering which is hypothesized to result from low concentrations of the small particles that cause backscattering in the water column.

In Chapter 3, models for remotely estimating primary production are evaluated and optimized for the PAL/LTER region. Using measurements of primary production for two different seasons, we determine that over 60% of the variability in primary production can be explained by surface chlorophyll concentrations alone. Unique from other regions, the vertical profile of normalized primary production is found to be more uniform with depth. Also, the maximum chlorophyll-normalized primary production,  $P_{opt}^B$ , is found to be low for these data compared to other regions. Irradiance plays a very limited role in estimating primary production and only improves model performed by about 5%. Very little relationship is evident between surface irradiance and the photo-adaptive variables. The optimized primary production model developed in this chapter explains over 70% of the variability in the PAL/LTER dataset and in an independent historic dataset collected in the region.

Chapter 4 utilizes the models developed in Chapters 1 and 2 to estimate primary production from satellite-derived chlorophyll concentrations for both the Palmer Station area and the Southern Ocean. First, the SeaWiFS-derived radiance concentrations are compared to *in situ* radiance levels. Then, chlorophyll concentrations are compared to concurrent measurements of chlorophyll both for nearshore CCSZ waters and offshore waters of the POOZ and PFZ. We find that, as predicted, SeaWiFS generally underestimates chlorophyll concentrations. By applying the polynomial correction algorithm developed in Chapter 2 to the SeaWiFS chlorophyll, the adjusted chlorophyll concentrations closely

match the in situ chlorophyll ( $r^2=70\%$ ) both at Palmer Station and across the Drake Passage.

Chapter 5 estimates primary production for the Antarctic Peninsula and Southern Ocean using the algorithms from Chapters 2 and 3. While the interannual variability in primary production is extremely high near Palmer Station (varying by a factor of seven), the variability in the last two summers near station has been relatively low. The primary production estimated for the whole Southern Ocean,  $2.7 \times 10^{15} \text{ g C yr}^{-1}$ , is in the range of past estimates made from CZCS satellite data. Most of the production occurs within the larger area of the collective POOZ and PFZ, even though production rates are higher within the CCSZ and SIZ. We hypothesize that interannual variability in primary production is likely to be greatest in the nearshore CCSZ and SIZ, which are subject to the annual advance and retreat of sea ice and the presence of highly productive polynyas.

The Southern Ocean is characterized by extremely cold water, high winds, seasonal variability in solar irradiance, and the annual advance and retreat of sea ice. In response to the extreme environment, it is not surprising that the phytoplankton are different from other regions of the world's oceans. This dissertation shows that the waters of the Antarctic Peninsula have unique bio-optical properties when compared to temperate waters. The phytoplankton are generally more shade-adapted and appear to be operating near their maximal chlorophyll-normalized productivity for much of the water column. Due to the low levels of small submicron detritus in the water, we hypothesize that back-scattering is lower than for other regions. Therefore, the general algorithms for estimating chlorophyll and primary production from satellite data are inaccurate when applied to these unique waters. By using the modified algorithms presented in this dissertation, remotely sensed estimates of both chlorophyll and

primary production are shown to more accurately reflect the *in situ* concentrations.

## References

- Arrigo, K.R., and C.R. McClain, Spring phytoplankton production in the western Ross Sea, *Science*, 266, 261-262, 1994.
- Bathmann, U.V., Ecology and biogeochemistry in the Atlantic sector of the Southern Ocean during austral spring: the first JGOFS expedition aboard RV 'Polarstern'. *Journal of Marine Systems*, 17, 77-85, 1998.
- Clarke, G.K., G.C. Ewing, and C.J. Lorenzen, Spectra of backscattered light from the sea obtained from aircraft as a measure of chlorophyll concentration. *Science*, 167, 1119-1121, 1970.
- Dierssen, H.M., R.C. Smith, and M. Vernet, Optimizing models for remotely estimating primary production in Antarctic coastal waters. *Antarctic Science*, 12 (1), 20-32, 2000.
- El-Sayed, S.Z., On the productivity of the Southern Ocean, in *Antarctic Ecology*, edited by M.W. Holdgate, pp. 119-135, The Scientific Committee on Antarctic Research by Academic Press, London, 1970.
- Jeandel, C., D. Ruiz-Pino, E. Gjata, and e. al., KERFIX, a time series station in the Southern Ocean: a presentation. *Journal of Marine Systems*, 17, 555-569, 1998.
- Lancelot, C., S. Mathot, C. Veth, and H. de Baar, Factors controlling phytoplankton ice-edge blooms in the marginal ice-zone of the northwestern Weddell Sea during sea ice retreat 1988: field observations and mathematical modelling, *Polar Biology*, 13, 377-387, 1993.
- LeFevre, J., and P. Treguer, Preface. *Journal of Marine Systems*, 17, 1-3, 1998.

- Rabouille, C., and e. al., Recycling of organic matter in Antarctic sediments: A transect through the polar front in the Southern Ocean (Indian Sector). *Limnology and Oceanography*, 43 (3), 420-432, 1998.
- Smith, R.C., H.M. Dierssen, and M. Vernet, Phytoplankton biomass and productivity in the Western Antarctic Peninsula Region, in *Foundations for Ecosystem Research West of the Antarctic Peninsula*, edited by R.M. Ross, E.E. Hofmann, and L.B. Quetin, pp. 333-356. AGU Antarctic Research Series, 1996.
- Smith, W.O., and D.M. Nelson, Importance of ice edge phytoplankton production in the Southern Ocean. *Bioscience*, 36 (4), 251-257, 1986.
- Treguer, P., and G. Jacques, Dynamics of nutrients and phytoplankton, and fluxes of carbon, nitrogen and silicon in the Antarctic Ocean. *Polar Biology*, 12, 149-162, 1992.
- Zwally, H.J., J.C. Comiso, C.L. Parkinson, and e. al., Antarctic sea ice, 1973-1976: Satellite passive-microwave observations. National Aeronautics and Space Administration, Washington D.C., 1983.

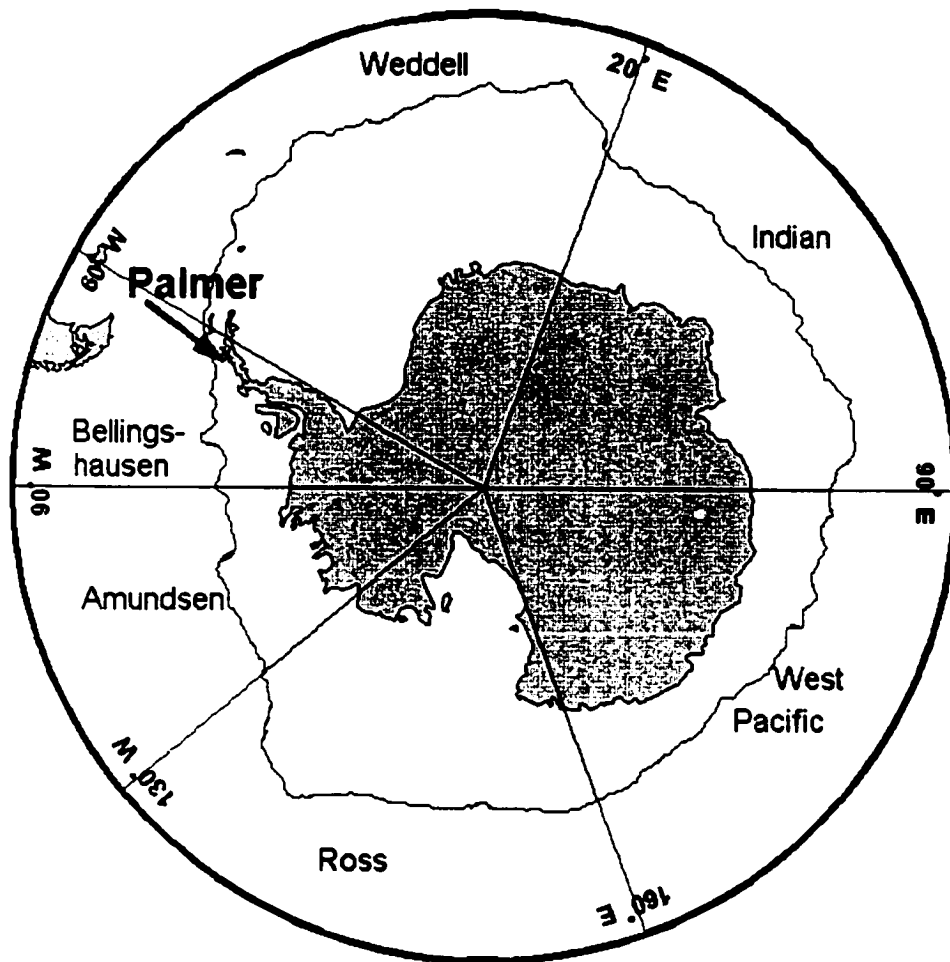


**Figure 1.** Location of the meridional sectors of the Southern Ocean. The lightly shaded region represents the area defined as the Coastal and Continental Shelf Zone and the Seasonal Ice Zone. The white area represents the Permanently Open Ocean Zone and the Polar Front Zone.

## **Chapter 2**

### **Bio-optical Properties and Remote Sensing Ocean Color Algorithms for Antarctic Peninsula Waters**

Dierssen, H.M. and R.C. Smith

Institute for Computational Earth System Science  
Department of Geography  
University of California at Santa Barbara  
Santa Barbara, California 93106

*In press*

*Journal of Geophysical Research*

**Abstract.** Increasing evidence suggests that bio-optical properties of Antarctic waters are significantly different than those at temperate latitudes. Consequently, retrieval of chlorophyll concentrations from remotely sensed reflectance measurements using standard ocean color algorithms are likely to be inaccurate when applied to the Southern Ocean. Here we utilize a large bio-optical data set (>1000 stations) collected in waters west of the Antarctic Peninsula in conjunction with the Palmer Long Term Ecological Research program to assess ocean optical properties and associated ocean color algorithms. We find that the remote sensing reflectance spectrum as a function of chlorophyll concentrations appears significantly different from the SeaBAM data set collected from other regions of the world's oceans. For Antarctic waters, remote sensing reflectance is significantly higher in the blue and lower in the green region of the spectrum for high chlorophyll concentrations ( $>1 \text{ mg Chl m}^{-3}$ ). Therefore, applying general processing algorithms for both CZCS and SeaWiFS in these Antarctic waters results in an underestimate of chlorophyll by roughly a factor of two. From modeled estimates of absorption and backscattering, we hypothesize that both low chlorophyll-specific absorption and low backscattering contribute to the high reflectance ratios.

## 1. Introduction

In assessing the oceanic role in possible climate change, it is important to understand and quantify the processes that control the temporal fluxes of carbon into the ocean. The major carbon flux in the ocean is carbon dioxide uptake by phytoplankton during photosynthesis which can be directly related to the amount of phytoplankton biomass. For Antarctic coastal waters, *Dierssen et al.* [in press] have shown that primary production is tightly coupled to chlorophyll concentrations and can be accurately modeled. However, large-scale shipboard estimates of chlorophyll concentrations for the Southern Ocean are relatively limited. The use of remotely sensed observations from satellites is, therefore, essential in order to gain a synoptic understanding of the abundance and distribution of phytoplankton. This paper is directed at understanding the bio-optical properties of the Antarctic Peninsula waters and determining optimum algorithms for retrieving chlorophyll concentrations from remotely sensed ocean color observations in these waters.

Recent studies present evidence that bio-optical properties, and hence the relationship between water-leaving radiance and pigment concentrations, are significantly different in the Southern Ocean compared to other oceanic regions [*Mitchell and Holm-Hansen, 1991; Mitchell, 1992; Sullivan et al., 1993; Fenton et al., 1994; Arrigo et al., 1998*]. The general processing algorithm for retrieving pigment biomass concentrations from the Coastal Zone Color Scanner (CZCS) was found to underestimate low chlorophyll concentrations ( $< 1.5 \text{ mg Chl m}^{-3}$ ) in the Southern Ocean by a factor of 2.4 [*Mitchell and Holm-Hansen, 1991; Sullivan et al., 1993*]. Therefore, a regional algorithm was developed for the Southern Ocean [*Sullivan et al., 1993*]. The underestimation by the general algorithm was hypothesized to be due to the low concentrations of detritus and



the large pigment packaging effects in this region, which alter the absorption coefficients in Antarctic waters [Mitchell and Holm-Hansen, 1991]. Both pigment packaging effects and low concentrations of colored dissolved and detrital material would result in a reduced absorption coefficient, an increase in remote sensing reflectance, and an underestimation of chlorophyll concentrations. However, pigment-specific absorption in Southern Ocean waters may vary depending on the species composition of the water column [Brody *et al.*, 1992; Arriago *et al.*, 1998].

While absorption properties may be different for Antarctic waters, backscattering coefficients may also play a role in defining the unique relationship between water-leaving radiance and pigment concentrations. Indeed, recent measurements of backscattering in the Ross Sea have found low levels of backscattering [Stramski *et al.*, 1998]. Modeling results suggest that particles  $<0.1$   $\mu\text{m}$  are responsible for the majority of backscattering in the oceans [Morel, 1991; Stramski and Kiefer, 1991]. While submicron microbes and viruses contribute to the total backscattering, the majority of backscattering is thought to come from submicron detrital particles ("Koike" particles  $<0.06$   $\mu\text{m}$ ) that have high water content and corresponding low refractive index [Stramski and Kiefer, 1991; Balch *et al.*, 1998]. Although little is known about the concentrations of Koike particles in the Antarctic, the concentrations of submicron bacterial populations have been found to be low. Compared to most oceanic regions where bacterial biomass is  $\geq 10\%$  of the contemporaneous phytoplankton standing stock, bacterial biomass in the Antarctic Peninsula region is found to be  $<1-2\%$  of phytoplankton standing stock and generally uncoupled from phytoplankton populations [Karl *et al.*, 1996]. Moreover, low bacterial biomass has been found for nearly all Southern Ocean marine ecosystems studied [Lancelot *et al.*,

1989; Cota *et al.*, 1990; Zdanowski and Donachie, 1993]. Given low populations of the submicron bacterial populations and the possibility that microbial decomposition may contribute to the formation of Koike particles [Stramski and Kiefer, 1991], the concentrations of backscattering Koike particles might also be similarly low. If particulate backscattering is generally lower in Antarctic waters, then the water-leaving radiance and remote sensing reflectance ( $R_{rs}(\lambda)$ ) would also be lower, and remote sensing pigment retrieval algorithms for the Southern Ocean would also be different when compared to low latitudes.

In this study, we use a multiyear data set collected in waters west of the Antarctic Peninsula from 1991-1997 to investigate the bio-optical properties for this region. Optical measurements have been collected with several instruments including: the Bio-Optical Profiling System (BOPS-II) [Smith *et al.*, 1997], the Optical Free-Fall Instrument (OFFI) [Waters *et al.*, 1990], and a Bio Spherical Instruments Profiling Reflectance Radiometer (PRR) operated in a free-fall configuration. The data have been collected over different seasons and years and in waters with both low and high pigment biomass concentrations. Optical observations in this region are especially challenging due to low sun angles, a corresponding long atmospheric path length, frequent cloudiness (typically 95%), and the presence of sea ice and snow. In the following methods section we describe in detail the various data quality issues involved in compiling and processing this Antarctic bio-optical data set. This data set is unique because of the varied spatial and temporal coverage, the careful calibration history for each optical sensor, and the intercomparison of data from different ships, instrumentation, and sampling methodology. These LTER data are compared to a large global data set compiled primarily from temperate waters (SeaBAM) [O'Reilly *et al.*,

1998] and to the CZCS and Sea-viewing Wide Field of View Sensor (SeaWiFS) pigment retrieval algorithms.

## **2. Methods**

### **2.1. Data Collection**

Bio-optical data were collected west of the Antarctic Peninsula and from near Palmer Station (64°S, 64°W, Fig. 1) from November 1991 – March 1998. Data were obtained using two basic modes of sampling: 1) weekly time series data collected roughly between November to March over a fine-scale grid near Palmer Station; 2) regional data collected during six week research cruises that covered a large-scale fixed sampling grid [*Waters and Smith, 1992*]. Table 1 lists the various cruises and optical instrumentation from which data were obtained for this paper. For the seasonal time series data from 1991 to 1994, an Optical Free Fall Instrument (OFFI) was used to mitigate potential perturbation effects of the ship [*Waters et al., 1990*]. This instrument was replaced by a free-falling Profiling Reflectance Radiometer (PRR) which was used for the near-shore time series data from 1994 onward and for the January 1998 cruise. The BOPS-II instrument [*Smith et al., 1997*] was used to collect optical data for all of the research cruises prior to January 1998. Coincident chlorophyll and CTD data were also collected with the optical data. Chlorophyll *a* concentrations were estimated by subtracting the phaeopigment concentration determined by sample acidification [*Smith et al., 1981*].

### **2.2. Optical Calibration**

Wherever possible, we used long-term average calibration values to process the bio-optical data. With the exception of a few wavelength channels that degraded over time (and were subsequently replaced), the calibrations generally

varied by less than a few percent over the many years of sampling [Smith *et al.*, 1997]. Following standard radiometric procedures, instrument calibrations were performed periodically (typically before and after each field deployment) and were carried out at the UCSB Ocean Optics Calibration Facility, which participates in the SeaWiFS optical calibration laboratory round robin exercises [Mueller and Austin, 1995]. Immersion coefficients were measured for each instrument individually and applied to the calibration of down- ( $E_d$ ) and upwelling ( $E_u$ ) irradiance data. The measured immersion coefficients for the BOPS-II resulted in irradiances that were 2-6% lower than those measured using the manufacturer-supplied immersion coefficients. Immersion coefficients on upwelling radiance,  $L_u$ , were theoretically computed from different refraction indices for water and the clear acrylic window.

### 2.3. Depth Offsets

The zero depth offset was individually determined for each instrument and each cast. Once the zero depth offset was determined for each cast, we corrected for the positioning of each of the sensors on the instrumentation. For each of the instruments and their respective configurations, we applied an offset to the measured depths to account for the distances between the downwelling and upwelling sensors on the instrumentation package. Thus, the data matrices from each sensor were realigned such that the depth corresponded to the true depth of each individual sensor in the water column and not the depth of the pressure sensor. Table 1 shows the size of each instrument and the distance between the downwelling and upwelling sensors for each of the three instruments.

## 2.4. Extrapolation to the Surface

For typical sea states it is not practical to make optical measurements precisely at an infinitesimal depth below (or above) the surface. Consequently, profiles of irradiance ( $E_d(z, \lambda)$ ) and radiance ( $L_u(z, \lambda)$ ) were measured in the upper few optical depths and estimates just beneath the sea surface ( $z=0^-$ ) were obtained by propagating the measurements back to the sea surface using a least squares regression technique to estimate the down- and up-welling attenuation coefficients,  $K_d(\lambda)$  or  $K_L(\lambda)$  [Smith and Baker, 1984], such that:

$$\ln(E_d(0^-, \lambda)) = \ln(E_d(z, \lambda)) + K_d(\lambda)z \quad (1)$$

$$\ln(L_u(0^-, \lambda)) = \ln(L_u(z, \lambda)) + K_L(\lambda)z \quad (2)$$

$$R_{rs}(0^-, \lambda) = \frac{L_u(0^-, \lambda)}{E_d(0^-, \lambda)} \quad (3)$$

Measured radiation from different depth intervals of 0.5 -5 m. were used in the regression to obtain estimates of  $L_u(0^-, \lambda)$  and  $E_d(0^-, \lambda)$ . As confirmation of our extrapolation process, we found a strong coherence between  $R_{rs}(0^+, \lambda)$  estimated from  $E_d(0^+, \lambda)$  and  $R_{rs}(0^+, \lambda)$  estimated from measured downwelling irradiance above the sea surface,  $E_d(0^+, \lambda)$  (as measured from a ship-board sensor). Spectral remote sensing reflectance just below the air-water interface,  $R_{rs}(0^-, \lambda)$ , was then estimated as the ratio of  $L_u(0^-, \lambda)$  to  $E_d(0^-, \lambda)$  (Eq. 3).

## 2.5. Remote Sensing Reflectance, $R_{rs}(0^+, \lambda)$

For much of the following analyses, we use remote sensing reflectance estimated just above the sea surface,  $R_{rs}(0^+, \lambda)$ . We estimate  $R_{rs}(0^+, \lambda)$  using the

reflectance measured just beneath the surface  $R_{rs}(0^-, \lambda)$  (Eq. 3) in the following relationship [Smith and Baker, 1986; Mobley, 1994; Mueller, 1995]:

$$R_{rs}(0^+, \lambda) = t_r(\lambda) R_{rs}(0^-, \lambda) \quad (4)$$

$$t_r(\lambda) = \frac{1 - \rho(\lambda, \theta)}{n_w^2(\lambda)} t_d \quad (5)$$

Here, we assume that the Fresnel reflectance from water to air,  $\rho(\lambda, \theta)$ , is 0.021-0.022. Depending on the wavelength, we use the wavelength-specific index of refraction,  $n_w$ , for water at 0°C [Austin and Halikas, 1976; Mobley, 1994] and assume that the transmittance of  $E_d(0^+)$  across the sea surface,  $t_d$ , is 0.96 [Smith and Baker, 1986; Dierssen and Smith, 1996]. The resultant transmittance factor,  $t_r$ , used to convert  $R_{rs}(0^-, \lambda)$  to  $R_{rs}(0^+, \lambda)$  varied from 0.515-0.524 depending on wavelength. This is consistent with the methodology used to process the Sea-BAM data set [O'Reilly et al., 1998] and with modeling results from Hydrolight [Mobley, 1994] which show that 51-54% of the  $R_{rs}(0^-, \lambda)$  signal is propagated through the sea surface depending on the wavelength, absorption, scattering, wind and sky conditions.

## 2.6. Instrument self-shading

In order to avoid significant instrument self shading, the instrument radius ( $r$ ) must be less than  $(30a(\lambda))^{-1}$  for  $E_u(\lambda)$  and  $(100a(\lambda))^{-1}$  for  $L_u(\lambda)$  [Gordon and Ding, 1992], where  $a$  is the absorption coefficient for the water column. In these waters, chlorophyll concentrations over  $30 \text{ mg Chl m}^{-3}$  are known to occur and estimates of absorption can be over  $0.4 \text{ m}^{-1}$  (see Section 4.2). Conse-

quently, under high chlorophyll situations, the radius of our instruments would need to be less than 2.5 cm to obtain accurate upwelling radiance measurements. Since the BOPS-II instrument is mounted on a large diameter rosette (radius 42 cm; Table 1), we investigated techniques for correcting instrument self-shading effects on the upwelling radiance and irradiance data. Self-shading correction techniques have been derived and tested primarily for low chlorophyll situations in which the product of  $a$  and  $r$  is less than 0.1 [Gordon and Ding, 1992; Mueller and Austin, 1995; Zibordi and G.Z., 1995]. Because we did not have coincident absorption measurements for these data, we followed an approach recently tested in more productive coastal waters [Aas and Korsbo, 1997] which used the upwelling diffuse attenuation coefficients ( $K_L$ ) combined with the instrument radius ( $r$ ) and a scaling factor ( $B$ ), such that:

$$\ln(L_u^{meas}(\lambda)) = \ln(L_u^{true}(z, \lambda)) - BK_L(\lambda)r \quad (6)$$

Aas and Korsbo [1997] found that this approach was applicable to highly absorbing waters and yielded error estimates that were within 7% of those estimated from the model of Gordon and Ding [1992]. From their measurements, the scaling factor,  $B$ , was found to be dependent both on wavelength and sun angle and ranged between 1.6 and 2.5. To process the BOPS-II data, we used  $B$  coefficients of 2.0, 2.3, 1.8, 1.6, 2.2, 2.5 corresponding to a sun angle of 50° and the wavelengths 410, 441, 488, 520, 565, 625 nm, respectively. The BOPS-II  $E_u$  data were processed using the above  $B$  coefficients scaled by 0.586 (i.e.,  $k_{sky}(E_u)/k_{sky}(L_u)$  from Zibordi and Ferraro [1995]). Determining the appropriate radius was problematic for the BOPS-II instrument because the upwelling radiance sensor was mounted on one side of the instrument and hence it was not

shaded symmetrically by the instrument. To be conservative, we assumed that the instrument was shaded equally by the full instrument radius (0.42 m).

The self-shading corrections varied from a few percent for the low chlorophyll concentrations to around 40% for the higher chlorophyll concentrations. Because of the numerous uncertainties inherent in these self-shading corrections, the corrected BOPS-II data were carefully compared to the PRR and OFFI data, which are smaller instruments that do not have significant self-shading problems. In Fig. 2, we compare median  $R_{rs}(0^+, \lambda)$  estimated for the free-falling PRR (Fig. 2A), OFFI instruments (Fig. 2B), and the BOPS-II instrument (Fig. 2C) for different chlorophyll concentrations ( $\sim 20\%$ ). Overall, the corrected  $R_{rs}(0^+, \lambda)$  for the BOPS-II match up closely in magnitude and overall shape to the PRR and OFFI data. When used concurrently, the corrected BOPS-II estimates were found to be within the experimental error of data obtained using the OFFI or PRR instruments and are used throughout the remainder of this paper.

## 2.7. Wavelength Differences

The spectral bands for discrete wavelength filters on the BOPS-II and OFFI radiometers (410, 441, 488, 520, 565, 625/765 nm) are different from the recommended SeaWiFS spectral bands incorporated in the PRR (412, 443, 490, 510, 555, 665 nm). The first three wavelengths for these instruments are within 2 nm of each other and are used interchangeably throughout this paper. The last three wavelengths have larger differences between the three instruments ( $>10$  nm). Since the spectral shape of remote sensing reflectance is unique for these data as compared to temperate data, wavelength corrections determined for low chlorophyll temperate waters [O'Reilly *et al.*, 1998] may not be appropriate for these waters. Therefore, rather than applying wavelength corrections, we pres-



ent the data separately for each instrument and wavelength ratio so as to ensure that no bias is presented by using mixed wavelength ratios.

## 2.8. Data Quality Assurance

The presence of inorganic particles in the water column (e.g., from glacial runoff) can cause the water's optical properties to be uncoupled from chlorophyll concentrations. Under these conditions, the waters are considered to be Case 2 and should be treated separately from Case 1 waters [*Gordon and Morel, 1983*]. While specific delineations have not been established to distinguish between Case 1 and Case 2 waters for the Southern Ocean, we generally find a tight coupling between the reflectance ratios and chlorophyll concentrations which is indicative of Case 1 waters. Approximately 165 of our 1248 stations were deemed to have anomalously high reflectance and a flatter spectral shape that was consistent with Case 2 waters. These Case 2 data were predominantly associated with glacial melt conditions (i.e., low salinity surface lens) and are excluded from this analysis of Case 1 data. A discussion of Case 2 waters will be presented elsewhere. Without these Case 2 data, the final data set used in the remainder of this paper consisted of 1083 stations.

## 3. Results

In order to understand how the bio-optical properties of Antarctic waters differ from other oceanic regions, we have compared the Antarctic LTER data to the global SeaBAM data [*O'Reilly et al., 1998*]. The SeaBAM data set (n=919) is a compilation of coincident chlorophyll and remote sensing reflectance measurements primarily from non-polar mesotrophic Case I waters. Both data sets have lognormally distributed chlorophyll concentrations and cover a wide range of pigment biomass concentrations. The SeaBAM data set has more

stations in the lower range of chlorophyll concentrations (median of 0.2 mg Chl m<sup>-3</sup>) and ranges from 0.02 to 33 mg Chl m<sup>-3</sup>. In contrast, the median chlorophyll concentrations for these LTER data is higher at around 1 mg Chl m<sup>-3</sup> and ranges from 0.7 to 43 mg Chl m<sup>-3</sup> (Fig. 3). In comparison to the SeaBAM data, the LTER data has considerably more high chlorophyll stations (>5 mg Chl m<sup>-3</sup>) and virtually no oligotrophic data (<0.1 mg Chl m<sup>-3</sup>). However, both data sets are large and overlap in their ranges.

Figs. 4 shows measurements of chlorophyll versus  $R_{rs}(0^+, 443)$  for the SeaBAM data (Fig. 4A) and the LTER data from the BOPS-II (Fig. 4B and 4C), OFFI (Fig. 4D), and PRR (Fig. 4E) instruments, respectively. The data are presented for each instrument and then combined in Fig. 4F for ease of illustration and discussion. For data from all three LTER instruments,  $R_{rs}(0^+, 443)$  is generally higher than the best polynomial fit to the SeaBAM (shown as the dotted line on all of the subplots). The data collected during the winter cruises in early November 1991 and August 1993 were consistently found to be lower than the SeaBAM data (Fig. 4C). This could be due to the low incoming irradiance and very high solar zenith angles associated with winter months in the Antarctic. If we exclude the BOPS-II winter data, it is evident that the blue reflectance values from the LTER data set are consistently higher than the SeaBAM data set. Above values of about 10 mg Chl m<sup>-3</sup>, too few SeaBAM data are available to make a reliable comparison.

The panels in Fig. 5 are identical to those in Fig. 4 except the data are from the green region of the spectrum,  $R_{rs}(0^+, 555-565)$ . The reflectance data for the BOPS-II and OFFI are for a waveband centered at 565 nm, whereas the PRR and most of the SeaBAM data are centered at 555 nm. Because significant dif-

ferences in reflectance can occur between 555 and 565 nm, caution must be taken when concluding from Fig. 5 that  $R_{rs}(0^+, 555)$  is generally lower for the LTER data than the SeaBAM data. As shown in Fig. 5A, the SeaBAM data set also contains reflectance measured at both 555 and 565 nm. Because the SeaBAM  $R_{rs}(0^+, 555)$  are primarily from low chlorophyll stations ( $< 1 \text{ mg Chl m}^{-3}$ ) and because the reflectance spectra is most steeply sloped at low chlorophyll concentrations, these data were found to be approximately 20% lower than  $R_{rs}(0^+, 555)$  [Balch *et al.*, 1998; O'Reilly *et al.*, 1998]. At higher chlorophyll concentrations, however, the difference between reflectance at these two wavelengths is reduced and  $R_{rs}(0^+, 565)$  can be equal to or even greater than  $R_{rs}(0^+, 555)$ . From the 555 nm PRR data (Fig. 5E), we can conclude that the green reflectance for the LTER data is lower than the corresponding SeaBAM for high chlorophyll concentrations ( $> 5 \text{ mg Chl m}^{-3}$ ). This difference is statistically significant, as discussed below.

We have also averaged the data to compare wavelength-specific  $R_{rs}(0^+, \lambda)$  measured for increasing concentrations of chlorophyll ( $\pm 20\%$ ) for the SeaBAM and LTER data (Fig. 6). Consistent with Fig. 4 and 5, the LTER and SeaBAM reflectance spectra are significantly different both in the blue and green regions. At high chlorophyll concentrations ( $> 5 \text{ mg Chl m}^{-3}$ ), the LTER reflectance is lower in the green than the SeaBAM data. In addition, the LTER reflectance in the blue region of the spectrum (410-443 nm) is generally higher than the SeaBAM at chlorophyll concentrations greater than  $0.1 \text{ mg Chl m}^{-3}$ .

Statistical t-tests comparing the SeaBAM and the PRR data for each wavelength and chlorophyll category are shown in Table 2. Because of the wavelength differences between the SeaBAM data and the BOPS-II and OFFI

data, we have only used the PRR data for this statistical comparison. This is also a conservative statistical test because only 311 of the 1124 stations are from the PRR instrument. For a given wavelength and chlorophyll concentration, Table 2 presents the relative percent difference between the mean value from each data set and the results of the hypothesis test that the means of the two data sets are equal. A value of 0 indicates that we would accept the null hypothesis that the means are equal at a significance level of 0.05. A value of 1 or -1 indicates that the mean of the LTER data is significantly greater or less, respectively, than the SeaBAM data. The PRR reflectance is significantly lower than the SeaBAM data (up to 40% lower) for high chlorophyll concentration and green wavelengths. The PRR reflectance is significantly greater than SeaBAM at chlorophyll concentrations of 0.5 mg Chl m<sup>-3</sup> across most of the spectrum. The PRR reflectance at 412 nm is also statistically greater at 5 mg Chl m<sup>-3</sup>. For nearly all chlorophyll levels, the LTER reflectance is on average lower than the SeaBAM data for greener wavelengths (>490 nm) and is greater than the SeaBAM data for bluer wavelengths (<490 nm).

The standard satellite pigment-retrieval algorithms for both CZCS and SeaWiFS utilize the fact that the ratios of remotely sensed radiance vary in a systematic way with chlorophyll concentration. As seen from the spectral shapes in Fig. 6, chlorophyll can be estimated by comparing the reflectance in the blue to that in the green. The ratios of blue to green reflectance should be greater than one for low chlorophyll concentrations and less than one at high chlorophyll concentrations. However, because the LTER reflectance spectra is significantly different from the SeaBAM spectra (Table 2), we expect the resulting waveband ratios also to be significantly different. The general processing algorithm for CZCS makes use of the ratio of  $L_u(443)/L_u(555)$  for chloro-

phyll and phaeopigment concentrations less than  $1.5 \text{ mg Chl m}^{-3}$  and the ratio  $L_u(520)/L_u(555)$  for concentrations greater than  $1.5 \text{ mg Chl m}^{-3}$ . For concentrations less than  $1.5 \text{ mg Chl m}^{-3}$ , Southern Ocean researchers have found that the CZCS general processing algorithm underestimates biomass by a factor of approximately 2.4 [Mitchell and Holm-Hansen, 1991; Sullivan et al., 1993].

Fig. 7 compares the performance of the CZCS general processing algorithms for the LTER data. For chlorophyll and phaeopigment less than  $1.5 \text{ mg Chl m}^{-3}$ , the  $L_u(443)/L_u(555)$  algorithm (Fig. 7A) tends to underestimate LTER chlorophyll concentrations by roughly a factor of two. Our data is consistent with the RACER data also collected west of the Antarctic Peninsula [Mitchell and Holm-Hansen, 1991] and with data collected from cryptophyte-dominated waters in the Ross Sea [Arrigo et al., 1998]. Our best model II regression line [Laws and Archie, 1981] ( $r^2=0.56$ ) is significantly higher than the general processing CZCS algorithm [Gordon and Morel, 1983] and reflectance data collected from diatom and *P. antarctica*-dominated waters in the Ross Sea [Arrigo et al., 1998]. For chlorophyll and phaeopigment greater than  $1.5 \text{ mg Chl m}^{-3}$ , the CZCS general processing algorithm using  $L_u(520)/L_u(555)$  (dot-dashed line) is also inaccurate for these LTER data. When compared to the LTER regression line ( $r^2=0.78$ ), the CZCS algorithm underestimates chlorophyll for concentrations greater than  $10 \text{ mg Chl m}^{-3}$  and overestimates chlorophyll for concentrations greater than  $10 \text{ mg Chl m}^{-3}$ . Thus, chlorophyll determined from CZCS is underestimated not only at low chlorophyll concentrations, as previously noted [Sullivan et al., 1993], but also at concentrations up to approximately  $10 \text{ mg Chl m}^{-3}$ .

Table 3 presents the coefficients for the CZCS radiance ratio algorithms derived from these LTER data and also presents the corrections that can be applied to the chlorophyll concentrations once they have already been processed with the CZCS algorithm. The factor of approximately 2.22 can be linearly applied to the CZCS satellite-derived chlorophyll concentrations less than 1.5 mg Chl m<sup>-3</sup>. For Antarctic coastal waters, chlorophyll concentrations derived from the  $L_w(520)/L_w(555)$  CZCS algorithm can be corrected using a log-linear equation (Table 3) to increase concentrations less than 10 mg Chl m<sup>-3</sup> and decrease concentrations greater than 10 mg Chl m<sup>-3</sup>.

The ocean color algorithm for SeaWiFS (OC2V2) utilizes a modified cubic polynomial function to derive chlorophyll concentrations from the reflectance ratio  $R_{rs}(490)/R_{rs}(555)$  [McClain *et al.*, 1998; O'Reilly *et al.*, 1998]. By normalizing water-leaving radiance ratios to the downwelling irradiance (i.e., using  $R_{rs}$  instead of  $L_w$ ), the data appear less variable compared to the CZCS algorithms, and the SeaWiFS algorithm explains more of the variability in the data. For nearly the entire range of chlorophyll, the LTER  $R_{rs}(490)/R_{rs}(555)$  ratios are consistently higher per unit of chlorophyll than those derived with the OC2V2 algorithm (Fig. 8). Fig. 8A presents the reflectance ratios versus measured chlorophyll concentrations for the LTER data. Fig 8B presents the measured chlorophyll versus the chlorophyll that would be derived using the measured reflectance ratios and the OC2V2 algorithm. As shown, the OC2V2 algorithm would underestimate the SO chlorophyll concentrations on average by a factor of 2.5.

However, few datapoints are available at the high and low ends of the chlorophyll range. At the tail ends of the chlorophyll distribution, data from the

BOPS-II and PRR instruments appear to diverge. For low chlorophyll stations ( $0.1 \text{ mg Chl m}^{-3}$ ), the PRR reflectance ratios tend to be lower per unit chlorophyll than the BOPS-II ratios and centered more closely around the OC2V2 algorithm. At high chlorophyll ( $>10 \text{ mg Chl m}^{-3}$ ), the PRR reflectance ratios tend to be a bit higher than the BOPS-II ratios. Because the PRR data fit the OC2V2 wavelengths precisely (490 and 555 nm) compared to the BOPS-II (488 and 565 nm) and because instrument self-shading is a bigger problem on the BOPS-II, we have chosen to fit a polynomial line through just the PRR data. The polynomial line follows the best fit log-linear regression ( $r^2=0.83$ ) for most of the chlorophyll range and only curves at the tail ends of the range. This polynomial fit describes the factor of 2.5 difference, but does not distort the chlorophyll retrieval from the OC2V2 algorithm at the extreme ranges where we have little data. The coefficients for the fitted lines are presented in Table 3.

The factor of 2.5 and the general consistency in the LTER data is different from recent Ross Sea results which show that the performance of the CZCS and SeaWiFS processing algorithms depend strongly on species composition [Arrigo *et al.*, 1998] (Fig. 8A: lines expressed over data ranges from which algorithm were derived). Within the Antarctic Peninsula waters of the LTER, we typically find large blooms of diatoms and intermittently cryptophytes [Moline and Prezelin, 1996; Vernet *et al.*, 1996; Dierssen *et al.*, in press]. Even with these two different types of blooms, our data indicate that the CZCS and SeaWiFS algorithms consistently underestimate chlorophyll concentrations by roughly a factor of two. Moreover, developing algorithms for a limited range of chlorophyll can lead to large errors in estimating biomass outside of the range.

#### 4. Discussion

For these waters west of the Antarctic Peninsula, blue-to-green reflectance ratios are higher than the global ratios and satellite pigment-retrieval algorithms significantly underestimate chlorophyll concentrations by at least a factor of two. As shown in the previous section, the higher Antarctic blue-to-green reflectance ratios per unit chlorophyll are due to a combination of both higher blue reflectance and lower green reflectance. Here, we investigate the possible influences of the inherent optical properties (IOPs) on the differences in the LTER and SeaBAM reflectance spectra. Radiance reflectance is proportional to the backscattering coefficient,  $b_b$ , and inversely proportional to the absorption coefficient,  $a$ . [Morel and Gentili, 1991], such that:

$$R_{rs} \approx \frac{f}{Q} \frac{b_b}{a} \quad (7)$$

In order to explore the factor of two difference between measured and satellite-derived pigment concentrations, the ratio  $f/Q$ , absorption, and backscattering are discussed below in relation to the LTER reflectance data.

#### 4.1. Ratio $f/Q$

The  $Q$  factor expresses the nonisotropic character of the radiance distribution and relates a given upwelling radiance,  $L_u$ , to the corresponding upwelling irradiance,  $E_u$ , such that:

$$Q = \frac{E_u}{L_u} \quad (8)$$

$Q$  has been shown to be strongly dependent on the sun angle and to lesser degree wavelength. The  $f$  factor, which relates  $R_{rs}(0^+, \lambda)$  to the inherent optical properties of the water body, is also dependent on sun angle. Because of the parallel



dependencies of  $f$  and  $Q$  on sun angle, the ratio of these two parameters,  $f/Q$ , has been found to be relatively stable ( $\pm 20\%$ ) [Gordon, 1986; Morel and Gentili, 1993]. While the ratio is more constant than either of the parameters individually,  $f/Q$  ratios can still vary from 0.12 for low-pigment waters and blue wavelengths down to 0.08 for high pigment waters and red wavelengths [Morel and Gentili, 1993].

Modeling results suggest that there are regional differences in  $f/Q$ . In contrast to temperate regions, polar regions have large solar zenith angles (always  $>40^\circ$  at Palmer Station) and the proportion of diffuse skylight is high, especially in the blue regions of the spectrum [Dierssen and Smith, 1996]. Morel and Gentili [1993] model the changing trends in  $f/Q$  with latitude and determine that across the visible spectrum,  $f/Q$  ratios are approximately 5% greater in polar regions than in temperate regions. The latitudinal differences in  $f/Q$  ratios are more pronounced at chlorophyll greater than  $0.3 \text{ mg m}^{-3}$ , which is generally the case for most of our LTER data (Fig. 3). Because  $f/Q$  is proportional to  $R_{rs}(0^+, \lambda)$  (Eq. 7), a higher  $f/Q$  would result in a higher  $R_{rs}(0^+, \lambda)$  for these polar waters. However, the LTER reflectance in the green is lower, not higher, than the SeaBAM data. While  $f/Q$  may play a minor role in explaining the increased reflectance in the blue, the magnitude of difference between the SeaBAM and LTER data is generally greater than 5% (Table 2).

## 4.2. Absorption

The total spectral absorption coefficient,  $a$ , is comprised of several components:

$$a = a_w + a_p + a_{DS} \quad (9)$$

where  $a_w$  is absorption due to water,  $a_p$  is absorption due to total particulates (i.e., phytoplankton and detrital materials), and  $a_{DS}$  is absorption due to colored dissolved organic materials [Sakshaug *et al.*, 1997]. These properties are discussed below in relation to their effects on  $R_{rs}(0^+, \lambda)$ . Since  $R_{rs}(0^+, \lambda)$  is inversely proportional to  $a$  (Eq. 7), higher  $a(\lambda)$  would result in lower  $R_{rs}(0^+, \lambda)$ .

To analyze the absorption characteristics of these waters, we estimated total absorption  $a(0^+, \lambda)$  from the BOPS-II data using the relationship derived by *Gershun* (1936) to estimate  $a$  from the depth rate of change of the net irradiance,  $K_E$ , and the average cosine for total light,  $\mu$ , where:

$$a = K_E(\lambda, z) \mu(\lambda, z) \quad (10)$$

$$\mu(\lambda, z) = \frac{E_d - E_u}{E_o} \quad (11)$$

The value of  $\mu(\lambda, z)$  is estimated from the downwelling ( $E_d$ ), upwelling ( $E_u$ ) and scalar irradiances ( $E_o$ ) (Eq. 11). For the *Gershun* approximation, internal sources of radiant energy are assumed to be negligible.

We estimated  $a(0^+, \lambda)$  from Eq. 10 using the  $E_d$ ,  $E_u$ , and  $E_o$  data from the BOPS-II instrument. By subtracting  $a_w$  [Pope and Fry, 1997] from the total absorption, we arrived at surface estimates of absorption due to particulates and colored dissolved organic materials,  $a_{p+DS}(0^+, \lambda)$ . As shown in Fig. 9A, the magnitude of  $a_{p+DS}(0^+, \lambda)$  increases with increasing chlorophyll concentration up to around  $0.25 \text{ m}^{-1}$  for chlorophyll of  $10 \text{ mg Chl m}^{-3}$ . We compared these  $a_{p+DS}(0^+, \lambda)$  with modeled estimates using two different chlorophyll-specific relationships [Morel, 1991; Bricaud *et al.*, 1995]. The shape and magnitude of

the LTER  $a_{p+DS}(0, \lambda)$  could be best approximated by using the *Bricaud* [1995] model with an additional 30%  $a_{DS}(0, \lambda)$  (modeled with an exponential decay slope of 0.02). Because the *Morel* [1991] model has higher pigment-specific absorption coefficients, this model was closest to the LTER data with no additional contribution of  $a_{DS}(0, \lambda)$ . However, both models tend to underestimate  $a_{p+DS}(0, \lambda)$  at low pigment concentrations. We speculate that  $a_{DS}(0, \lambda)$  is underestimated when total absorption is low and a fixed percentage (i.e., 30%) is used throughout the chlorophyll range to estimate the contribution of  $a_{DS}(0, \lambda)$ .

When the  $a_{p+DS}(0, \lambda)$  are normalized to chlorophyll concentration (Fig. 9B), the resulting pigment-specific absorption,  $a^*_{p+DS}(0, \lambda)$ , tends to be high for low chlorophyll concentrations ( $<1 \text{ mg m}^{-3}$ ) and low for high chlorophyll concentrations ( $5\text{-}20 \text{ mg m}^{-3}$ ). This is consistent with pigment-package effects in which pigment-specific absorption decreases with increasing chlorophyll concentrations. We have also compared our estimates of  $a^*_{p+DS}(0, \lambda)$  with previously published absorption measurements in the Southern Ocean. In the LTER region, diatoms are the major bloom-forming plankton, although cryptophytes are occasionally dominant in the water column [*Kozłowski et al.*, 1995; *Moline and Prezelin*, 1996; *Dierssen et al.*, in press]. For cryptophytes collected both in the Antarctic Peninsula and the Ross Sea (Fig. 9B) [*Brody et al.*, 1992; *Arrigo et al.*, 1998],  $a^*_p(0, \lambda)$  was quite high and in the range measured for temperate species.

Diatoms from these two regions, however, had vastly different  $a^*_p(0, \lambda)$ . In the Ross Sea, the diatom  $a^*_p(0, \lambda)$  spectra was found to be quite

similar to cryptophytes, whereas in the Antarctic Peninsula,  $a^*_{p}(0^-, \lambda)$  was low for the diatom populations [Mitchell and Holm-Hansen, 1991; Brody *et al.*, 1992]. The discrepancy in absorption between the two diatom populations can be explained by comparing the various cell sizes of the organisms. The diatoms reported for Antarctic Peninsula waters tend to be much larger (diameter  $> 20 \mu\text{m}$ ) [Brody *et al.*, 1992] than the diatoms reported for Ross Sea waters (total volume of  $30 \mu\text{m}^3$ ) [Arrigo *et al.*, 1998]. For the LTER data, we find that as chlorophyll increases the cell sizes also increase. For chlorophyll greater than  $5 \text{ mg m}^{-3}$ , over 90% of the chlorophyll occurs in cells greater than  $20 \mu\text{m}$ . Our low estimates of  $a^*_{p+DS}(0^-, \lambda)$  at high chlorophyll concentrations are, therefore, consistent with large diatoms generally associated with Antarctic Peninsula waters.

Because absorption is inversely proportional to reflectance (Eq. 7), lower absorption results in greater reflectance. Consistent with past finding in the western Antarctic Peninsula region [Mitchell and Holm-Hansen, 1991], we postulate that low  $a^*_{p+DS}(0^-, \lambda)$ , especially at high chlorophyll concentrations, could result in the increased  $R_{rs}(0^-, \lambda)$  observed in the blue region of the spectrum. However, absorption generally influences the blue and red portions of the spectrum and not the green where we observe a low reduced reflectance at 555 nm. If the phytoplankton contained pigments that absorbed highly in the green region of the spectra, higher  $a_p(0^-, 555)$  could hypothetically result in a lower  $R_{rs}(0^-, 555)$ . Of the major bloom-forming plankton in this region, diatoms and cryptophytes both contain pigments that can absorb light in the green region of the spectra (500-600 nm). However, neither the LTER data nor the other Southern Ocean data give any indication of anomalously high absorption in the green region of the spectrum which would cause the depressed  $R_{rs}(0^-, 555)$ . This

suggests that high  $a_p(555)$  is unlikely to be the cause of the low measurements of  $R_{rs}(0^+, 555)$  with increasing chlorophyll concentrations. Therefore, we hypothesize that backscattering must also play an important role in the factor two of difference in remote sensing pigment-retrieval algorithms for this region.

### 4.3. Backscattering

With increased concentration of total particulates in a water body, the amount of backscattered light generally increases at all wavelengths. However, when the particles are predominantly algae, certain parts of the visible spectra (i.e., blue and red) are highly absorbed and the resulting shape of the  $R_{rs}(0^+, \lambda)$  curve is low in blue and red and high in green (as shown in the high chlorophyll SeaBAM data, Fig. 4A). The presence of the so-called  $R_{rs}(0^+, \lambda)$  spectral hinge point in which high and low chlorophyll  $R_{rs}(0^+, \lambda)$  cross at approximately 500 nm has been a commonly observed characteristic of ocean color data sets. However, the LTER green reflectance is significantly lower than SeaBAM, especially as chlorophyll concentrations increase above  $5 \text{ mg Chl m}^{-3}$ . Because backscattering is proportional to reflectance (Eq. 7), reduced backscattering could explain the low green reflectance observed in the LTER data.

Because of the low refractive index of living cells relative to water [Kirk, 1994], backscattering from phytoplankton is considered to be minimal. Theoretical studies suggest that most of particulate backscattering is due to detrital particles less than  $0.6 \mu\text{m}$  (i.e., Koike particles) and not phytoplankton [Morel and Ahn, 1990; Stramski and Kiefer, 1991; Ulloa et al., 1994; Balch et al., 1998]. Nevertheless, phytoplankton concentrations have been found to covary with the amount of backscattered light. Ulloa et al. [1994] present an explana-

tion for this paradox by showing that an inverse relationship exists between pigments and the shape of the total particle-size distribution, which is in turn the principle control on the ratio of backscattering to total scattering. If concentrations of minute backscattering detrital particles covary with phytoplankton, backscattering will increase with higher phytoplankton concentrations. Because of their minute size, submicron detritus have only recently been demonstrated to occur in large numbers in most regions of the world's ocean [Koike *et al.*, 1990] and little is known of their abundance in the Antarctic.

If backscattering is found to be lower in the Southern Ocean, then one could hypothesize that concentrations of submicron detrital particles are also low. The relationships between other submicron populations (e.g., viral and microbial) and phytoplankton in the Antarctic may be fundamentally different from other marine habitats. Karl *et al.* [1996] have shown that Antarctic bacterial productivity is generally uncoupled to phytoplankton concentrations and is consistently low relative to phytoplankton productivity. Even during the spring bloom, bacterial biomass are <1-2% of the contemporaneous phytoplankton standing stock compared to  $\geq 10\%$  for most other oceanic regions [Karl *et al.*, 1996]. Moreover, virus particle abundance has also been found to be consistently low in the surface waters of the Antarctic [Karl *et al.*, 1996]. This is not unique to Antarctic Peninsula waters, but is ubiquitous for all Southern Ocean ecosystems studied [Lancelot *et al.*, 1989; Cota *et al.*, 1990; Zdanowski and Donachie, 1993]. Given that microbial activities may contribute to the formation of submicron detritus with low refractive index (i.e., Koike particles) [Stramski and Kiefer, 1991], the reduced microbial populations in the Antarctic may be correlated with a low abundance of submicron detritus that causes most of the backscattering in the ocean. Therefore, we postulate that low backscattering at high chlorophyll may be a feature of parts of the Southern Ocean and may influ-

ence the performance of ocean color algorithms. Future efforts will be directed at characterizing the absorption and backscattering coefficients in relation to the reflectance spectra and the factor of two difference in pigment-retrieval algorithms.

## 5. Acknowledgements

This research was supported by NASA Training Grants NGT-30063 (Earth System Science Fellowship) and NGT-40005 (California Space Institute) to H. Dierssen, and NSF Grant OPP90-11927 and NASA Grant NAGW 290-3 to R.C. Smith. Karen Baker provided data management and Sharon Stammerjohn, Maria Vernet, and Brad Seibel gave helpful comments on the manuscript. Dave Menzies carried out instrument repair and optical calibration. Also acknowledged are the many people who helped acquire the data at sea: in particular, Tim Newberger, Phil Handley and Janice Jones. We further wish to thank the anonymous reviewers for their helpful comments on this manuscript.

## 6. References

- Aas, E., and B. Korsbo. Self-shading effect by radiance meters on upward radiance observed in coastal waters, *Limnology and Oceanography*, 42 (5), 968-974, 1997.
- Arrigo, K., D. Worthen, A. Schnell, and M.P. Lizotte, Primary production in Southern Ocean waters, *Journal of Geophysical Research*, 103 (C8), 15587-15600, 1998.
- Austin, R.W., and G. Halikas. The index of refraction of seawater, pp. 121. Scripps Institute of Oceanography, La Jolla, CA, 1976.

- Balch, W., J. Vaughn, J. Novotny, D. Drapeau, and e. al., Light scattering by viral suspensions, in *Ocean Optics XIV*, edited by S. Ackleson, and J. Campbell. Offic of Naval Research, Kailua-Kona Hawaii, 1998.
- Bricaud, A., M. Babin, A. Morel, and H. Claustre, Variability in the chlorophyll-specific absorption coefficients of natural phytoplankton: Analysis and parameterization. *Journal of Geophysical Research*, 100 (C7), 13,321-13,332, 1995.
- Brody, E., B.G. Mitchell, O. Holm-Hansen, and M. Vernet, Species-dependent variations of the absorption coefficient in the Gerlache Strait, *Antarctic Journal, Review*, 160-162, 1992.
- Cota, G.F., S.T. Kottmeier, D.H. Robinson, W.O. Smith, and C.W. Sullivan, Bacterioplankton in the marginal ice zone of the Weddell Sea: biomass, production, and metabolic activities during austral autumn. *Deep-Sea Research*, 37, 1145-1167, 1990.
- Dierssen, H.M., and R.C. Smith, Estimation of irradiance just below the air-water interface, in *Ocean Optics XIII*, pp. 204-209, SPIE, Halifax, Nova Scotia, Canada, 1996.
- Dierssen, H.M., R.C. Smith, and M. Vernet, Optimizing models for remotely estimating primary production in Antarctic coastal waters, *Antarctic Science*, in press.
- Fenton, N., J. Priddle, and P. Tett, Regional variations in bio-optical properties of the surface waters in the Southern Ocean, *Antarctic Science*, 6 (4), 443-448, 1994.
- Gordon, H.R., Ocean color remote sensing: influence of the particle phase function and the solar zenith angle. *EOS Trans. Amer. Geophys. Union*, 14, 1055, 1986.



- Gordon, H.R., and K. Ding, Self shading of in-water optical instruments, *Limnology and Oceanography*, 37, 491-500, 1992.
- Gordon, H.R., and A.Y. Morel. *Remote Assessment of Ocean Color for Interpretation of Satellite Visible Imagery: A Review*. Springer-Verlag, New York, 1983.
- Karl, D.M., J.R. Christian, and J.E. Dore, Microbiological oceanography in the region west of the Antarctic Peninsula: Microbial dynamics, nitrogen cycle, and carbon flux, in *Foundations for Ecosystem Research West of the Antarctic Peninsula*, edited by R.M. Ross, E.E. Hofmann, and L.B. Quetin, pp. 303-332, AGU Antarctic Research Series, 1996.
- Kirk, J.T.O., *Light and Photosynthesis in Aquatic Ecosystems*, Cambridge University Press, Cambridge, 1994.
- Koike, I., S. Hara, T. Terauchi, and K. Kogure, Role of submicrometer particles in the ocean. *Nature*, 345, 242-244, 1990.
- Kozlowski, W., S.K. Lamerdin, and M. Vernet, Palmer LTER: Predominance of cryptomonads and diatoms in Antarctic coastal waters. *Antarctic Journal of the U.S.*, in press, 1995.
- Lancelot, C., G. Billon, and S. Mathot, *Ecophysiology of Phyto- and Bacterioplankton Growth in the Southern Ocean*. *Belgian Scientific Research Programme on Antarctica Scientific Results of Phase One (Oct 85-Jan 89)*, 97 pp., 1989.
- Laws, E.A., and J.W. Archie, Appropriate use of regression analysis in marine biology. *Marine Biology*, 65, 13-16, 1981.
- McClain, C.R., M.L. Cleave, G.C. Feldman, W.W. Gregg, and e. al., Science quality SeaWiFS data for global biosphere research. *Sea Technology*, 10-16, 1998.

- Mitchell, B.G.. Predictive bio-optical relationshs for polar oceans and marginal ice zones. *Journal of Marine Systems*, 3, 91-105, 1992.
- Mitchell, B.G., and O. Holm-Hansen. Bio-optical properties of Antarctic Peninsula waters: differentiation from temperate ocean models. *Deep-Sea Research*, 38 (8/9), 1009-1028, 1991.
- Mobley, C.D.. *Light and water: Radiative transfer in natural waters*, Academic Press, San Diego, 1994.
- Moline, M., and B.B. Prezelin. Long-term monitoring and analyses of physical factors regulating variability in coastal Antarctic phytoplankton biomass, in situ productivity and taxonomic composition over subseasonal, seasonal, and interannual time scales. *Marine Ecology Progress Series*, 145 (1-3), 143-160, 1996.
- Morel, A.. Light and marine photosynthesis: a spectral model with geochemical and climatological implications. *Prog. Oceanography*, 26, 263-306, 1991.
- Morel, A., and Y.H. Ahn, Optical efficiency factors of free-living marine bacteria: influence of bacterioplankton upon the optical properties and particulate organic carbon in oceanic waters. *Journal of Marine Research*, 48, 145-175, 1990.
- Morel, A., and B. Gentili, Diffuse reflectance of oceanic waters: its dependence on Sun angle as influenced by the molecular scattering contribution. *Applied Optics*, 30 (30), 4427-4438, 1991.
- Morel, A., and B. Gentili, Diffuse reflectance of oceanic waters. II. Bidirectional aspects. *Applied Optics*, 32 (33), 6864-6879, 1993.
- Mueller, J.L.. Comparison of irradiance immersion coefficients for several marine environmental radiometers (MERs), in *Volume 27, Case Studies for SeaWiFS Calibration and Validation, Part 3.*, edited by S.B. Hooker.

- E.R. Firestone, and J.G. Acker, NASA Technical Memorandum 104566: SeaWiFS Technical Report Series, Goddard Space Flight Center, 1995.
- Mueller, J.L., and R.W. Austin, *Volume 25, Ocean Optics Protocols for SeaWiFS Validation, Revision 1*, NASA Technical Memorandum 104566: SeaWiFS Technical Report Series, Goddard Space Flight Center, 1995.
- O'Reilly, J.E., S. Maritorena, B.G. Mitchell, D.A. Siegel, and e. al., Ocean color chlorophyll algorithms for SeaWiFS, *Journal of Geophysical Research*, *103* (C11), 24,937-24,953, 1998.
- Pope, R., and E. Fry, Absorption spectrum of pure water: 2. Integrating cavity measurements, *Applied Optics*, *36* (33), 8710-8723, 1997.
- Sakshaug, E., A. Bricaud, Y. Dandonneau, P.G. Falkowski, and e. al., Parameters of photosynthesis: definitions, theory and interpretation of results, *Journal of Plankton Research*, *19* (11), 1637-1670, 1997.
- Smith, R.C., and K.S. Baker, The analysis of ocean optical data, *SPIE - Ocean Optics VII*, *489*, 119-126, 1984.
- Smith, R.C., and K.S. Baker, Analysis of ocean optical data II, *SPIE - Ocean Optics VIII*, *637*, 95-107, 1986.
- Smith, R.C., K.S. Baker, and P. Dustan, Fluorometer techniques for measurement of oceanic chlorophyll in the support of remote sensing, Visibility Laboratory, Scripps Institution of Oceanography, San Diego, CA, 1981.
- Smith, R.C., D.W. Menzies, and C.R. Booth, Oceanographic Bio-optical Profiling System II, in *Ocean Optics XIII*, edited by S.G. Ackleson, and R. Frouin, pp. 777-786. SPIE, Halifax, Nova Scotia, 1997.
- Stramski, D., and D.A. Kiefer, Light scattering by microorganisms in the open ocean, *Prog. Oceanog.*, *28*, 343-393, 1991.

- Stramski, D., R. Reynolds, and B.G. Mitchell, Relationships between the back-scattering coefficient, beam attenuation coefficient and particulate organic matter concentrations in the Ross Sea, in *Ocean Optics XIV*, edited by S. Ackleson, and J. Campbell, Office of Naval Research, Kailua-Kona Hawaii, 1998.
- Sullivan, C.W., K.R. Arrigo, C.R. McClain, J.C. Comiso, and J. Firestone, Distributions of phytoplankton blooms in the Southern Ocean, *Science*, 262, 1832-1837, 1993.
- Ulloa, O., S. Sathyendranath, and T. Platt, Effect of the particle-size distribution on the backscattering ratio in seawater, *Applied Optics*, 33 (30), 7070-7077, 1994.
- Vernet, M., W. Kozlowski, and T. Ruel, Palmer LTER: Temporal variability in primary productivity in Arthur Harbor during the 1994/1995 growth season, *Antarctic Journal of the United States*, 1996.
- Waters, K.J., and R.C. Smith, Palmer LTER: A sampling grid for the Palmer LTER program, *Antarctic Journal of U.S.*, 27, 236-239, 1992.
- Waters, K.J., R.C. Smith, and M.R. Lewis, Avoiding ship-induced light-field perturbation in the determination of oceanic optical properties, *Oceanography*, November, 18-21, 1990.
- Zdanowski, M.K., and S.P. Donachie, Bacteria in the sea-ice zone between Elephant Island and the South Orkneys during the Polish sea-ice expedition, *Polar Biology*, 13, 245-254, 1993.
- Zibordi, G., and F. G.Z., Instrument self-shading in underwater optical measurements: experimental data, *Applied Optics*, 34 (15), 2750-2754, 1995.

**Table 1.** Optical Instrumentation used for LTER Sampling

name	Optical	Size (m) <sup>f</sup>	Instrument	wavelengths			
	Instrument	Dia. x Len.	ID numbers	E <sub>d</sub>	E <sub>u</sub>	L <sub>u</sub>	E <sub>s</sub>
<b>cruise</b>							
nov91	BOPS-II	0.83 x 1 <sup>g</sup>	8714 <sup>a</sup> /8715 <sup>c</sup> /8709	1	1	1	2
jan93	BOPS-II	0.83 x 1 <sup>g</sup>	8714 <sup>a</sup> /8715 <sup>c</sup> /8709	1	1	1	2
aug93	BOPS-II	0.83 x 1 <sup>g</sup>	8714 <sup>a</sup> /8715 <sup>c</sup> /8709	1	1	1	2
jan94	BOPS-II	0.83 x 1 <sup>g</sup>	8714 <sup>a</sup> /8715 <sup>c</sup> /8709	1	1	1	2
jan95	BOPS-II	0.83 x 1 <sup>g</sup>	8714 <sup>b</sup> /8715 <sup>c</sup> /8722	3	1	1	7
jan96	BOPS-II	0.83 x 1.3 <sup>h</sup>	8714 <sup>b</sup> /8715 <sup>d</sup> /8709	3	1	1	2
jan97	BOPS-II	0.83 x 1.3 <sup>h</sup>	8714 <sup>b</sup> /8715 <sup>d</sup> /8709	3	1	1	2
jan98ab	PRR	0.2 x 0.40	9628 <sup>e</sup> /9629	4	--	4	4
<b>station</b>							
pal9192	OFFI	0.2 x 0.75	8722/8709	5	--	5	2
pal9293	OFFI	0.2 x 0.75	8722/8709	5	--	5	2
pal9394	OFFI	0.2 x 0.75	8722/8709	5	--	5	2
pal9495	PRR	0.2 x 0.40	9603/9614	6	--	6	6
pal9596	PRR	0.2 x 0.40	9628/9629	4	--	4	4
pal9697	PRR	0.2 x 0.40	9628/9629	4	--	4	4
pal9798	PRR	0.2 x 0.40	9628 <sup>e</sup> /9629	4	--	4	4
pal9899	PRR	0.2 x 0.40	9603/9614	6	--	6	6

Wavelength Key (nm)

1- 410, 441, 488, 520, 565, 625  
2- 410, 441, 488, 560  
3- 410, 412, 441, 443, 488, 490, 510, 520,  
555, 565, 589, 625, 665  
4- 412, 443, 490, 510, 555, 665  
5- 410, 441, 488, 520, 565, 765  
6- 412, 443, 490, 510, 555, 656  
7- 38 channels

Notes

<sup>a</sup> pre-Nov. 1994 long-term average, 8 channels  
<sup>b</sup> post-Nov. 1994 long-term average, 13 channels  
<sup>c</sup> pre-Oct. 1995 long-term average  
<sup>d</sup> post-Oct. 1995 long-term average, decreased the acceptance angle on sensor  
<sup>e</sup> new teflon diffuser put on 9628  
<sup>f</sup> except where specified, the length is the distance between the  $E_d$  and  $L_v/E_v$  sensors and the sensors are centered on the instrumentation array  
<sup>g</sup>  $L_v$  sensor 10 cm above bottom of array and mounted on one side of instrument.  
<sup>h</sup>  $L_v$  sensor 40 cm above bottom of array and mounted on one side of instrument

**Table 2.** Statistical results from a t-test<sup>a</sup> comparing measured SeaBAM and PRR  $R_{rs}(0^-, \lambda)$  for different chlorophyll concentrations<sup>b</sup>

Chl <sup>b</sup> mg m <sup>-3</sup>	Wavelength [nm]				
	412	443	490	510	555
0.1	0 (-20%)	0 (-19%)	0 (-13%)	0 (5%)	0 (3%)
0.5	1 (36%)	1 (24%)	1 (22%)	1 (18%)	0 (-7%)
1	0 (10%)	0 (4%)	0 (-1%)	0 (-3%)	-1 (-20%)
5	1 (46%)	0 (16%)	0 (-6%)	0 (-15%)	-1 (-36%)
10	0 (18%)	0 (-9%)	0 (-25%)	0 (-29%)	-1 (-40%)

<sup>a</sup> Assuming a significance level of 0.05, the statistical results are as follows:

0 = accept the null hypothesis that the means are equal.

1 = reject the null hypothesis and accept the alternative hypothesis that the LTER mean is greater than the SeaBAM mean.

-1 = reject the null hypothesis and accept the alternative hypothesis that the LTER mean is less than the SeaBAM mean.

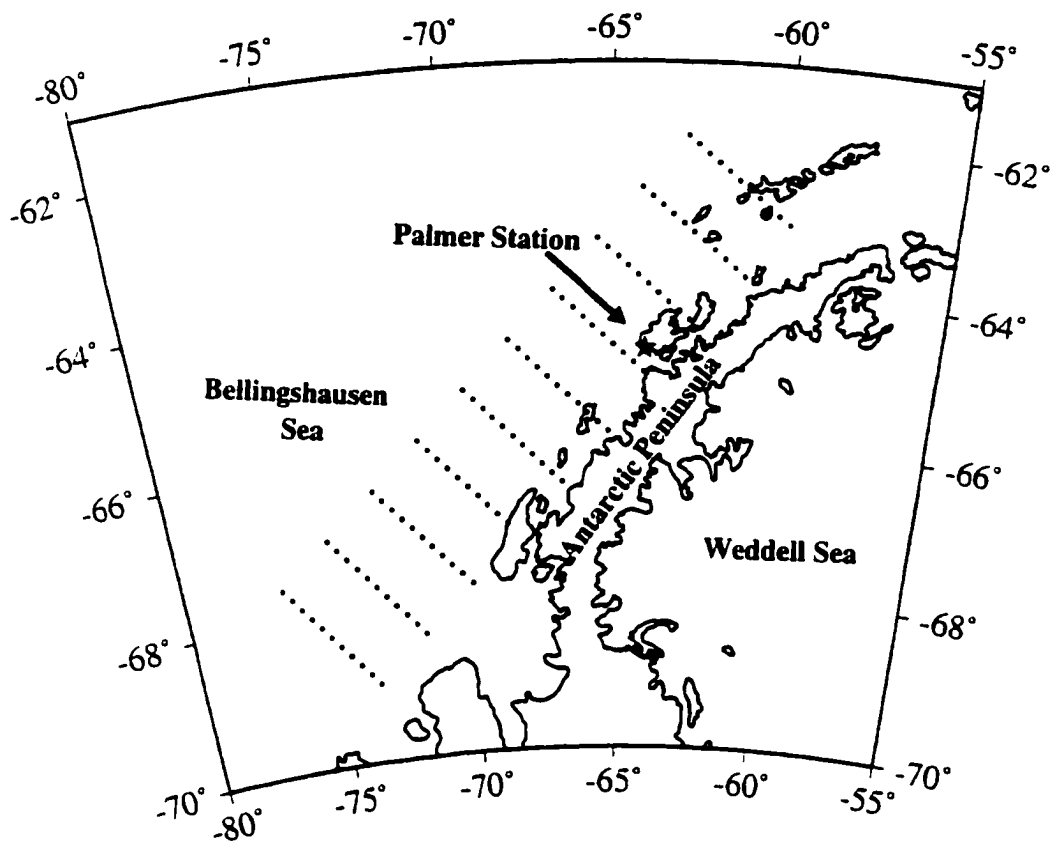
( %) = number in parenthesis represents the percent difference between mean LTER and SeaBAM values.

<sup>b</sup> chlorophyll categories are ±20% of value given

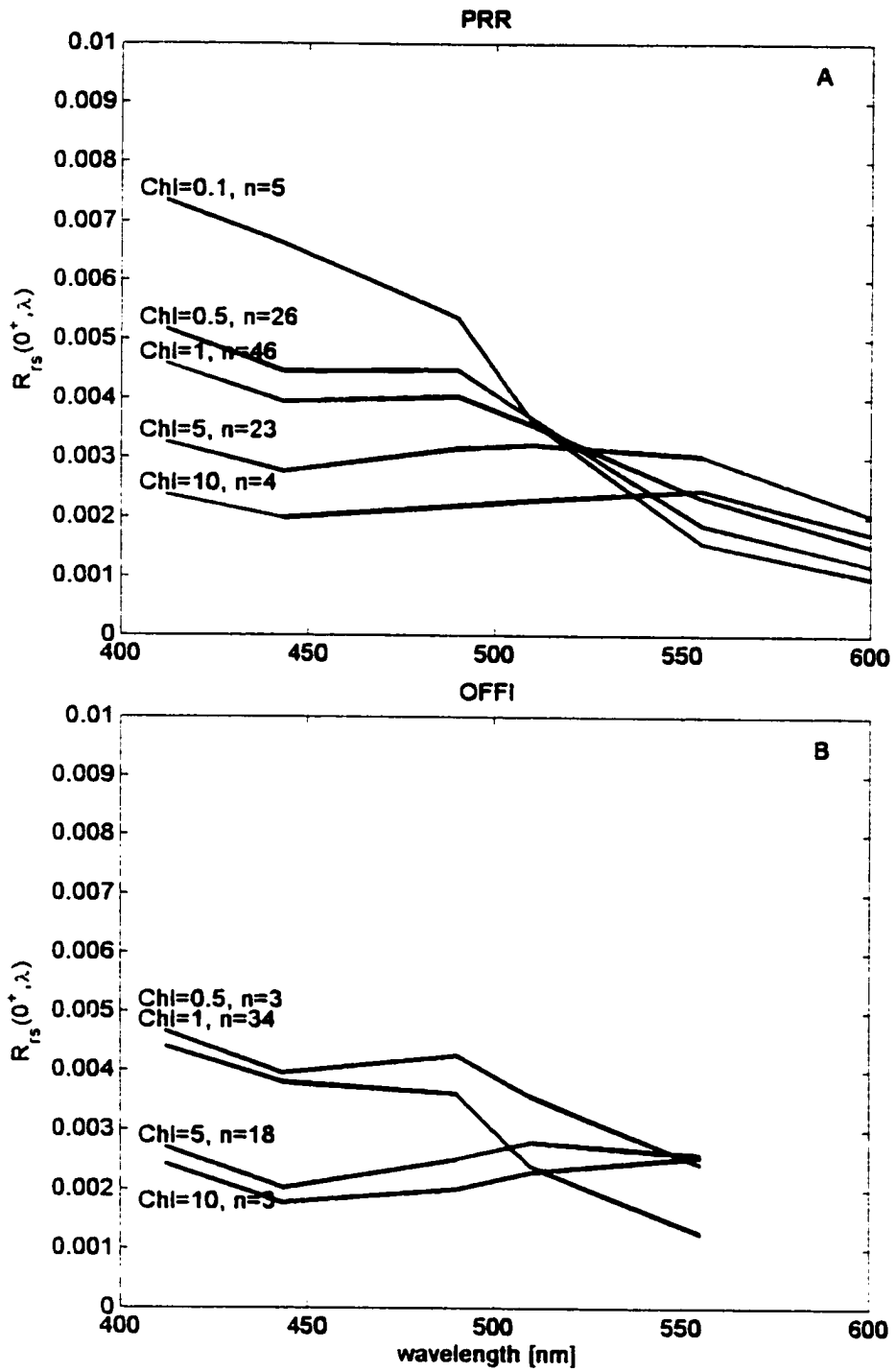
**Table 3.** Southern Ocean chlorophyll algorithms using reflectance ratios and satellite-derived chlorophyll

Algorithm Input (X)	Formu- lation	Coefficient				
		a	b	c	d	e
<b><u>CZCS &lt; 1.5 mg m<sup>-3</sup></u></b>						
log(L <sub>w</sub> (440)/L <sub>w</sub> (555))	power	0.51	-1.69			
CZCS-derived Chl	linear	0	2.22			
<b><u>CZCS &gt; 1.5 mg m<sup>-3</sup></u></b>						
log(L <sub>w</sub> (520)/L <sub>w</sub> (555))	power	0.78	-2.52			
log(CZCS-derived Chl)	power	0.45	0.53			
<b><u>SeaWiFS OC2V2</u></b>						
log(R <sub>rs</sub> (490)/R <sub>rs</sub> (555))	3-poly.	0.641	-2.058	-0.442	-1.140	
log(OC2V2-derived Chl)	4-poly.	0.3914	1.0176	-0.3114	0.0186	0.0610
Formulations: linear, C = a + bX; power, C = 10 <sup>(a+bX)</sup> ; 3-degree polynomial,						
C = 10 <sup>(a+bX+cX<sup>2</sup>+dX<sup>3</sup>)</sup> ; 4-degree polynomial, C = 10 <sup>(a+bX+cX<sup>2</sup>+dX<sup>3</sup>+eX<sup>4</sup>)</sup>						





**Figure 1.** Location of the large-scale LTER sampling grid in reference to Palmer Station Antarctica.



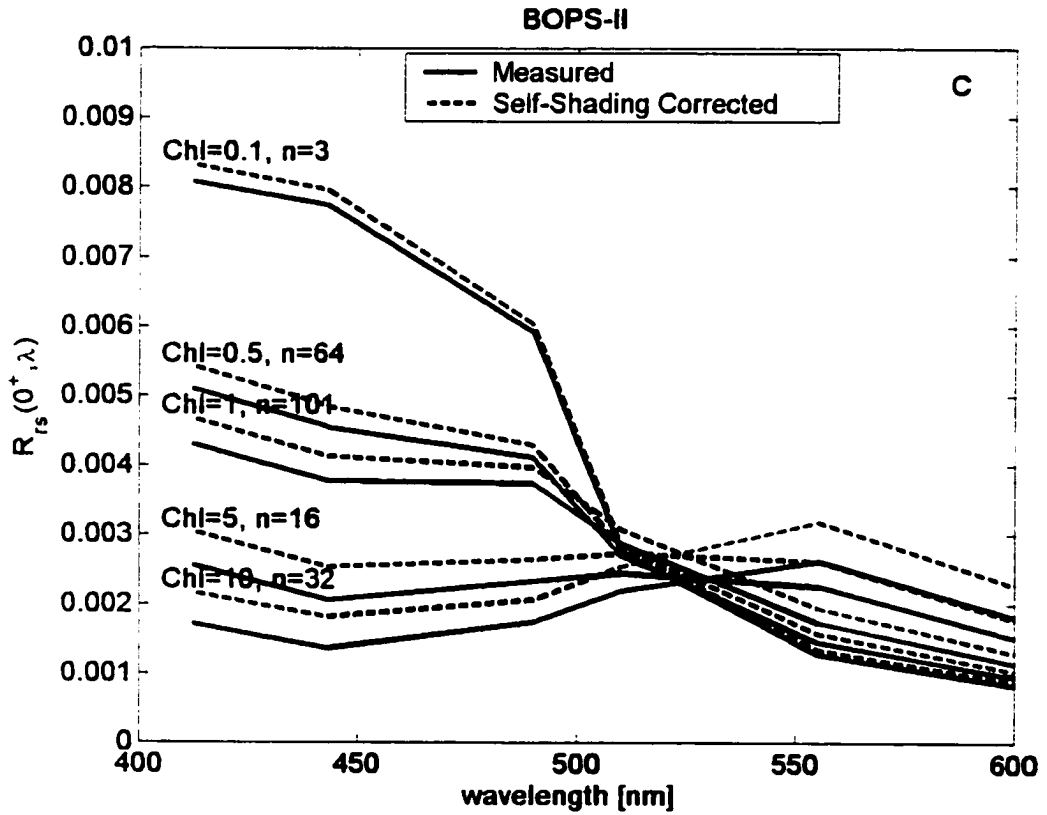


**Figure 2.** Median spectral measurements of  $R_{rs}(0^+, \lambda)$  for various concentrations of chlorophyll ( $\approx 20\%$ ) using data from: A) PRR; B) OFFI; C) BOPS-II measured and self-shading corrected.

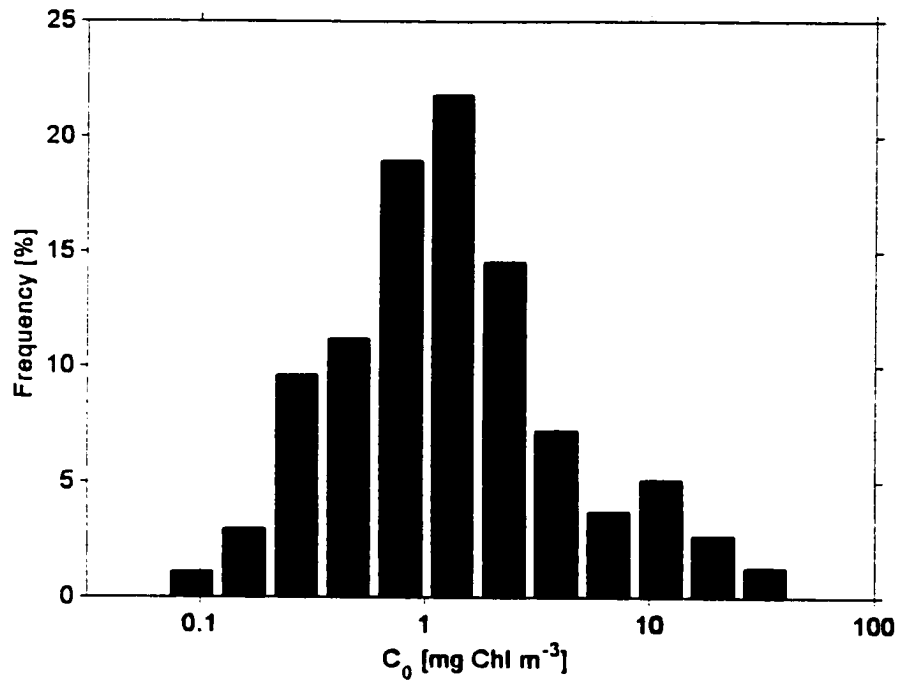
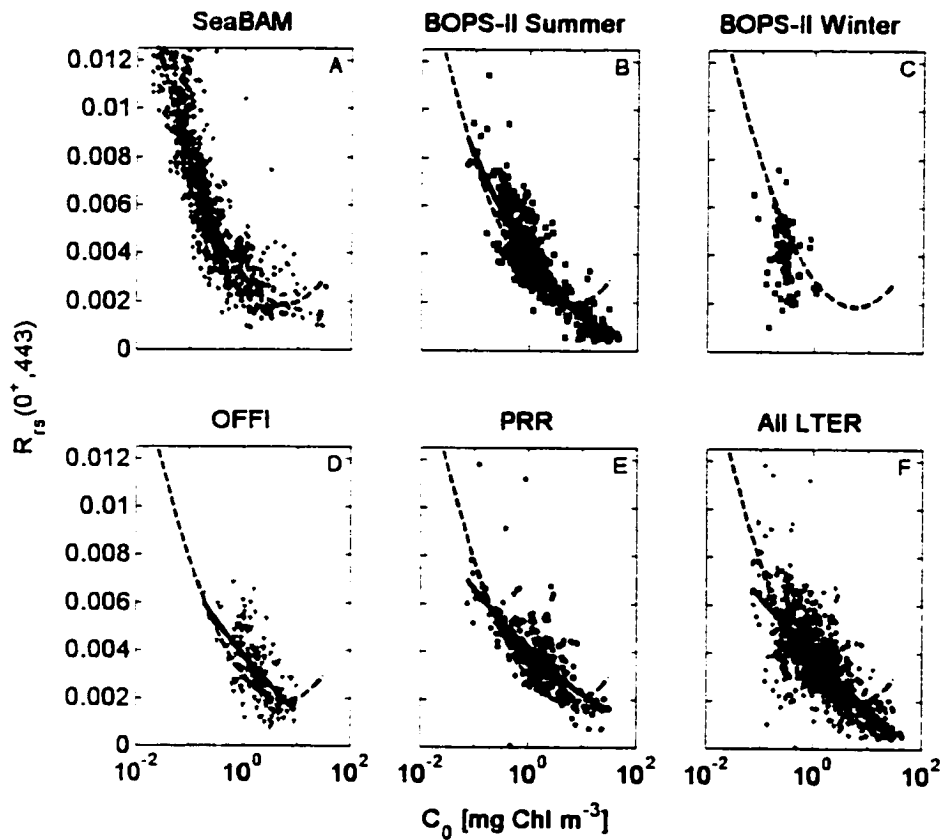


Figure 3. Lognormal frequency distribution of all LTER surface chlorophyll concentrations.



**Figure 4.** Surface chlorophyll versus  $R_{rs}(0^+,443)$  for A) SeaBAM; B) BOPS-II summer (December – March); C) BOPS-II winter (April-November); D) OFFI; E) PRR; F) All LTER data. On all panels, solid line is best fit to plotted data and dotted line is best fit to SeaBAM data derived in Panel A. No best fit was possible for Panel C.

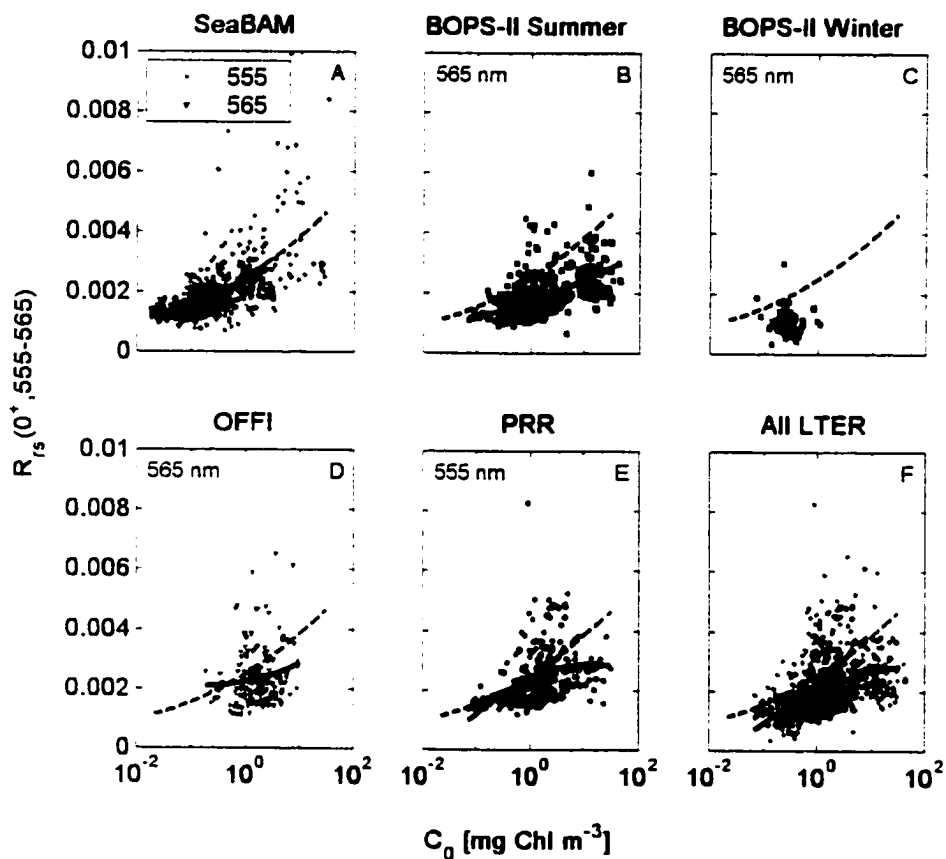
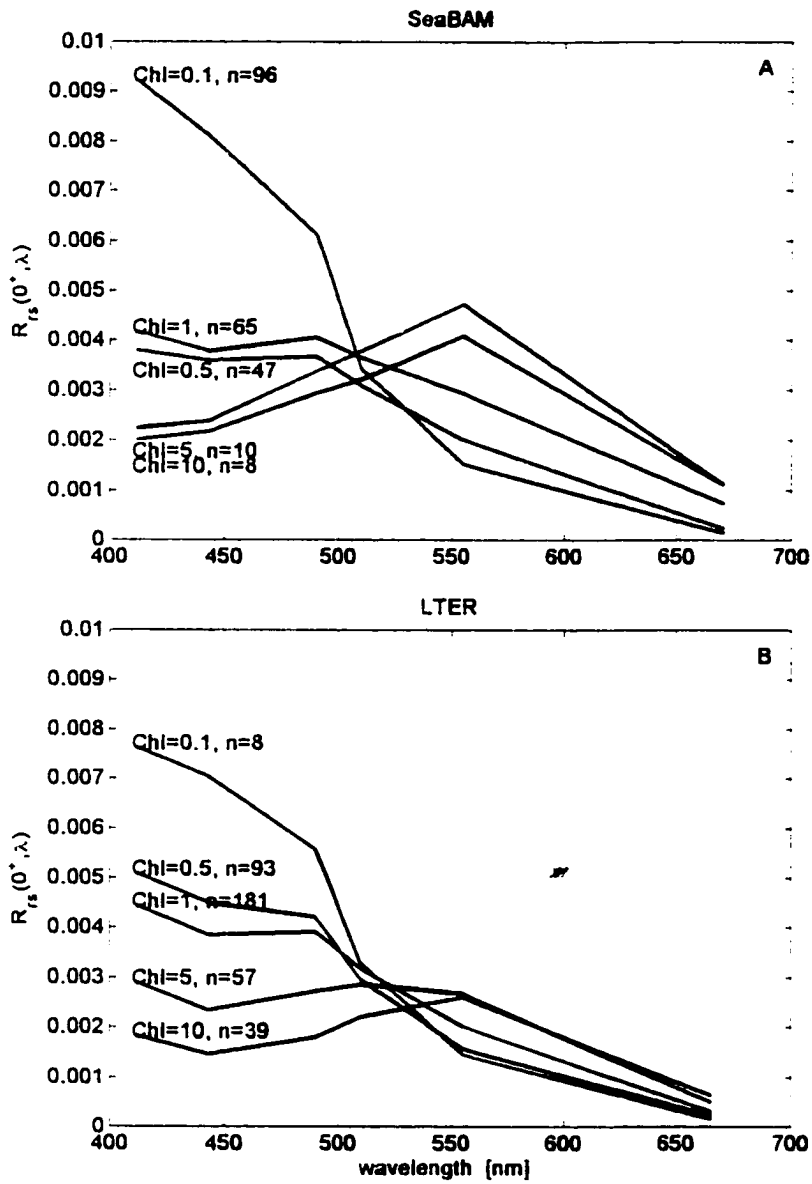
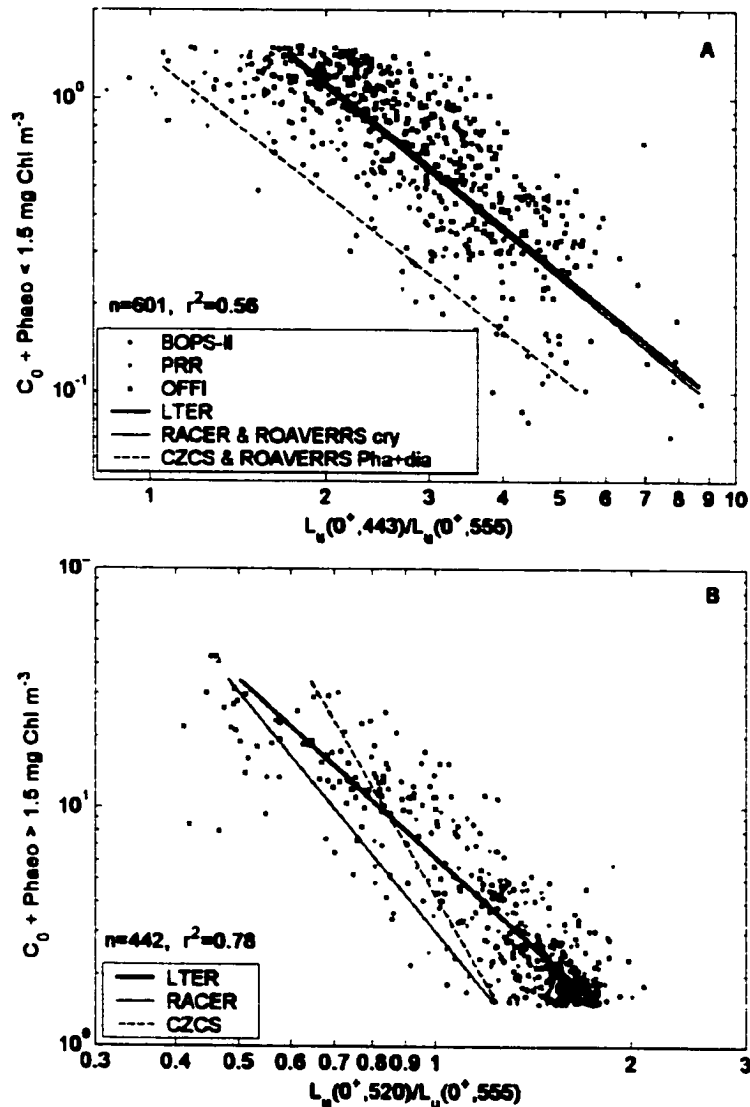


Figure 5. Same as Figure 4, except for a different wavelength,  $R_{rs}(0^+, 555)$ . BOPS-II and OFFI data (panels B-D) are  $R_{rs}(0^+, 565)$ .



**Figure 6.** Median spectral measurements of  $R_{rs}(0^+, \lambda)$  for various concentrations of chlorophyll ( $\approx 20\%$ ) using data from: A) SeaBAM; B) LTER.



**Figure 7.** Water-leaving radiance ratios used in the CZCS general processing algorithm. A) The ratio of  $L_u(443)/L_u(555)$  for chlorophyll and phaeopigment concentrations less than  $1.5 \text{ mg Chl m}^{-3}$ . B) The ratio  $L_u(520)/L_u(555)$  for chlorophyll concentrations greater than  $1.5 \text{ mg Chl m}^{-3}$ . The thick solid lines are the best-fit line for all LTER data and the dotted lines represent the general processing CZCS algorithms [Gordon and Morel, 1983]. The RACER data is from Antarctic Peninsula waters [Mitchell and Holm-Hansen, 1991]. The ROAVERRS data is from the Ross Sea [Arrigo et al., 1998], where cry=cryptophytes, Pha=*Phaeocystis Antarctica* and dia=diatoms.



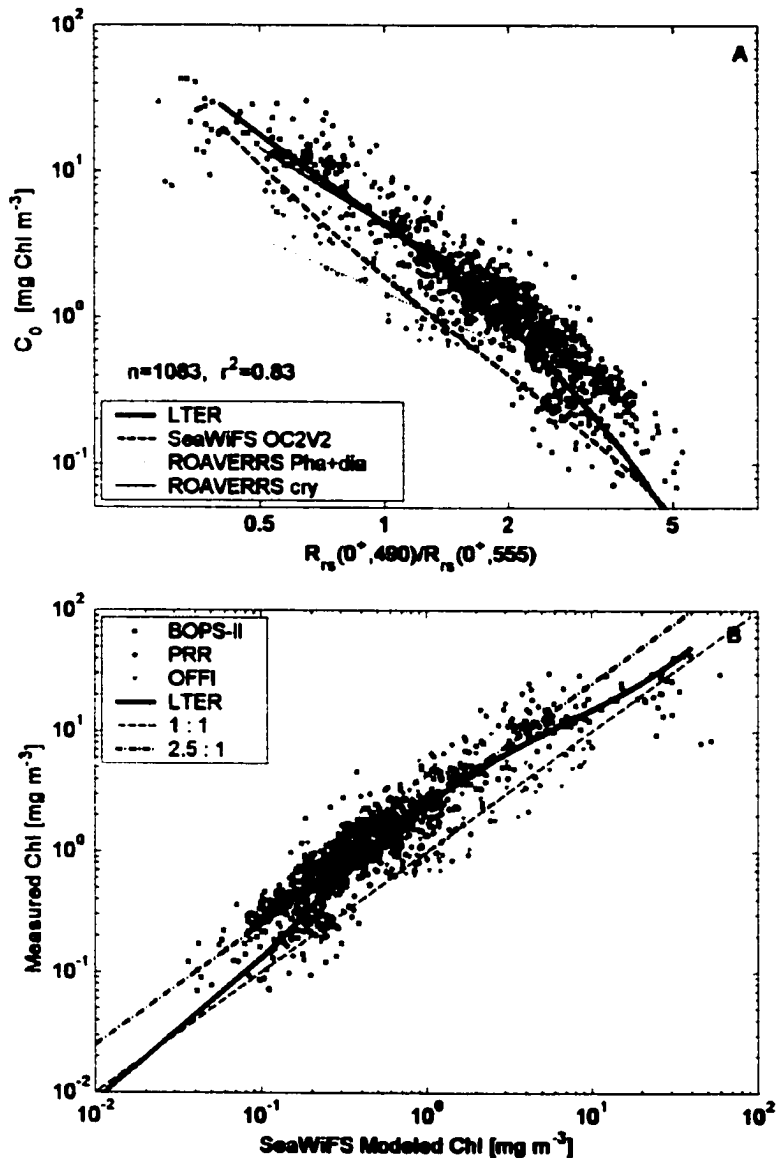


**Figure 8.** A) Chlorophyll concentrations versus  $R_{rs}(490)/R_{rs}(555)$  for the three LTER instruments. The thick solid line is the best fit regression line for all LTER data. Also shown are the OC2V2 algorithm used for SeaWiFS and Ross Sea ROAVERRS algorithms from Arrigo [1998], where cryp=cryptophytes, Pha=*Phaeocystis Antarctica* and dia=diatoms. B) Measured chlorophyll versus chlorophyll modeled using OC2V2 algorithm. The dashed line presents the 1:1 correlation line. Note the similarity between the 2.5:1 line (dot-dashed line) and the best fit regression line (solid line).

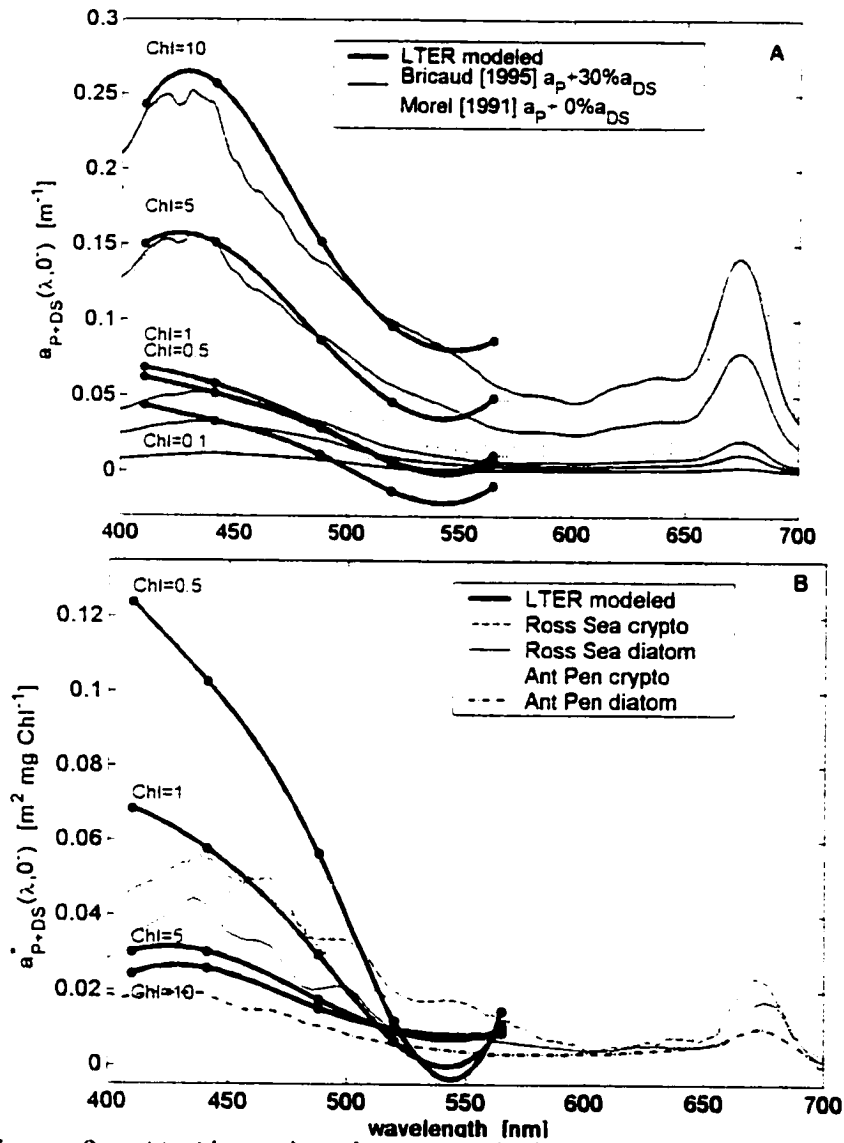


**Figure 9.** A) Absorption due to particulates and dissolved organic matter  $a_{P+DS}(\lambda, 0')$ , estimated from the BOPS-II data using *Gershun's Law* (Eq. 8) and subtracting  $a_w$  [Pope and Fry, 1997]. Modeled estimates of  $a_{P+DS}(\lambda, 0')$  from *Bricaud et al.* [1995] and *Morel* [1991]. Mean standard deviation is  $\pm 0.032$ . B) Pigment-specific absorption,  $a^*_{P+DS}(\lambda, 0')$ , for different chlorophyll concentrations. Ross Sea data from [Arrigo et al., 1998] and Antarctic Peninsula data from [Brody et al., 1992].

### **Chapter 3**

#### **Optimizing models for remotely estimating primary production in Antarctic Coastal Waters**

Dierssen, H.M.<sup>1</sup>, M. Vernet<sup>2</sup>, R.C. Smith<sup>1</sup>

<sup>1</sup>Department of Geography  
Institute for Computational Earth System Science  
University of California at Santa Barbara  
Santa Barbara, California 93106

<sup>2</sup>Marine Research Division  
Scripps Institution of Oceanography  
University of California, San Diego  
La Jolla, California 92093

Dierssen, H.M., R.C. Smith, and M. Vernet, Optimizing models for remotely estimating primary production in Antarctic coastal waters. *Antarctic Science*. 12 (1), 20-32, 2000.

## Abstract

Primary productivity and associated biogeochemical fluxes within the Southern Ocean are globally significant, sensitive to change and poorly known compared to temperate marine ecosystems. This relative lack of knowledge, as well as the inaccessibility, large area and often severe environmental conditions are compelling reasons for the study and optimization of models to estimate phytoplankton production remotely. We present seasonal time series data of chlorophyll, primary productivity and in-water irradiance measured in the coastal waters of the Western Antarctica Peninsula and build upon existing models to provide a more optimum parameterization for the estimation of primary productivity in Antarctic coastal waters. These and other data provide strong evidence that bio-optical characteristics and phytoplankton productivity in Antarctic waters are different than in temperate waters. For these waters we show that over 60% of the variability in primary production can be explained by the surface chlorophyll concentration alone, a characteristic, which lends itself to remote sensing models. If chlorophyll concentrations are accurately determined, then the largest source of error (13-18%) results from estimates of the photoadaptive variable ( $P_{opt}^B$ ). Further, the overall magnitude of  $P_{opt}^B$  is low (median  $1.09 \text{ mg C mg Chl}^{-1} \text{ h}^{-1}$ ) for these data compared to other regions and generally fits that expected for a cold water system. However, the variability of  $P_{opt}^B$  over the course of a season ( $0.4$  to  $3 \text{ mg C mg Chl}^{-1} \text{ h}^{-1}$ ) is not consistently correlated with other possible environmental parameters, such as chlorophyll, sea surface temperature, incident irradiance, day length, salinity, or taxonomic composition. Nonetheless, by tuning a standard depth-integrated primary productivity model to fit representative  $P_{opt}^B$  values and the relatively uniform chlorophyll-normalized production profile found in these waters, we can improve the model to account for approximately 72-73% the variability in

primary production both for these LTER data as well as independent historic Antarctic data for this area.

## Introduction

In order to better understand and quantify global oceanic primary productivity and the flux of carbon in the world's ocean, considerable effort has been directed towards developing satellite algorithms to model this production. Such algorithms may be used to estimate the rate of primary productivity from the concentration of biomass in a water column using different scales of integration (e.g., depth, time, and wavelength). Aside from the simplest empirical correlation between chlorophyll and primary productivity (Smith *et al.*, 1982), all primary productivity models generally invoke some photoadaptive variable that varies linearly with biomass concentration (e.g., the maximum carbon fixation rate within a water column  $P_{opt}^B$ , water-column averaged light utilization  $\psi$ , etc.). Recently, Behrenfeld and Falkowski (1997a) have shown that given the same biomass concentrations, much of the error in primary productivity models is associated with uncertainties in the photoadaptive variable and not with the specific structure of the algorithm. These workers suggest that improvements in productivity algorithm performance will depend less on improved mathematical formulations and more on improved understanding of phytoplankton ecology and photoadaptive variability (Longhurst *et al.*, 1995; Antoine *et al.*, 1996; Behrenfeld and Falkowski, 1997b).

Not only are Antarctic coastal waters much colder than temperate waters, the annual range of temperature variability is relatively small (-2 to +2°C). However, the Antarctic ecosystem is characterized by large variations in solar radiation both on a daily and seasonal basis. Water column stability and the opposing influence of high winds and consequent deep mixing are also highly

variable and have long been recognized as an important controlling factor for phytoplankton biomass buildup (Hart, 1934; Mitchell and Holm-Hansen, 1991; Nelson and Smith, 1991; Priddle *et al.*, 1994). Indeed, wind forcing, atmospheric variability, sea ice and snow cover, and changing ocean optical properties combine to cause a highly variable light regime for Antarctic phytoplankton. In spite of often unfavorable conditions, high biomass concentrations ( $> 30 \text{ mg Chl m}^{-3}$ ) have been observed (Hart, 1934; El-Sayed, 1978; Smith *et al.*, 1996a).

How the Antarctic phytoplankton respond to this variable environment, both on a daily and seasonal basis, remains a key question in our attempt to understand primary productivity in this region. Past research has shown that the phytoplankton are generally adapted to the low light and low temperatures (El-Sayed, 1978; Tilzer *et al.*, 1986; Smith and Sakshaug, 1990; Smith *et al.*, 1996a), but the phytoplankton ecology and inherent variability in photoadaptation is far from understood. The efficiency of how phytoplankton use light for primary production is determined both by the extent to which aquatic plants succeed in competing with the other components of the system for quanta and by the efficiency with which the absorbed light energy is converted to chemical energy. Here we make use of a time series of biological and optical data collected in conjunction with the Palmer Long-Term Ecological Research (LTER) project (Smith *et al.*, 1995) to: (1) investigate the underlying causes of photoadaptive variability of phytoplankton over the course of the growing season; (2) evaluate the relative accuracy of productivity models; and (3) inquire how best to parameterize a productivity model so as to enhance model performance in Antarctic coastal waters.

## Methods

We analyze time series data obtained in 1994-95 and 1995-96 from two in-shore stations (B and E) near Palmer Station, Antarctica (64° 46'S; 64° 03'W) and from a larger area, the Palmer LTER large scale study grid, during a January-February 1995 cruise (Fig. 1). Nearshore sampling was conducted weekly from approximately November to the end of March (weather and ice permitting) for both field seasons at stations B and E (Waters and Smith, 1992). Samples were collected at depths corresponding to the following percent surface irradiance as measured using a LICOR 193-SA Quantum Sensor: 100%, 55%, 27%, 11%, 5%, and 2%. Duplicate productivity samples were estimated for each light level by 24-hour simulated *in situ* incubations with <sup>14</sup>C-bicarbonate (Vernet *et al.*, 1996). The temperature of the incubations was maintained using the seawater intake system both at Palmer Station and during the cruise. For Palmer station, the seawater is collected from the harbor near the station and is representative of the SST within the near shore sampling grid. The SST at stations B and E is quite similar over the course of the season (mean standard deviation between stations of 0.30°C and demonstrate a general warming trend over the course of the season (discussed below). For the cruise data, the temperature of the incubations is that of the water through which the ship is traveling and may not always represent the SST from which the phytoplankton were collected, but is accurate to  $\pm 2^\circ\text{C}$ .

Total chlorophyll was quantified from filtered samples (Millipore HA filters) using standard fluorometric techniques on a digital Turner Fluorometer (Smith *et al.*, 1981). Chlorophyll *a* (Chl) was calculated by subtracting phaeopigment concentration determined by sample acidification. All samples were analyzed within 2-3 days of collection. Additional algal pigments were determined by using high-performance liquid chromatography with a gradient



system and a reverse-phase C-18 column (Kozłowski *et al.*, 1995). The taxonomic composition was determined by analyzing the ratio of specific pigments to Chl. The concentration of fucoxanthin (Fuco) was used to indicate diatoms, alloxanthin (Allo) for cryptophytes, chlorophyll *b* (Chl *b*) for green algae, and the sum of 19'-hexanoyloxyfucoxanthin and 19'-butanoyloxyfucoxanthin for chromophytes (Hex + But). Multiple regression was performed on the pigment concentrations ( $\text{mg m}^{-3}$ ) of the surface waters (depths corresponding to 100% and 55% light levels) against Chl concentrations for both 1994-95 and 1995-96 seasons (Bidigare *et al.*, 1986; Gieskes *et al.*, 1988; Claustre *et al.*, 1997). The equation used was:

$$\text{Chl}(a) = 1.58\text{Fuco} + 3.28\text{Allo} + 0.56(\text{Hex} + \text{But}) + 2.33\text{Chl}(b) \quad (1)$$

We assume that multicollinearity of the input variables was negligible. This method only approximates dominant taxonomic groups in a phytoplankton assemblage.

We also compiled a set of historical Chl and primary productivity data collected primarily from the Antarctic Peninsula region from 1972-1990 (Smith *et al.*, 1996a; Behrenfeld and Falkowski, 1997b). The historical dataset consists of a relatively large number of Chl observations ( $n=438$ ) and a smaller subset of both Chl and primary productivity with sufficient ancillary data to generate depth-integrated values ( $n=86$ ) within the euphotic zone. When the euphotic depth ( $Z_{eu}$ ) was not provided for the data, we estimated  $Z_{eu}$  to the 2% light level using a relationship developed from the LTER data ( $r^2=0.37$ ,  $p<0.01$ ):

$$Z_{eu} = 46.8C_0^{-0.36} \quad (2)$$

The reliability of historical phytoplankton production data is of some concern.

especially data collected subsequent to the mid 1980's when "clean" techniques were not in use. Martin et al (1990) suggest that clean techniques are most important in open oligotrophic regions where iron is limiting (Martin *et al.*, 1990). As most of the data we discussed was obtained in coastal waters where iron is not considered to be as limiting, we would expect little difference between "clean" and "classical" techniques for the data presented here. These historical data are discussed in detail by Smith *et al.* (1996a).

Downwelling photosynthetically available radiation (400-700 nm) at the ocean surface,  $E_d(0^+, 400-700)$ , is estimated for each 24-hour incubation period using measurements taken from a spectroradiometer located at Palmer Station (Booth *et al.*, 1995). This instrument provided hourly measurements of downwelling light integrated from 400-600 nm. Irradiance is then extrapolated out to 700 nm using a site-specific modeled relationship between irradiance integrals from 400-600 versus 400-700 nm:

$$E_d(0^+, 400 - 700) = 1.42 E_d(0^+, 400 - 600) - 1.15 \quad (3)$$

This relationship has been derived using the atmospheric radiative transfer model SBDart (Gautier and Frouin, 1992) with different modeled cloud layers, surface albedos, and solar zenith angles. These estimates of  $E_d(0^+)$  are highly correlated with measurements of scalar  $E_0(0^+)$  made using a Biospherical Instrument QSR250 located near the primary productivity incubators at Palmer Station ( $r^2 = 0.82$ ; data not shown). For the ship incubations, this correlation was used to estimate  $E_d(0^+, 400-700)$  from the scalar measurements of  $E_0(0^+)$  made from a QSR250 onboard ship.

A method of evaluating the relationship between rates of primary productivity and the *in situ* irradiance (P vs. E) is to treat the water column as a

compound photosynthetic system and estimate P vs. E parameters for the entire water column (Talling, 1957; Behrenfeld and Falkowski, 1997b). This approach is different from P vs. E curves measured under conditions of constant irradiance, because the productivity for each sample is measured under irradiance conditions that can vary from light-limiting to photoinhibiting over the course of an incubation. These in-water P vs. E curves have different physiological interpretations and terminology than the short-term P vs. E curves (see Table I for terminology used throughout this paper). Vollenweider (1996) and, more recently, Behrenfeld and Falkowski (1997b) have discussed the differences between parameters used in time-integrated models and photosynthesis-irradiance variables (Vollenweider, 1966; Behrenfeld and Falkowski, 1997a). Measured values of productivity normalized by Chl,  $P_z^B$ , are normalized to the Chl-specific maximum rate of water column photosynthesis,  $P_{opt}^B$ , and modeled as a function of the daily irradiance using the P vs. E equation (Platt and Sathyendranath, 1988; Behrenfeld and Falkowski, 1997b):

$$\frac{P_z^B}{P_{opt}^B} = \frac{P_s^B}{P_{opt}^B} \left( 1 - \exp\left(-\frac{E_z}{E_{max}}\right) \right) \exp(-\beta E_z) \quad (4)$$

where  $E_z$  is the irradiance at a given optical depth.  $E_{max}$  is the irradiance at the inflection point between light limitation and light saturation in the absence of photoinhibition.  $P_s^B$  is the maximum normalized productivity in the absence of photoinhibition, and  $\beta_d$  is the variable slope for surface photoinhibition. Daily production was converted to hourly production using the photoperiod. Equation (4) is the same as Behrenfeld and Falkowski (1997b), but explicitly contains the factor of  $P_s^B$  to  $P_{opt}^B$  required for proper scaling of the model. The observed patterns of

$P_z^B$  were fit to Eq. (4) using a Gauss-Newton non-linear curve fitting routine with Levenburg-Marquardt modifications (Zimmerman *et al.*, 1987) Model II regression techniques (Laws and Archie, 1981) were utilized throughout this manuscript in cases where both the independent and the dependent variable were subject to natural variability.

## Results and Discussion

### *Distribution of chlorophyll and primary production*

Water column integrated values for both Chl ( $C_{cu}$ ) and daily primary production ( $PP_{cu}$ ) over the 1994-95 and 1995-96 field seasons at the inshore stations B and E are shown in Fig. 2. As shown, Chl and  $PP_{cu}$  are highly correlated throughout the season. Both biomass and productivity show significant interannual variability with 1995-96 levels being higher than the 1994-95 levels. For the 1994-95 field season at Palmer Station, the median  $C_{cu}$  is 69 mg Chl  $m^{-2}$  and ranges from 22 to 280 mg Chl  $m^{-2}$ . The median  $PP_{cu}$  is 1.0 g C  $m^{-2} d^{-1}$  and ranges from 0.3 to over 4 g C  $m^{-2} d^{-1}$ . For 1995-96, the median  $C_{cu}$  is 101 mg Chl  $m^{-2}$  and ranges from 20 up to 600 mg Chl  $m^{-2}$  and the median  $PP_{cu}$  is 1.5 g C  $m^{-2} d^{-1}$  and ranges from 0.13 to over 6 g C  $m^{-2} d^{-1}$ . Because biomass and productivity are lognormally distributed and blooms occur infrequently, the median values for  $C_{cu}$  and  $PP_{cu}$  are significantly lower than the mean values. Fig. 2 also shows that both years of data typically display two to three phytoplankton blooms during each growing season. One bloom generally occurs in January with additional blooms occurring in fall and/or spring. These blooms persist for approximately one to two weeks. This general pattern also was observed in earlier time series data from these stations (Moline and Prezelin, 1996).

Vertical profiles of Chl, productivity, and Chl-normalized productivity

( $P^B_z$ ) for the Palmer nearshore and offshore LTER data are shown in Fig. 3a-c. The profiles have been normalized to the mean value in the profile and the shaded area represents one standard deviation from the mean. In general, the vertical structure of all three variables shows a maxima at or near the surface and a gradual decrease with depth. Also, the vertical structure of Chl (Fig. 3a) is fairly uniform within the top two optical depths of the water column. Thus, the highest concentrations of Chl are generally well within the layer of water that can be remotely sensed by an ocean color satellite (i.e., one optical depth which is shown by the dotted lines in Figs. 3) (Gordon and McGluney, 1975; Smith, 1981). Because the vertical structure of Chl within the water column is fairly consistent amongst all profile data, the surface concentrations of Chl ( $C_0$ ) explains nearly 84% of the integrated water column Chl variance with a log-log regression (Fig. 4), such that:

$$C_{eu} = 42.7C_0^{-0.66} \quad (5a)$$

This relationship is nearly identical both to that determined with the historical data and estimated using Eq. 2. Lines 2 and 3 on Fig. 4 show almost identical relationships to Eq. 5a. However, these relationships differ significantly from that developed previously for high latitudes (Morel and Berthon, 1989), which underestimates integrated Chl (Fig. 4, line 5).

We also compared these results to relationships developed using chlorophyll integrated to 50 m,  $C_{50}$ , and found them also to be very similar (Holm-Hansen and Mitchell, 1991). As expected,  $C_{50}$  underestimates  $C_{eu}$  for low Chl concentrations and overestimates  $C_{eu}$  for high Chl concentrations (data not shown), such that:

$$C_{50} = 2.17 C_{cu}^{0.75} \quad (5b)$$

While Chl concentrations can remain high at depths beneath the euphotic zone (Holm-Hansen and Mitchell, 1991), generally the highest biomass concentrations are found near the surface where most of the primary production occurs. For these waters, the euphotic zone is generally found within the wind mixed layer, which is consistent with a more uniform vertical profile of Chl.

Primary productivity generally peaks at an optical depth of 0.6 or when approximately 50-55% of the incoming  $E_d(0^+)$  has been attenuated (Fig 3b). Hence, the rates of primary production at the surface appear to be photoinhibited when compared to the rates at the 55% light level. However, this peak generally occurs within the top optical depth of the water column, well within the depth from which a satellite signal can be received. The presence of a  $C_0$  and primary productivity maxima is consistent with past findings in this region of the Southern Ocean (Smith *et al.*, 1996a). The daily profile of  $PP_{cu}$  decreases more rapidly with depth than either the Chl or Chl-normalized productivity profiles.

When productivity is normalized to Chl, photoperiod and optical depth ( $P^B_{\zeta}$ ), the vertical profile still exhibits the same basic shape as the productivity profile (Fig. 3c). When compared to the vertical structure of data collected from all of world's oceans (Behrenfeld and Falkowski, 1997b), the actual profiles of normalized productivity for the Palmer data are both much more uniform with depth and of a lower magnitude than for the global data (Fig. 5a). The shaded region in Fig. 5a represents the normalized productivity data used in the global productivity algorithm developed by Behrenfeld and Falkowski (1997a, Fig. 1b). As shown, the  $P^B_{\zeta}$  profiles for the Antarctic data peak around  $1 \text{ mg C mg Chl}^{-1}$

$\text{h}^{-1}$ , which is significantly lower than for other oceanic waters. Both the shape and the magnitude of the LTER data shown in Fig. 5a have significant implications for modeling primary productivity in Antarctic waters.

If the median of the Palmer nearshore and offshore Chl-normalized productivity data from Fig. 5a (white squares) are plotted against the corresponding percent transmission of incident irradiance, this relatively uniform vertical structure can be transformed into a type of time-integrated P vs. E curve representing the water column. As shown in Fig. 5b, this curve has a steep slope indicative of a relatively low  $E_k^*$ , rising to a  $P_{\text{opt}}^B$  above  $0.9 \text{ mg C mg Chl}^{-1} \text{ h}^{-1}$ , followed by a gradual decreasing slope indicative of photoinhibition.  $E_k^*$  is defined as the irradiance at the inflection point between light limitation and light saturation observed from measured  $P_{\zeta}^B$  in the water column. On average,  $E_k^*$  occurs when approximately 7% of the surface light remains ( $E_k^*/E_0 = 0.07$ ). Because  $E_k^*$  generally occurs deep within the water column, much of the daily production occurs at irradiance levels above  $E_k^*$ . In other words, Chl-normalized productivity does not decrease as rapidly with depth as it does for phytoplankton from other regions of the world. Having both a low  $E_k^*$  and  $P_{\text{opt}}^B$  is characteristic of phytoplankton that are adapted to low-light conditions and/or low water temperatures and is consistent with past studies from this region (Smith and Sakshaug, 1990; Holm-Hansen and Mitchell, 1991; Smith *et al.*, 1996b).

For these Antarctic waters, the median  $P_{\text{opt}}^B$  for our data set is  $1.09 \text{ mg C mg Chl}^{-1} \text{ h}^{-1}$ , with  $P_{\text{opt}}^B$  varying by nearly a factor of seven over the course of a season. Fig. 6 shows a time series of  $P_{\text{opt}}^B$  as it varies over the course of the 1994-95 and 1995-96 field seasons, respectively. The  $P_{\text{opt}}^B$  measured for stations B and E have been averaged (shading represents one standard deviation

from the mean) and are highly variable over the course of a season. As shown in Fig. 6, no obvious seasonal trend is evident in  $P_{opt}^B$  for the two field seasons. For 1994-95,  $P_{opt}^B$  approaches 1.5 in late December to early January and are less than 1 both before and after this period. For 1995-96,  $P_{opt}^B$  is high (approaching 2) from November through December and then closer to 1 throughout the remainder of the year. Additionally, the variability in  $P_{opt}^B$  over the course of a season does not appear to follow the corresponding variability in productivity (Fig. 2b), nor does it follow the seasonal variability in water temperature, which shows a general warming trend throughout the season (Fig. 6). For example,  $P_{opt}^B$  is low for the 1994-95 mid-January phytoplankton bloom, relatively high for the early 1995-96 bloom, and only average for the late 1995-96 bloom. Both the lower magnitude of  $P_{opt}^B$  and the more uniform vertical structure of normalized productivity are discussed below in the context of primary productivity models.

#### *Environmental influence on photoadaptation*

Behrenfeld and Falkowski (1997a,b) have shown that model performance in estimating depth-integrated primary productivity is critically dependent on the ability to accurately represent the space/time variability of the photoadaptive parameter,  $P_{opt}^B$ , and suggest that model improvement will depend upon a mechanistic understanding of how environmental variability affects the physiological state of phytoplankton assemblages. While Chl explains most of the variability in  $PP_{eu}$ , variability in  $P_{opt}^B$  and the vertical distribution of the Chl-normalized productivity can also significantly impact estimates of  $PP_{eu}$ . Here we seek to identify environmental variables that may explain the variability in these parameters and emphasize those that may be remotely sensed and could potentially allow more accurate modeling of  $PP_{eu}$ .



from remotely sensed biomass.

As photosynthesis is the result of an enzymatically controlled rate process, it is sensitive to ocean temperatures (Tilzer *et al.*, 1986). Recent estimates of global ocean primary production have used sea surface temperature (SST) to predict the magnitude of a photoadaptive variable (Antoine and Morel, 1996; Behrenfeld and Falkowski, 1997b). Such an approach is advantageous because SST can be determined remotely and used to delimit biogeochemical provinces for global modeling. Antarctic phytoplankton south of the polar front live in the coldest surface waters, with temperatures from nearly -2 to 2° C. While some thermal adaptation may occur,  $P_{opt}^B$  ranges from 0.4 - 3 mg C (mg Chl)<sup>-1</sup> h<sup>-1</sup>, which is in the range expected for a cold water system (Smith *et al.*, 1996b). However, within this limited temperature range, no significant relationship appears to exist between SST and  $P_{opt}^B$  for our nearshore and offshore data (Figs. 6 and 7). The polynomial model described by Behrenfeld and Falkowski (1997a) (Fig. 7) tends to overestimate  $P_{opt}^B$  for the temperatures between 0 and 2° C and  $P_{opt}^B$  varies by a factor of seven within this temperature range. The poor fit of the global model to this low temperature range is not surprising since this is the temperature range where the global data set showed the greatest variability. Indeed, as shown in Fig. 7, no temperature trend within this low temperature range is evident in either our Palmer or cruise data.

We also investigated several other environmental factors that may influence the variability in  $P_{opt}^B$  and may be remotely sensed. However, no single parameter or group of parameters that we analyzed (e.g.,  $E_d(0^-)$ , SST, Chl, daylength, cloud ratio, salinity, mixed layer depth) produces a statistically significant relationship to  $P_{opt}^B$ . Furthermore, considering the variables together only explained up to 20% of the variability in  $P_{opt}^B$  using multiple regression. We considered that variable light histories might influence the  $P_{opt}^B$  of the

phytoplankton, but found no relationship between  $E_d(0^+)$  from days prior to the incubation. We also analyzed whether Antarctic phytoplankton blooms were correlated to sea surface salinity based upon water column stability from melting sea ice and coastal glaciers, but no discernible relationship was found. Past findings from this region also found that photosynthesis-irradiance parameters were poorly correlated to physical forcing and nutrient regimes (Moline *et al.*, 1998).

Because different species of phytoplankton in this region have different carbon to Chl ratios (C:Chl) and pigment-specific absorption coefficients (Brody *et al.*, 1992), some of the variability in  $P_{opt}^B$  could be due to the presence of different bloom forming phytoplankton (e.g., diatoms vs. cryptophytes). Fig. 8a and 8b show  $P_{opt}^B$  for sampling events from the inshore Palmer data when the phytoplankton were mainly diatoms (high in fucoxanthin/Chl ratio) and mainly cryptophytes (high in alloxanthin/Chl ratio), respectively. Fig. 8c shows the relationship between  $P_{opt}^B$  and  $C_0$  for all of the Palmer data regardless of taxonomic composition. As shown, cryptophytes are estimated to be the dominant taxa (>60%) in the water column less frequently than diatoms. Moreover, the very large blooms ( $C_0 > 10 \text{ mg Chl m}^{-3}$ ) tend to be diatom blooms. Cryptophytes cover a smaller range in  $P_{opt}^B$  and have a median value of 1.20 and a standard deviation of  $0.47 \text{ mg C mg Chl}^{-1} \text{ h}^{-1}$ . The range in  $P_{opt}^B$  is greater for the diatoms, which vary from  $0.9\text{-}2.44 \text{ mg C mg Chl}^{-1} \text{ h}^{-1}$ , but there is no statistically significant difference between  $P_{opt}^B$  for the two taxa. In addition to the more numerous diatom blooms, another reason for the larger range in  $P_{opt}^B$  could be because different species of diatoms can be either larger or smaller than cryptophytes, which may contribute to different internal ratios of C:Chl. Over the course of a season, the dominant diatom taxa at Palmer Station can vary to include both large and small diatoms, which will similarly cause variance in

$P_{opt}^B$ . Such a difference may not be as evident from data collected over a restricted time period (Brody *et al.*, 1992). While  $P_{opt}^B$  tends to decrease with increasing  $C_0$  on all three panels (Fig. 8a-c), the concentration of  $C_0$  is not a good predictor of  $P_{opt}^B$  because  $P_{opt}^B$  still varies by a factor of seven for low Chl concentrations.

Another parameter that also plays a role in modeling primary productivity is the relationship of  $P_{opt}^B$  to the mean Chl-normalized productivity ( $P_Z^B$ ). The function  $F$  is used to describe the loss in potential photosynthesis due to light limitation and photoinhibition and can be estimated as the ratio of the mean  $P_Z^B$  with depth versus  $P_{opt}^B$  (Wright, 1959; Behrenfeld and Falkowski, 1997a). While  $F$  does not explain much of the variability in  $PP_{eu}$  (<2%),  $F$  is a linear term in the model and hence is important in determining the overall magnitude of primary production. In the absence of photoinhibition,  $F$  should demonstrate an irradiance-dependence such that the  $F$  function is lower when  $E_d(0^-)$  is low (more of the water column is light-limited), and  $F$  approaches a maximum when  $E_d(0^-)$  is high (more of the water column is light-saturated) (Behrenfeld and Falkowski, 1997a). Because the vertical structure of Chl-normalized productivity for these Antarctic data are much more uniform with depth (Fig. 5), the phytoplankton are operating close to  $P_{opt}^B$  throughout much of the water column and consequently  $F$  is higher (mean of 0.64) for these Antarctic data than the mean of 0.55 estimated for the global dataset (Behrenfeld and Falkowski, 1997a).

The  $F$  parameter is commonly compared to the ratio of  $E_d(0^-)$  to  $E_K^*$ , the light intensity corresponding to the intersection between the light-limited slope of primary productivity in the water column and  $P_{opt}^B$  (Fig. 9a). While our  $F$  is higher than that derived from the global dataset (Behrenfeld and Falkowski,

1997a), it is lower than the theoretical derivation of  $F$  assuming no photoinhibition (Talling, 1957). Because  $E_K^*$  is low and often occurs near the bottom of the euphotic zone, the range of  $E_d(0^+)/E_K^*$  extends to much higher values than previously published (i.e., >25). The tight correlation shown in Fig 9a is expected because the vertical profile of Chl-normalized production, and thereby  $F$ , can be derived from the photosynthesis-irradiance parameters used to describe the water column (i.e.,  $E_K^*$ ). However, this relationship (Fig. 9a) cannot be used to model  $F$  because either  $E_K^*$  or the ratio  $E_d(0^+)/E_K^*$  must be known *a priori*. As shown in Fig. 9b,  $E_K^*$  is not readily estimated from  $E_d(0^+)$  for these data.  $E_K^*$  varies between 0 and 8  $\text{Ein m}^{-2} \text{d}^{-1}$  and displays little relationship to  $E_d(0^+)$ . The dashed line on Fig. 9b was developed for the global dataset (Behrenfeld and Falkowski, 1997a) and does not fit these data. It is possible that this lack of correlation could be due to the extremely variable light environment to which these phytoplankton are exposed.

The relationship between  $F$  and  $E_d(0^+)$  (Fig. 9c), however, is statistically significant ( $p < 0.01$ ), although it explains little of the variability in  $F$  ( $r^2 = 0.23$ ). We derive the following empirical relationship:

$$F = \frac{E_d(0^+)}{E_d(0^+) + 11.77} \quad (6)$$

#### *Optimization of primary productivity model*

Behrenfeld and Falkowski (1997a) have shown that, in general, depth-integrated models can be reduced to a relationship describing depth-integrated primary productivity from phytoplankton biomass ( $C_{eu}$ ), a photoadaptive

variable ( $P_{opt}^B$ ), an irradiance-dependent function ( $F$ ), and daylength ( $D$ ). Further, they show that depth-integrated productivity models are fundamentally synonymous and most of the variability in estimating primary productivity involved differences in the input biomass and estimate of photoadaptive variability. Hence, more complex primary productivity models, involving additional levels of integration (i.e., time, wavelength, depth), are not likely to explain significantly more of the variability in primary productivity until the photoadaptive variability is better characterized. As discussed above, in investigating the environmental influences on photoadaptive variability, we found no consistent predictor or set of predictors that could be used to reliably predict  $P_{opt}^B$  for these Antarctic waters.

We utilize the standard depth-integrated model structure (Behrenfeld and Falkowski, 1997b) and tune the model to fit the Antarctic data (both the cruise data and the inshore Palmer data):

$$PP_{eu} = P_{opt}^B D C_0 Z_{eu} F \quad (7)$$

For our parameterization of the model, we use  $F$  estimated from  $E_d(0^+)$  (Eq. 6), the median value for  $P_{opt}^B$  ( $1.09 \text{ mg C mg Chl}^{-1} \text{ h}^{-1}$ ), and  $Z_{eu}$  derived from  $C_0$  (Eq. 2). Using measured values of  $C_0$  and  $E_d(0^+)$ , this model explains nearly 72% of the variability in the data on a log scale and closely follows a 1:1 correspondence line (Fig. 10a). If we further simplify the model and use a constant  $F$  of 0.64, the model only loses 5% of predictive capability. Because the median  $P_{opt}^B$  ( $1.01 \text{ mg C mg Chl}^{-1} \text{ h}^{-1}$ ) for the large blooms is very similar to the median  $P_{opt}^B$  ( $1.09 \text{ mg C mg Chl}^{-1} \text{ h}^{-1}$ ) from all nearshore and offshore LTER data, our model is more effective for days with extremely high  $PP_{eu}$ . This is important because a significant fraction of seasonal production occurs under

high bloom conditions.

In addition to applying this model to the LTER data from which it was derived, we also applied it to historic primary productivity data from the Antarctic (Fig. 10b). The historic data shown here were collected in the Antarctic Peninsula region and South Indian Sector of the Southern Ocean from 1972-1990 (Smith et al., 1996a). When irradiance data was not available within this data set, a constant  $F$  of 0.64 was used in the model instead of Eq. 6. Even without irradiance data, the model performed just as well on the historic data as on the LTER data and explained 73% of the variability in  $PP_{eu}$ . Moreover, we find nearly a 1:1 correspondence between the measured and modeled data ( $m=1.02$ ,  $b=-0.11$ ). It will be of interest to test the model for other regions of the Southern Ocean.

Table II presents a comparison of our model parameterization (Eq. 7) with various published algorithms. The VGPM model developed for the global oceans (Behrenfeld and Falkowski, 1997b) in its original form explains approximately 61% of the variability for the Antarctic data and tends to overestimate productivity for low  $PP_{eu}$  and underestimate for high  $PP_{eu}$ . In fact, for these waters it explains less of the variability in  $PP_{eu}$  than a simple regression on  $C_0$ . We believe this is primarily due to three sources of error when applying the model to Antarctic waters: (1) the equation relating  $P_{opt}^B$  and SST overpredicts  $P_{opt}^B$  at  $SST > 1^\circ C$  (Fig. 7); (2) the  $F$  function is generally underestimated (Fig. 9); and (3) the relationship (Morel and Berthon, 1989) used to estimate  $Z_{eu}$  generally underestimates  $C_{eu}$  (Fig. 4).

Using measured  $C_0$  and a constant light utilization index ( $\psi$ ), (Morel, 1991), the Laboratoire de Physique et Chimie Marines (LPCM) model (Antoine et al., 1996) explains 69% of the variability in the data. For these data,  $\psi$  (which

is related to the water column averaged functional absorption cross-section for photosynthetic carbon fixation  $\psi^*$ ) varies from 0.2 to 2 and has a median value of  $0.56 \text{ mg C m}^{-2} \text{ d}^{-1} (\text{mg Chl m}^{-2} \text{ Ein m}^{-2} \text{ d}^{-1})^{-1}$ . This is higher than that estimated for temperate waters and near the average  $\psi$  determined previously for this region (Claustre *et al.*, 1997). The parameter  $\psi$  can be related to  $P_{\text{opt}}^{\text{B}}$  by the following equation:

$$\psi = \frac{P_{\text{opt}}^{\text{B}} D F}{E_d(0^*)} \quad (8)$$

Because  $P_{\text{opt}}^{\text{B}}$  and  $F$  can nearly be approximated as constants for this region (Figs. 7 and 9), using a photoadaptive variable that represents the entire water column ( $\psi$ ) is nearly as effective as modeling with more specific formulations of  $P_{\text{opt}}^{\text{B}}$  and  $F$ . Moreover, because  $P_{\text{opt}}^{\text{B}}$  and  $\psi$  are so closely related, the possible environmental influences discussed in the previous section are applicable to both photoadaptive variables and no environmental predictors of  $\psi$  were found (data not shown).

The simplest primary productivity model is a log-linear regression between rates of primary production and Chl. Consistent with earlier reports for Antarctic waters (Minas and Minas, 1992; Moline and Prezelin, 1996; Smith *et al.*, 1996a), biomass seems to be a relatively good proxy for primary productivity (Fig. 11). For the LTER data, the best-fit relationship between  $C_0$  and  $PP_{\text{eu}}$  explains approximately 62% of the variability in  $PP_{\text{eu}}$ . As shown in Fig. 11, the lines labeled 1-3 are all from data collected in the Antarctic and are quite distinct from line 4, which is from low latitudes in the Atlantic (Falkowski *et al.*, 1998). If the low latitude regression were used for high latitude Antarctic data,  $PP_{\text{eu}}$  would be overestimated at low  $C_0$  and underestimated at high  $C_0$ .

This is likely a result of the more uniform Chl distribution with depth found in Antarctic waters. If Chl is low at the surface, then it remains low throughout the water column (i.e., few deep Chl maxima) and similarly if Chl is high at the surface, it remains high throughout the water column. Our tuned depth-integrated model (Eq. 7) explains only 10% more of the variability in  $PP_{eu}$  than this simple Chl regression. Thus, the accuracy of any depth-integrated primary productivity model for this region is primarily dependent on determining the appropriate biomass concentration and the correct relationship between  $PP_{eu}$  and  $C_{eu}$ .

### Conclusions

Using time series data of chlorophyll and daily net primary production measured in the coastal waters of Palmer Station, Antarctica, we have evaluated models to estimate photoadaptive variability and rates of primary production for Antarctic coastal waters. Over 62% of the variability in  $PP_{eu}$  ( $\text{mg C m}^{-2} \text{d}^{-1}$ ) can be explained by Chl alone (Fig. 2). Only 10% more of the variability in primary productivity (72%) can be explained by using measured  $C_0$  and  $E_d(0^{\tau})$  with site-specific parameterizations of the standard depth integrated model (Behrenfeld and Falkowski, 1997a). Our parameterization of the model (Eq. 7) takes into account three factors that are unique to this region compared to other regions (Behrenfeld and Falkowski, 1997b): (1) higher integrated Chl concentration predicted from  $C_0$  (Fig. 4); (2) low magnitude of  $P_{opt}^B$  (Fig. 5); and, (3) more uniform distribution of Chl-normalized productivity, which is manifested in the model by a higher F function (Fig. 9). Not only does this model parameterization perform well on the LTER data from which it was derived, it also explains 73% of the variability in the historic  $PP_{eu}$  data collected in these



waters (Fig. 10).

A better understanding of  $P_{opt}^B$  could potentially improve the model and explain up to 13% more of the variability in  $PP_{cu}$ . While low,  $P_{opt}^B$  still varies by a factor of seven during the course of a season (Figs. 6). However, no single parameter or group of parameters (e.g., SST,  $E_d(0^T)$ , Chl, daylength, cloud ratio, salinity, mixed layer depth) was found to be a significant predictor of  $P_{opt}^B$ . Contrary to expectation, we found no significant relationship between SST and  $P_{opt}^B$  (Fig. 7) although, as expected,  $P_{opt}^B$  is low compared to global values. In this region, phytoplankton exist in very cold waters and over a relatively restricted range (-2 to 2° C). Furthermore, both diatoms and cryptophytes exhibit a fairly large range in  $P_{opt}^B$  (Fig. 8), such that no significant difference was found in the magnitude of  $P_{opt}^B$  between these two taxa. Under very large bloom conditions ( $C_0 > 10 \text{ mg Chl m}^{-3}$ ), the phytoplankton in Antarctic coastal waters tend to be diatoms and generally exhibit a lower range of  $P_{opt}^B$  centered near the median value of  $1.09 \text{ mg C mg Chl}^{-1} \text{ h}^{-1}$ .

An interesting result of this analysis is that irradiance seems to play a very limited role in estimating  $PP_{cu}$  and only improves the performance of our primary productivity model by 5%. Furthermore, very little correlation was evident between surface irradiance and the photoadaptive variables,  $P_{opt}^B$  and  $F$ . If these parameters are dependent on enzymatic activity, their variability may depend on temperature and nutrient availability and not adaptations to light (Prezelin *et al.*, 1991). Previous experiments on phytoplankton from the cold and often well-mixed waters of the Antarctic have shown them to have slower cellular responses than their temperate counterparts. For example, Antarctic phytoplankton exhibit low respiration rates (Tilzer *et al.*, 1986), slow growth

rates (Nelson and Smith. 1991), and an absence in ability to repair damage to photosynthetic systems due to UV exposure (Neale *et al.*. 1998). Further understanding of the variability in these photoadaptive parameters could lead to improvements in the primary production model.

### **Acknowledgements**

This research was supported by NASA Training Grants NGT-40005 (California Space Institute) and NGT5-30063 (Earth System Science Fellowship) to H. Dierssen, National Science Foundation grants OPP90-11927 and OPP-96-32763 to R. Smith and M. Vernet, and NASA grant NAGW 290-3 to R. Smith. We thank Janice Jones, Wendy Kozlowski, Antarctic Support Associates, and the captain and crew of RV *Polar Duke* for their efforts in data collection. We also wish to acknowledge Karen Baker, Sharon Stammerjohn and Charleen Johnson for their help in data processing and manuscript preparation.

## References

- Antoine, D. and Morel, A. 1996. Oceanic primary production: 1) Adaptation of a spectral light-photosynthesis model in view of application to satellite chlorophyll observations. *Global Biogeochemical Cycles*, **10**, 43-55.
- Antoine, D., Andre, J. M. and Morel, A. 1996. Oceanic primary production: 2. Estimation at global scale from satellite (coastal zone color scanner) chlorophyll. *Global Biogeochemical Cycles*, **10**, 57-69.
- Behrenfeld, M. J. and Falkowski, P. G. 1997a. Consumers guide to phytoplankton primary productivity models. *Limnology and Oceanography*, **42**, 1479-1491.
- Behrenfeld, M. J. and Falkowski, P. G. 1997b. Photosynthetic rates derived from satellite-based chlorophyll concentration. *Limnology and Oceanography*, **42**, 1-20.
- Bidigare, R. R., Frank, T. J., Zastrow, C. and Brooks, J. M. 1986. The distribution of algal chlorophylls and their degradation products in the Southern Ocean. *Deep-Sea Research*, **33**, 923-937.
- Booth, C. R., Lucas, T. B., Mestechkina, R., Tusson, J. R., Neuschuler, D. A. and Morrow, J. H. 1995. NSF Polar Programs UV Spectroradiometer Network 1993-1994 Operations Report.eds. . San Diego, CA: Biospherical Instruments, Inc., 167.
- Brody, E., Mitchell, B. G., Holm-Hansen, O. and Vernet, M. 1992. Species-dependent variations of the absorption coefficient in the Gerlache Strait. *Antarctic Journal*, **27**, 160-162.
- Claustre, H., Moline, M. A. and Prezelin, B. B. 1997. Sources of variability in the column photosynthetic cross section for Antarctic coastal waters.

*Journal of Geophysical Research*, **102**, 25047-25060.

- El-Sayed, S. Z. 1978. Primary productivity and estimates of potential yields of the Southern Ocean. In M. A. McWhinnie, eds. *Polar Research: To the Present, and the Future*, vol. 7. Boulder, Colorado: Westview Press. 141-160.
- Falkowski, P. G., Behrenfeld, M. J., Esaias, W. E., Balch, W., Campbell, J. W., Iverson, R. L., Kiefer, D. A., Morel, A. and Yoder, J. A. 1998. Satellite primary productivity data and algorithm development: a science plan for mission to planet earth. In S. B. Hooker and E. R. Fireston, eds. *SeaWiFS Technical Report Series, NASA TM-1998-104566*, vol. 42. Greenbelt, Maryland: NASA/GSFC, Code 970.2, 36.
- Gautier, C. and Frouin, R. 1992. Net surface solar irradiance variability in the central equatorial Pacific during 1982-1985. *Journal of Climate*, **5**, 30-55.
- Gieskes, W. W. C., Kraay, G. W., Montji, A., Setiapermana, D. and Sumtumo. 1988. Monsoonal alternation of a mixed and alyaired structurein the phytoplankton of the euphotic zone of the Banda Sea (Indonesia): a mathematical analysis of algal pigment fingerprints. *Netherlands Journal of Sea Research*, **22**, 123-137.
- Gordon, H. R. and McGluney, W. R. 1975. Estimation of the depth of sunlight penetration in the sea for remote sensing. *Applied Optics*, **14**, 359-361.
- Hart, T. J. 1934. On the phytoplankton of the south-west Atlantic and the Bellingshausen Sea. 1929-31. *Discovery Reports*, **8**, 1-268.
- Holm-Hansen, O. and Mitchell, B. G. 1991. Spatial and temporal distribution of phytoplankton and primary production in the western Bransfield Strait region. *Deep-Sea Research*, **38**, 961-980.
- Kozlowski, W., Lamerdin, S. K. and Vernet, M. 1995. Palmer LTER:

- Predominance of cryptomonads and diatoms in Antarctic coastal waters. *Antarctic Journal of the United States*, **30**, 267-268.
- Laws, E. A. and Archie, J. W. 1981. Appropriate use of regression analysis in marine biology. *Marine Biology*, **65**, 13-16.
- Longhurst, A., Sathyendranath, S., Platt, T. and Caverhill, C. 1995. An estimate of global primary productivity in the ocean from satellite radiometer data. *Journal of Plankton Research*, **17**, 1245-1271.
- Martin, J. H., Gordon, R. M. and Fitzwater, S. E. 1990. Iron in Antarctic waters. *Nature*, **345**, 156-158.
- Minas, H. J. and Minas, M. 1992. Net community production in "high nutrient-low chlorophyll" waters of the tropical and Antarctic Oceans. *Oceanologica Acta*, **15**, 145-162.
- Mitchell, B. G. and Holm-Hansen, O. 1991. Observations and modeling of the Antarctic phytoplankton crop in relation to mixing depth. *Deep-Sea Research*, **38**, 961-1007.
- Moline, M. A. and Prezelin, B. B. 1996. Long-term monitoring and analyses of physical factors regulating variability in coastal Antarctic phytoplankton biomass, in situ productivity, and taxonomic composition over subseasonal, seasonal, and interannual time scales. *Marine Ecology-Progress Series*, **145**, 143-160.
- Moline, M. A., Schofield, O. and Boucher, N. P. 1998. Photosynthetic parameters and empirical modelling of primary production: A case study on the Antarctic Peninsula shelf. *Antarctic Science*, **10**, 45-54.
- Morel, A. and Berthon, J. F. 1989. Surface pigments, algal biomass profiles and potential production of the euphotic layer: relationships re-investigated in view of remote sensing applications. *Limnology and Oceanography*, **34**, 1545-1562.

- Morel, A. 1991. Light and marine photosynthesis: a spectral model with geochemical and climatological implications. *Progress in Oceanography*, **26**, 263-306.
- Neale, P. J., Davis, R. F. and Cullen, J. J. 1998. Interactive effects of ozone depletion and vertical mixing on photosynthesis of Antarctic phytoplankton. *Nature*, **392**, 585-589.
- Nelson, D. M. and Smith, W. O. 1991. Sverdrup revisited: Critical depths, maximum chlorophyll levels, and the control of Southern Ocean productivity by the irradiance-mixing regime. *Limnology and Oceanography*, **36**, 1650-1661.
- Platt, T. and Sathyendranath, S. 1988. Oceanic primary production: Estimation by remote sensing at local and regional scales. *Science*, **241**, 1613-1620.
- Prezelin, B. B., Tilzer, M. M., Schofield, O. and Haese, C. 1991. The control of the production processes of phytoplankton by physical structure of the aquatic environment with special reference to its optical properties. *Aquatic Sciences*, **53**, 1015-1621.
- Priddle, J., Brandini, F., Lipski, M. and Thorley, M. R. 1994. Pattern and variability of phytoplankton biomass in the Antarctic Peninsula region: an assessment of the BIOMASS cruises. In S. Z. El-Sayed, eds. *Southern Ocean Ecology: the BIOMASS Perspective*. Cambridge: Cambridge University Press, 49-126.
- Smith, R. C. 1981. Remote sensing and depth distribution of ocean chlorophyll. *Marine Ecology Progress Series*, **5**, 359-361.
- Smith, R. C., Baker, K. S. and Dustan, P. 1981. *Fluorometer techniques for measurement of oceanic chlorophyll in the support of remote sensing*. San Diego: Visibility Laboratory, Scripps Institution of Oceanography. SIO Ref. 81-17.

- Smith, R. C., Eppley, R. W. and Baker, K. S. 1982. Correlation of primary production as measured aboard ship in southern California coastal waters and as estimated from satellite chlorophyll images. *Marine Biology*, **66**, 281-288.
- Smith, R. C., Baker, K. S., Fraser, W. R., Hofmann, E. E., Karl, D. M., Klinck, J. M., Quetin, L. B. and etc. 1995. The Palmer LTER: A long-term ecological research program at Palmer Station, Antarctica. *Oceanography*, **8**, 77-86.
- Smith, R. C., Dierssen, H. M. and Vernet, M. 1996a. Phytoplankton biomass and productivity in the Western Antarctic Peninsula Region. In R. M. Ross, E. E. Hofmann and L. B. Quetin, eds. *Foundations for Ecosystem Research West of the Antarctic Peninsula*. Washington D.C.: American Geophysical Union Antarctic Research Series, 333-356.
- Smith, R. C., Stammerjohn, S. E. and Baker, K. S. 1996b. Surface air temperature variations in the Western Antarctic Peninsula Region. In R. M. Ross, E. E. Hofmann and L. B. Quetin, eds. *Foundations for Ecosystem Research West of the Antarctic Peninsula*. Washington D.C.: American Geophysical Union Antarctic Research Series, 105-122.
- Smith, W. O. and Sakshaug, E. 1990. Polar Phytoplankton. In W. O. Smith, eds. *Polar Oceanography: Part B Chemistry, Biology and Geology*. San Diego: Academic Press, Inc. 477-526.
- Talling, J. 1957. The phytoplankton population as a compound photosynthetic system. *The New Phytologist*, **56**, 133-149.
- Tilzer, M. M., Elbrachter, M., Gieskes, W. W. and Beese, B. 1986. Light-temperature interactions in the control of photosynthesis in Antarctic phytoplankton. *Polar Biology*, **5**, 105-111.
- Vernet, M., Kozlowski, W. and Ruel, T. 1996. Palmer LTER: Temporal



- variability in primary productivity in Arthur Harbor during the 1994/1995 growth season. *Antarctic Journal of the United States*, **30**, 266-267.
- Vollenwieder, R. A. 1966. Calculation models of photosynthesis-depth curves and some implications regarding day rate estimates in primary production measurements. In C. R. Goldman, eds. *Primary productivity in aquatic environments*. Berkeley: University of California Press.
- Waters, K. J. and Smith, R. C. 1992. Palmer LTER: A sampling grid for the Palmer LTER program. *Antarctic Journal of the United States*, **27**, 236-239.
- Wright, J. C. 1959. Limnology of Canyon Ferry Reservoir: Phytoplankton standing crop and primary production. *Limnology and Oceanography*, **4**, 235-245.
- Zimmerman, R. C., SooHoo, J. B., Kremer, J. N. and D'Argenio, D. Z. 1987. Evaluation of variance approximation techniques for non-linear photosynthesis-irradiance models. *Marine Biology*, **95**, 209-215.

**Table 1. Terminology**

Parameter	Units	Description
Chl	Chl	chlorophyll <i>a</i>
$C_z$	mg Chl	measured chlorophyll <i>a</i> at depth <i>z</i>
$C_{eu}$	mg Chl m <sup>-2</sup>	water column chlorophyll <i>a</i> integrated to euphotic depth
$C_{50}$	mg Chl m <sup>-2</sup>	water column chlorophyll <i>a</i> integrated to 50 m
$C_{11}$	mg Chl m <sup>-3</sup>	surface chlorophyll <i>a</i>
$PP_{eu}$	mg C m <sup>-2</sup> d <sup>-1</sup>	water column primary productivity integrated to euphotic depth
$Z_{eu}$	m	euphotic depth
$D$	h	photoperiod
$E_d(0^+)$	Ein m <sup>-2</sup> d <sup>-1</sup>	daily downwelling irradiance (400-700 nm) incident upon the sea surface
$E_0(0^+)$	Ein m <sup>-2</sup> d <sup>-1</sup>	scalar irradiance (400-700 nm) incident upon the sea surface
$E_z$	Ein m <sup>-2</sup> d <sup>-1</sup>	daily downwelling irradiance at optical depth. $\zeta$
$E_{max}$	Ein m <sup>-2</sup> d <sup>-1</sup>	daily downwelling irradiance at the inflection between light limitation and light saturation in the absence of photoinhibition
SST	°C	sea surface temperature
$P_z^B$	mg C mg Chl <sup>-1</sup> d <sup>-1</sup>	Chl-normalized primary productivity by discrete depth
$p_z^B$	mg C mg Chl <sup>-1</sup> d <sup>-1</sup>	Chl-normalized primary productivity by optical depth
$P_{opt}^B$	mg C mg Chl <sup>-1</sup> h <sup>-1</sup>	Chl-normalized maximum rate of photosynthesis normalized by photoperiod for the water column
$P_s^B$	mg C mg Chl <sup>-1</sup> h <sup>-1</sup>	Chl-normalized maximum rate of photosynthesis normalized by photoperiod in the absence of photoinhibition for the water column
$\alpha$	mg C mg Chl <sup>-1</sup> h <sup>-1</sup> ( $\mu\text{Ein m}^{-2} \text{s}^{-1}$ ) <sup>-1</sup>	Chl-specific rate of light-limited photosynthesis in the water column
$\beta_d$	( $\mu\text{Ein m}^{-2} \text{s}^{-1}$ ) <sup>-1</sup>	Photoinhibition slope for the water column
$E^*_K$	$\mu\text{Ein m}^{-2} \text{s}^{-1}$	saturation parameter of photosynthesis for the water column
$F$	(dimensionless)	ratio of mean chl-normalized productivity in the water column to $P_{opt}^B$
$\psi$	mg C m <sup>-2</sup> d <sup>-1</sup> (mg Chl m <sup>-2</sup> Ein m <sup>-2</sup> d <sup>-1</sup> ) <sup>-1</sup>	light utilization index

**Table 2.** Statistical comparison of measured versus modeled daily primary production

Model	Formulation	Regression Statistics <sup>1</sup>		Source
		r <sup>2</sup>	m,b	
Antarctic Model <sup>2</sup>	$PP_{cu} = P_{opt}^B D Z_{cu} C_0 F$	0.72	0.96, 0.1	[Eq. 6]
	<i><math>C_0</math></i>	<i>0.62</i>		
	<i><math>Z_{cu}</math></i>	<i>0.28</i>		
	<i><math>P_{opt}^B</math></i>	<i>0.18</i>		
	<i><math>F</math></i>	<i>0.02<sup>3</sup></i>		
	<i><math>D</math></i>	<i>0.02</i>		
VGPM Model	$PP_{cu} = P_{opt}^B D Z_{cu} C_0 F$	0.61	0.92, 0.2	[Behrenfeld & Falkowski 1997a]
LPCM Model	$PP_{cu} = \psi Z_{cu} C_0 E_d(0^-)$	0.69	1.06, -0.2	[Antoine et al. 1996]
Chl Regression	$PP_{cu} = 513 C_0^{0.725}$	0.62	1.0, 0	[Fig. 10]

<sup>1</sup> log-linear regressions were performed using Model II regression techniques (Laws and Archie 1981), where r<sup>2</sup>=correlation coefficient, m=slope, b=intercept of regression.

<sup>2</sup> Each component of this model was individually regressed against PP<sub>cu</sub>, as presented in italics below.

<sup>3</sup> For this parameter, linear regression had a higher correlation to PP<sub>cu</sub> than a log-linear regression.

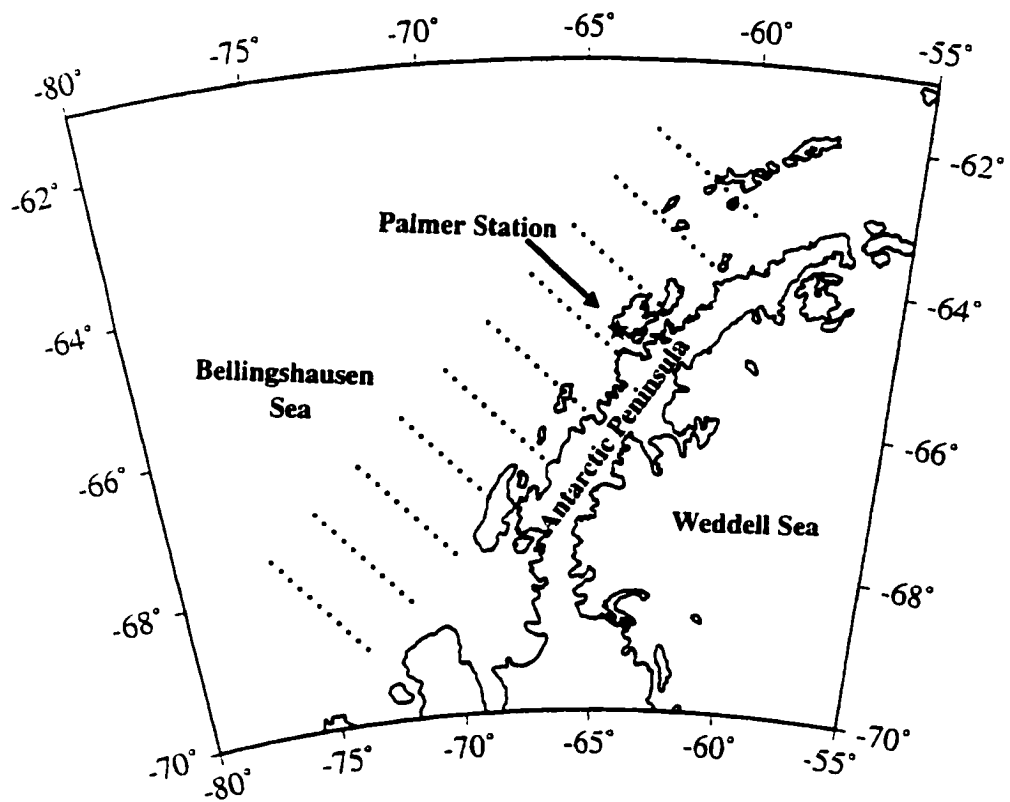


**Figure 1.** Location of Palmer Station and the LTER grid in reference to the Antarctic Peninsula.

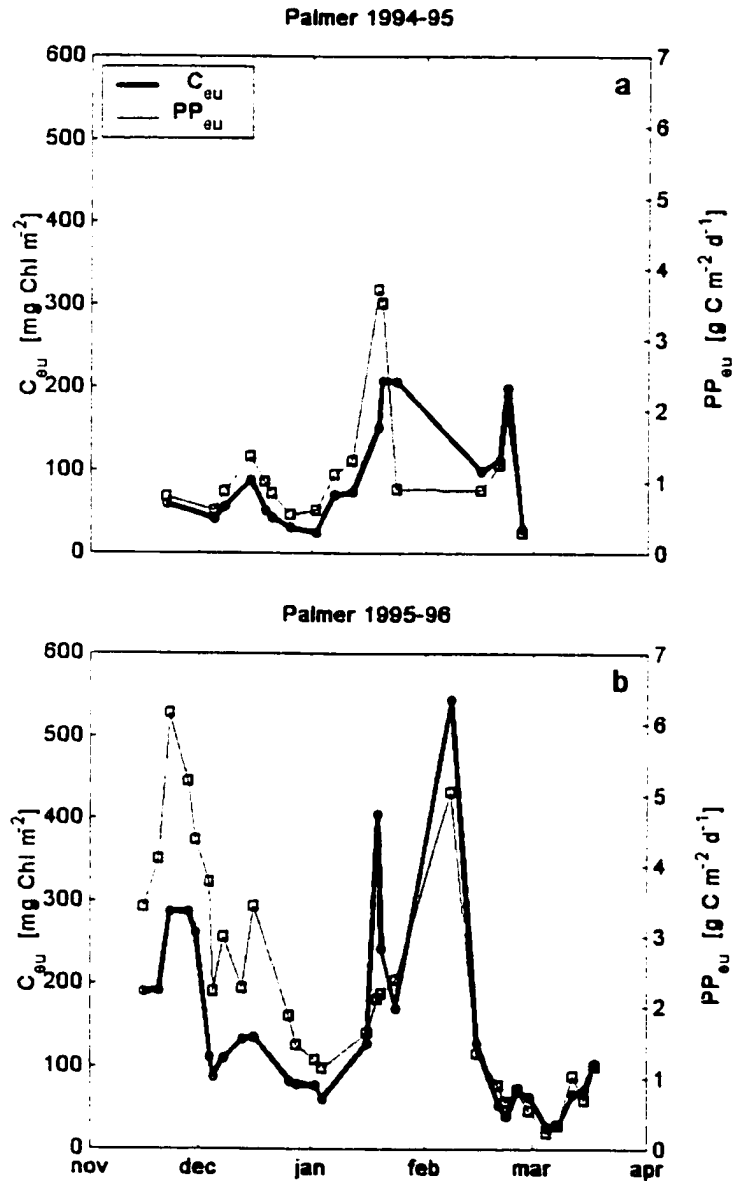


**Figure 2.** Distribution of water column integrated Chl and water column integrated daily primary production for: **a.** 1994-95 season; **b.** 1995-96 season. The data from stations B and E have been averaged. The mean standard deviation between these stations is  $25 \text{ mg Chl m}^{-2}$  for  $C_{eu}$  and  $0.35 \text{ g C m}^{-2} \text{ d}^{-1}$  for  $PP_{eu}$ .

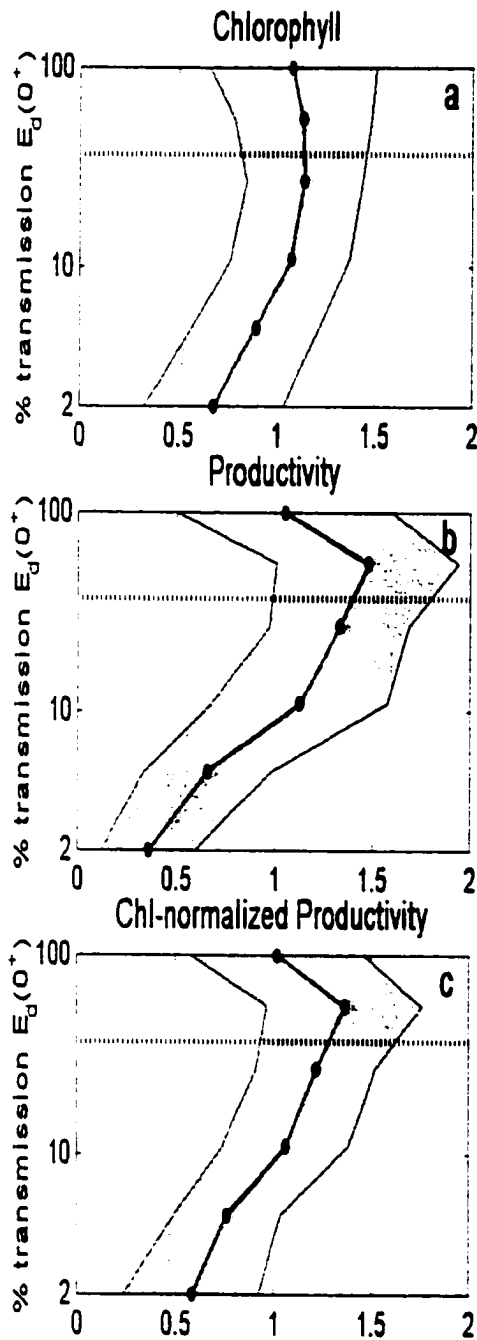


**Figure 3.** Mean vertical profiles of 177 stations from the Palmer nearshore and offshore area. Data have been normalized by the average concentration within the euphotic zone and are unitless. Shaded area represents one standard deviation from the mean and the dotted line represents the penetration depth of an ocean color sensor (i.e., 1 optical depth). **a.** Chl; **b.** Productivity; **c.** Chl-normalized productivity.

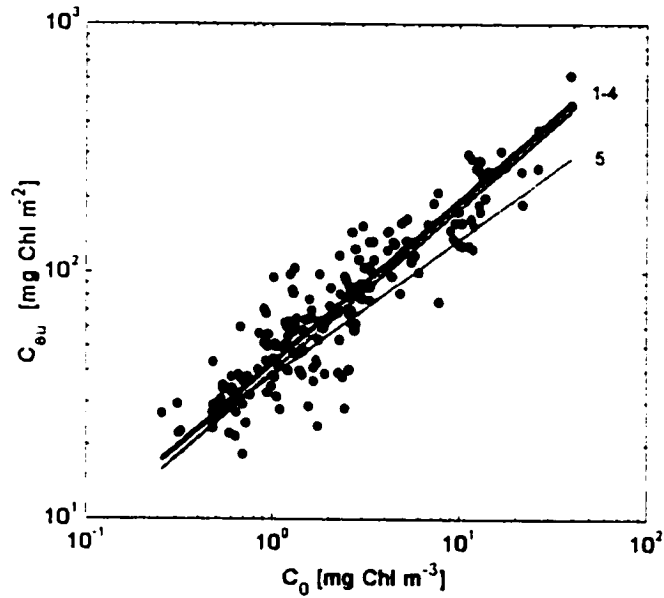


**Figure 4.** Relationship between the surface Chl concentrations ( $C_0$ ) and the water-column integrated Chl concentration ( $C_{eu}$ ). Numbered lines represent: 1) these data  $C_{eu} = 42.7 C_0^{0.66}$  ( $n=185$ ,  $r^2 = 0.84$ ); 2) Historic data; 3)  $C_0 \times Z_{eu}$  (Eq. 2); 4) Holm-Hansen and Mitchell (1991) using Eq. 5b to convert  $C_{50}$  to  $C_{eu}$ ; 5) Morel and Berthon 1989 for high latitudes.

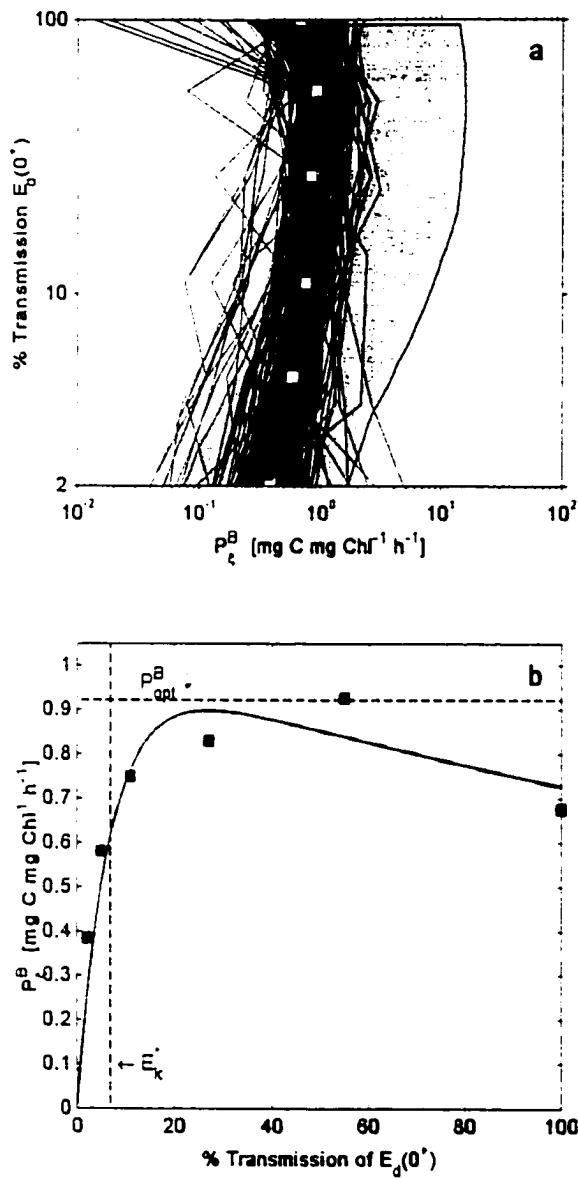


**Figure 5. a.** Vertical profiles of Chl-normalized productivity for the Antarctic data. Shaded region represents the data used in the global productivity algorithm developed by Behrenfeld and Falkowski (1997a, fig. 1b, p. 5). White squares represent the median for the Antarctic data.

**b.** Datapoints are the median vertical profile from Fig. 5a plotted against the corresponding percent transmission of incident light. These are time-integrated P vs E parameters representing the entire water column and the line represents the fit to the data using Eq. 4.



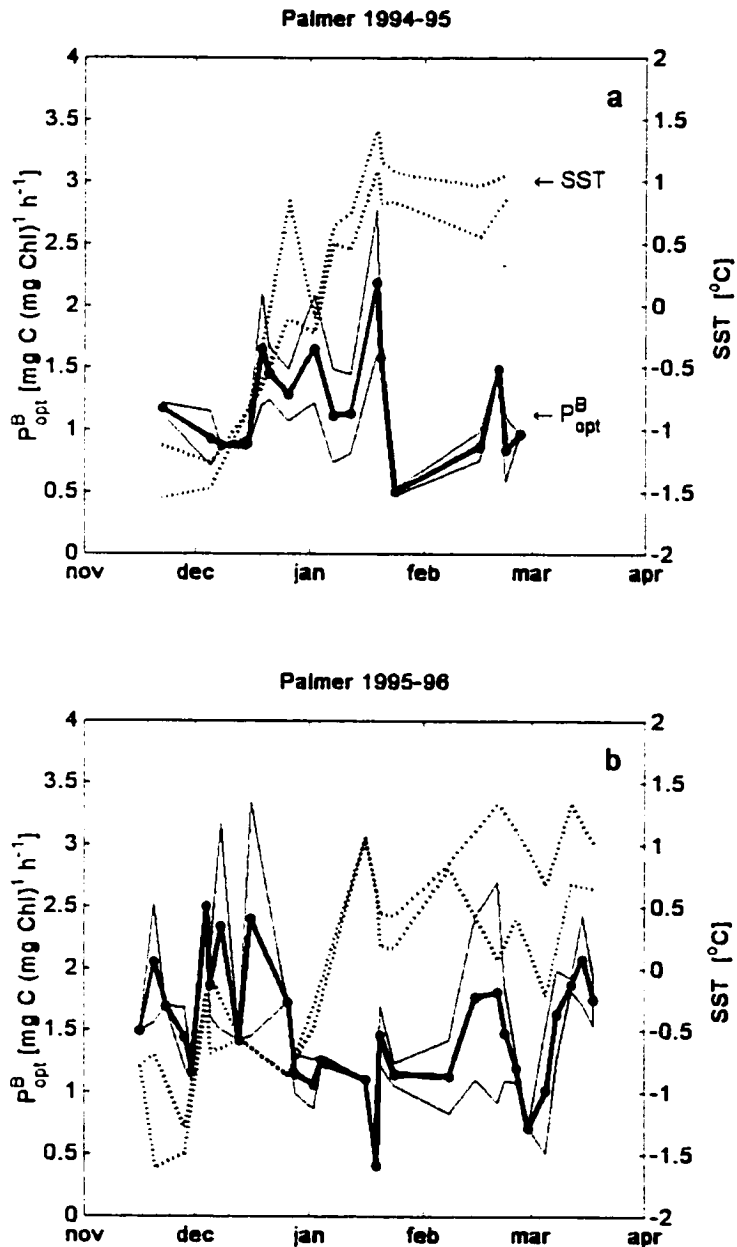
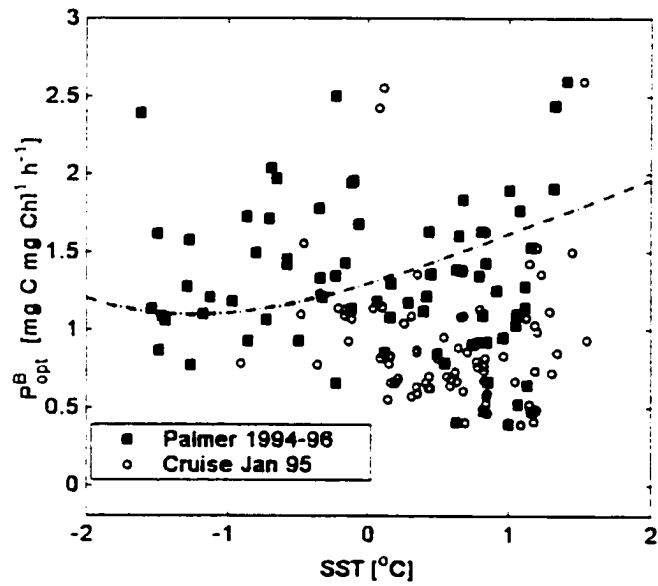
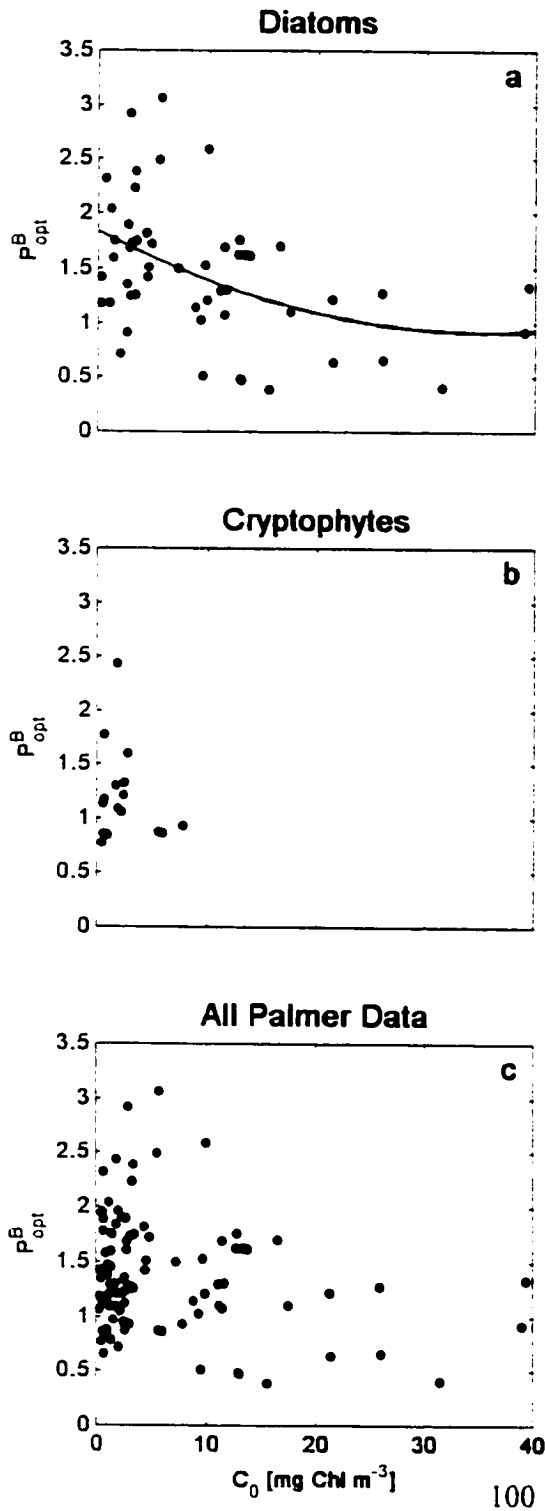


Figure 6. Measured estimates of  $P_{opt}^B$  over the field season averaged for stations B and E and shading represents one standard deviation from the mean for the two stations. Dotted line represents the SST of both stations B and E for each season. a. 1994-95 season; b. 1995-96 season.



**Figure 7.** Measured estimates of  $P_{opt}^B$  versus sea surface temperature. The dashed line is that corresponding to Behrenfeld and Falkowski (1997a; Eq. 11).



**Figure 8.** Comparison of  $P^B_{opt}$  [mg C mg Chl<sup>-1</sup> h<sup>-1</sup>] for nearshore Palmer data for when the water column is

- a. > 60% diatoms;
- b. > 60% cryptophytes;
- c. all Palmer data.

The line for the diatoms (Fig. 8a) is significant ( $p < 0.01$ ,  $r^2 = 0.14$ ). No significant trend was evident in the other two panels.

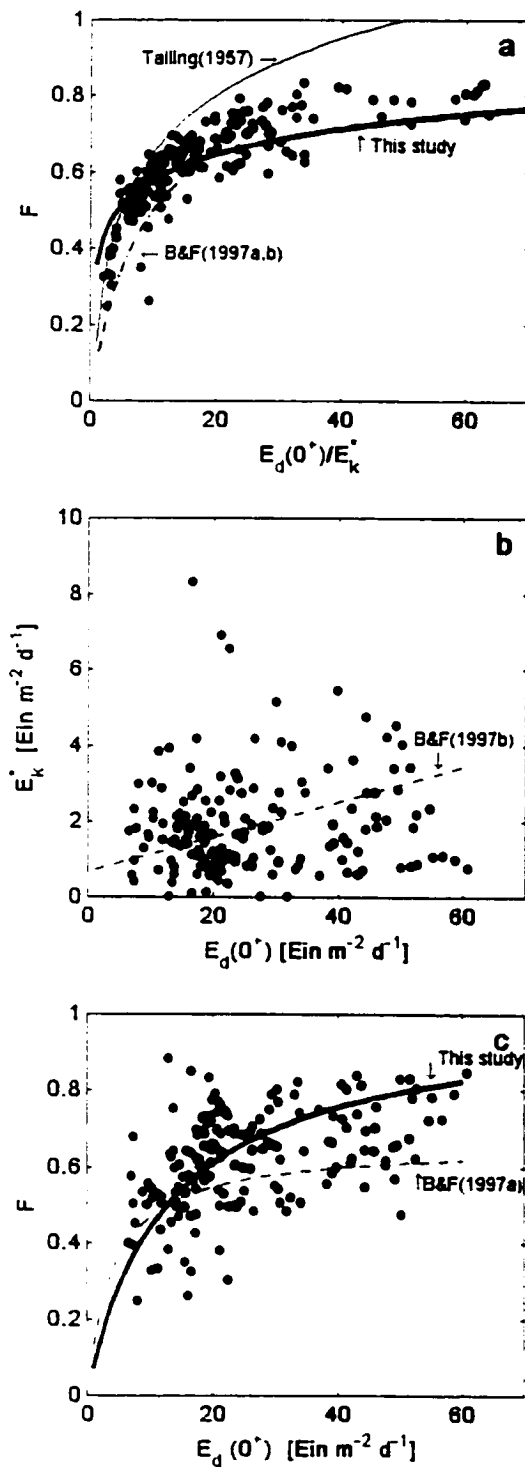


**Figure 9.**

a.  $F$ , which represents the mean Chl-normalized productivity with depth versus  $P_{opt}^B$ , as a function of  $E_d(0^+)/E_k^*$ . The thick line represents the best fit to this data. The thin line represents the fit by Talling (1997). Dashed line represents the fit using Eqs. 30 and 31 from Behrenfeld and Falkowski (1997b).

b. Comparison of the surface irradiance  $E_d(0^+)$  shown as a function of  $E_k^*$ . Dashed line represents the fit using Eqs. 31 from Behrenfeld and Falkowski (1997b).

c. Comparison of the surface irradiance ( $E_d(0^+)$ ) and the function  $F$ . Solid line represent fit using Eq. 6 ( $r^2 = 0.23, p < 0.01$ ). Dashed line represents the fit to the global data set (Behrenfeld and Falkowski 1997b; Eq. 30).

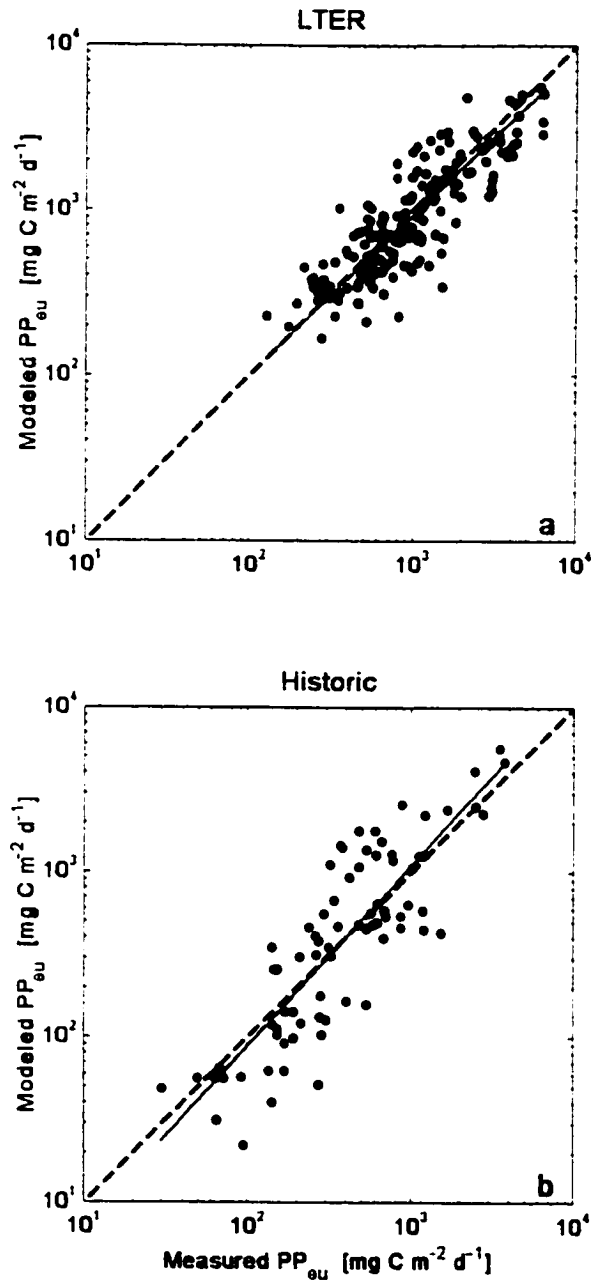


**Figure 10.** Measured primary productivity versus modeled primary productivity using Eq. 7 for the **a.** LTER data ( $n=186$ ,  $r^2=0.72$ ,  $m=0.96$ ); **b.** Historic data (Smith et al., 1996) ( $n=82$ ,  $r^2 = 0.73$ ,  $m=1.09$ ).

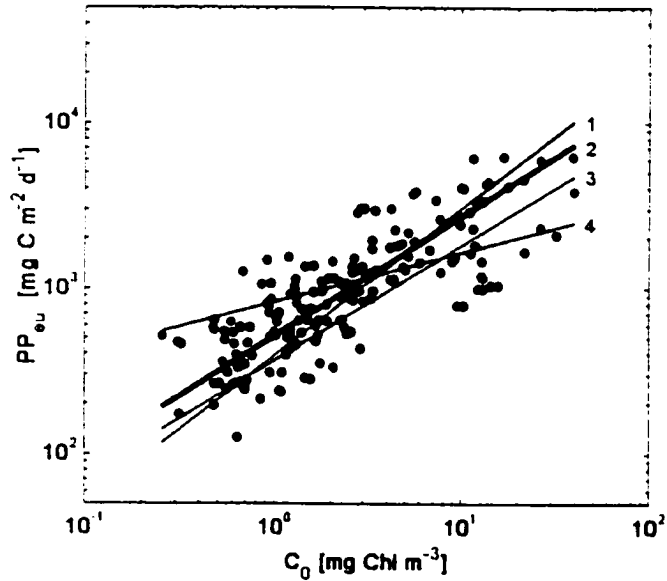


**Figure 11.** Best fit relationship between water-column integrated productivity,  $PP_{eu}$ , and surface Chl,  $C_0$ , for: 1) Holm-Hansen and Mitchell (1991) using  $C_{avg}$  instead of  $C_0$ ; 2) These LTER data, such that  $PP_{eu} = 512 C_0^{0.725}$  ( $n=186$ ,  $r^2=0.62$ ); 3) Historic Antarctic data; 4) Bermuda Atlantic Time-Series and Mid-Atlantic Bight data using  $C_{avg}$  instead of  $C_0$  (Falkowski *et al.*, 1998).

## **Chapter 4**

### **Validating remotely sensed chlorophyll from the SeaWiFS ocean color sensor for waters west of the Antarctic Peninsula**

*H.M. Dierssen and R.C. Smith*

Institute for Computational Earth System Science.

University of California Santa Barbara

Santa Barbara, CA 93106

## Abstract

Using data from the Palmer Long Term Ecological Research (PAL/LTER) program, we compare water-leaving radiance and chlorophyll derived from the ocean color sensor, SeaWiFS (Sea-viewing Wide Field-of-view Sensor). Comparisons are made between SeaWiFS-derived chl with over 370 chlorophyll measurements from the summer months of January/February in both 1998 and 1999. No consistent offsets are found between SeaWiFS monthly-binned normalized water leaving radiance,  $L_{WN}$ , and *in situ*  $L_{WN}$  measured at the same locations. However, the SeaWiFS-derived chlorophyll from the OC2V2 general processing algorithm tends to underestimate *in situ* chlorophyll at concentrations greater than  $0.1 \text{ mg Chl m}^{-3}$ . These results corroborate previous work that indicates that these Southern Ocean waters are bio-optically unique from other regions and do not conform to the OC2V2 algorithm developed primarily with data from temperate waters. Using the polynomial Southern Ocean (SO) algorithm previously derived from over 1000 bio-optical profiles collected from the PAL/LTER region, the SO-adjusted SeaWiFS chlorophyll concentrations closely match the *in situ* chlorophyll and explain over 70% of the variability in measured chlorophyll both at Palmer Station and across the Drake Passage.



## 1.0 Introduction

The Sea-viewing Wide Field of View Sensor, SeaWiFS, has been in orbit since September 1997 and is currently providing quantitative data on the global ocean bio-optical properties. This satellite is the successor to the Coastal Zone Color Scanner, CZCS, which was in operation from 1978-1986. Subtle changes in ocean color, as seen from an ocean color sensor, have been successfully used to estimate quantities of marine phytoplankton, which in turn can be used to elucidate primary production in the world's oceans [Gordon and Morel, 1983]. Use of remotely sensed data is especially important in the Southern Ocean, where the waters are characterized by extreme seasonal and interannual variability and are often inaccessible to sampling with other platforms. Currently, a general processing chlorophyll algorithm, OC2V2, is used to estimate chlorophyll throughout the world's oceans from ratios of remotely sensed reflectance derived from SeaWiFS.

Previous work has shown that the relationship between remotely sensed reflectance and chlorophyll is unique in the Southern Ocean when compared to the other regions [Mitchell and Holm-Hansen, 1991; Sullivan *et al.*, 1993; Dierssen and Smith, in press]. Using bio-optical measurements from over 1000 stations collected in conjunction with the Palmer Long-Term Ecological Research (PAL/LTER), the SeaWiFS OC2V2 algorithm was shown to underestimate measured chlorophyll concentrations by roughly a factor of 2.5 for waters west of the Antarctic Peninsula [Dierssen and Smith, in press]. As a result, a polynomial Southern Ocean (SO) algorithm was developed to adjust the OC2V2-derived chlorophyll to match *in situ* measurements. Earlier results from the now defunct CZCS also demonstrated that the general processing algorithm for retrieving pigment biomass concentrations underestimated low chlorophyll

concentrations ( $< 1.5 \text{ mg Chl m}^{-3}$ ) in the Southern Ocean by a factor of 2.4 [Mitchell and Holm-Hansen, 1991; Sullivan *et al.*, 1993]. The reason for this underestimation is believed to be due to both lower pigment-specific absorption coefficients and low backscattering coefficients, which render this area a unique bio-optical province [Dierssen and Smith, in press].

Because of the subpolar cyclonic pressure systems that cause frequent overcast conditions in the Southern Ocean [Rossow and Schiffer, 1991], generally only a few clear days per month occur in any given area sampled within the PAL/LTER program. Hence, ocean color remote sensing can be challenging in this region and time-averaged images are often necessary to obtain sufficient data coverage. In the spring and fall months, seasonal sea ice sweeps in and out of the continental shelf zone and can also interfere with ocean color retrieval. Moreover, in the winter months, the chronic darkness around Antarctica makes ocean color remote sensing impossible, even in open ocean regions that are not ice-covered. Thus, not only are the in-water bio-optical properties unique from other oceans, unique challenges exist in merely obtaining ocean color images in this polar region.

For this paper, we compare SeaWiFS-derived water leaving radiance and chlorophyll with measurements taken from PAL/LTER cruises in the summer months (January/February) of 1998 and 1999. Our comparison of radiance gives an indication as to the relative accuracy of the atmospheric correction algorithms used to process SeaWiFS radiances, which are largely untested for the Antarctic region. The atmospheric correction routines have been found to be particularly inaccurate for regions with clear atmospheres and low aerosol concentrations, such as in the Antarctic [Evans, 1999]. In addition, the correction routines assume a plane parallel atmosphere even in polar regions. In the Antarctic Peninsula, the sun reaches a minimum zenith angle of approximately  $40^\circ$

and is around 50-60° for much of the growing season (November through March). Secondly, we evaluate the performance of the polynomial SO algorithm in correcting chlorophyll that has been derived using SeaWiFS' OC2V2 algorithm. This validation is conducted on both nearshore and offshore data.

## Methods

In the following section, methods are described for the radiance and chlorophyll measurements collected as part of the PAL/LTER program. This is followed by a description of the SeaWiFS data used in this analysis.

### 2.1 PAL/LTER data

The field data presented in this paper was collected in collaboration with the Palmer Long Term Ecological Research (PAL/LTER) project [Smith *et al.*, 1995]. The region of study is shown in Fig. 1. Portions of the large grid sampling area [Waters and Smith, 1992] were sampled for chl in January-February 1998 and subsequently in 1999. Chlorophyll *a* concentrations (chl) were estimated using standard fluorometric techniques and subtracting the phaeopigment concentration determined by sample acidification [Smith *et al.*, 1981]. Vertical profiles of downwelling spectral irradiance and upwelling radiances were measured using a Bio Spherical Instruments Profiling Reflectance Radiometer (PRR) operated in a free-fall configuration. Normalized water-leaving radiance [Gordon *et al.*, 1988] was estimated by extrapolating the optical data across the sea surface [Dierssen and Smith, in press] and normalizing by the mean extraterrestrial solar irradiance.

## 2.2 SeaWiFS Data

Monthly SeaWiFS Level-3 Standard Mapped Images of chl *a* are provided from the National Aeronautics and Space Administration (NASA) Goddard Space Flight Center's Distributed Active Archive Center in June 1999. These images are global-area coverage data that has been averaged over each month using the maximum likelihood estimator mean. The resolution of each pixel in the image is approximately 0.088 degrees latitude and longitude, which translates to roughly 9.77 km per pixel in the north-south direction. Because the longitudinal lines converge at the South Pole, pixels derived from the PAL/LTER study area have a finer resolution in the east-west direction. The SeaWiFS images have been masked for land regions and for regions of cloud and ice. The SeaWiFS-derived chlorophyll was processed by NASA using the OC2V2 algorithm.

## 3.0 Results and Discussion

The following section compares normalized water-leaving radiance, nearshore chlorophyll, and offshore chlorophyll derived from SeaWiFS with *in situ* measurements collected in January-February 1998 and 1999. The PAL/LTER grid comprises a region along the coast of the Antarctic Peninsula out to the edge of the continental shelf, roughly 200 km offshore (Fig. 1). This grid falls primarily within the Coastal and Continental Shelf Zone of the Southern Ocean, which is swept by the annual advance and retreat of the Seasonal Ice Zone [Treguer and Jacques, 1992]. Fig. 2A and 2B depict the *in situ* stations sampled during the January 1998 and 1999 cruises and the corresponding SeaWiFS OC2V2 chl concentrations for that month. Dark black patches on the western side of the peninsula represent the regions that were cloudy for the en-

tire month and the dark region on the eastern side represents the Larsen Ice Shelf. These images illustrate the gradient in biomass from on- to offshore that is known to occur in this region [Smith *et al.*, 1996]. The highest chl concentrations in this region for these years tend to occur in Marguerite Bay (southernmost stations). Also evident is a tongue of low biomass extending off-shelf along the Antarctic Peninsula, which is representative of the low biomass Permanently Open Ocean Zone. Northward of this low biomass zone, the Polar Front Zone is found with increasing biomass. Because flow of water in between the Antarctic Peninsula and the tip of South America is constricted through the relatively narrow Drake Passage, the biogeochemical zones [Treguer and Jacques, 1992] are closer together and the accuracy of the SeaWiFS-derived chl and SO-adjusted can be evaluated in several different zones.

For this paper, we use monthly-composited SeaWiFS data because of the high level of cloud cover that occurs on any given day in this region. A SeaWiFS monthly composite may represent only one or two clear days for the entire month. Most of the *in situ* data were collected under cloudy conditions and, without this approach, would be excluded from the analysis. Even so, roughly 30-40% of the stations sampled had no corresponding SeaWiFS data because they were completely cloud covered for every SeaWiFS pass during that month. Therefore, the *in situ* measurements are not completely concurrent with the SeaWiFS data and some scatter is expected when comparing these two datasets.

### 3.1 Normalized Water-leaving Radiance

Fig. 3 presents *in situ* versus SeaWiFS-derived normalized water-leaving radiance ( $L_{WN}$ ) by wavelength for both the 1998 and 1999 field seasons.

Because radiance values have been collected from different times of day and days of the month, the SeaWiFS  $L_{WN}(\lambda)$  are not expected to match up exactly to *in situ* measurements. This analysis, therefore, is a rough comparison between the two datasets in order to determine whether the radiances are within a reasonable range of each other and whether a consistent bias occurs when comparing data from different wavelengths. As a first approximation, however, the data appear to be reasonably scattered around the 1:1 correspondence line for all wavelengths. The data from the bluer wavelengths (412 and 443 nm) cover a wider range and appear to be more scattered than data from the greener wavelengths (510-555 nm). Generally, the higher values of blue radiance represent low chl stations and the lower radiance values represent high chl stations that have absorbed much of the blue light. Atmospheric influences are likely to effect remotely sensed water-leaving radiance in the blue wavelengths most significantly because this light is most scattered by the atmosphere, especially in polar regions where the atmospheric path is longer due to the large solar zenith angles. As shown in earlier work [Dierssen and Smith, in press], water-leaving radiance for the green wavelengths is nearly independent of chl concentrations in this region and the variability in green reflectance is low. The OC2V2 algorithm uses radiance retrieved at 490 and 555 nm.

The mean percent difference between the satellite-derived and *in situ*  $L_{WN}$  for each wavelength is illustrated in Fig. 4. A positive percentage indicates that the SeaWiFS value is higher than the *in situ* value. As shown, the SeaWiFS data tends to overestimate  $L_{WN}$  for most wavelengths by about 20%. This trend is not robust, however, because the standard deviation from the mean, shown as errorbars in Fig. 4, are large and extend past the null line. In the blue region of the spectrum, the SeaWiFS  $L_{WN}(412)$  is on average about 90% of the corre-

sponding *in situ*  $L_{WN}(412)$ . Overall, however, this rough comparison of the monthly-composited global area coverage SeaWiFS data with *in situ* stations shows that the SeaWiFS radiance data are within the range of the *in situ* radiance measurements. Consistent differences between SeaWiFS-derived chl and *in situ* chl, therefore, are likely to be the result of differences in bio-optical properties of the water and not consistent radiometric errors.

### 3.2 Nearshore Chlorophyll

Fig. 5A compares the SeaWiFS-derived OC2V2 chl to the PAL/LTER measured chl concentrations in a given pixel during that same month. While a high correlation exists for most of the data ( $r^2=0.65$ ), significant differences exist in the slope comparing these two datasets. The SeaWiFS data matches the LTER data at concentrations around  $0.1 \text{ mg Chl m}^{-3}$ . As hypothesized, however, the SeaWiFS chl is on average roughly a factor of two lower than the measured concentrations. In Fig. 5B, we apply the SO correction algorithm [Dierssen and Smith, in press] to the SeaWiFS-derived chl, such that:

$$(1A)$$

$$\log Chl = 0.3914 + 1.0176X - 0.3114X^2 + 0.0186X^3 + 0.0610X^4$$

$$X = \log(Chl_{OC2V2}) \quad (1B)$$

The SO-adjusted SeaWiFS chl concentrations are a much better fit to the *in situ* measurements and tend to follow a 1:1 correspondence line. Not only is the slope unity, the polynomial SO algorithm improves the correlation coefficient between the two datasets to 0.70. The stations with low chl remain similar to the OC2V2 values, but the SO-adjusted chl are increased to match the *in situ* measurements.

While the SO relationship works well for the average chl concentration of  $1 \text{ mg m}^{-3}$ , the accuracy is less certain for high chl concentrations. A few stations have high measured chl and low SeaWiFS estimates while several have high SeaWiFS estimates and low measured chl. This discrepancy could be due to the use of monthly SeaWiFS composites that may be derived from a single clear pass during that month. For example, SeaWiFS could have captured a clear sky bloom episode and the corresponding measured chl was pre- or post-bloom. The presence of different phytoplankton populations with unique absorption and backscattering properties (i.e. cryptomonads vs. diatoms) could also play a role in this difference.

In Fig. 6, histograms are presented for SeaWiFS OC2V2 chl (Fig. 6A), SeaWiFS SO chl (Fig. 6B), and *in situ* chl (Fig. 6C). The OC2V2 SeaWiFS histogram is substantially lower than the *in situ* chl. The SeaWiFS SO chl and the PAL/LTER *in situ* chl have similar shapes centered around  $1 \text{ mg chl m}^{-3}$  indicating that Eq. 1 appears to be a good correction algorithm for this region. A median concentration of  $1 \text{ mg chl m}^{-3}$  is also consistent with the 1000 stations collected in previous years throughout the PAL/LTER grid [*Dierssen and Smith*, in press].

### 3.3 Offshore Chlorophyll

To test the accuracy of the polynomial SO algorithm on waters defined within the Polar Front Zone and the Permanently Open Ocean Zone of the Southern Ocean [*Treguer and Jacques*, 1992], we also compare measured surface chl and SeaWiFS-derived chl along a transect across the Drake Passage. Fig. 7A shows the location of the sampled stations and the SeaWiFS chl for the Drake Passage region. The transect contains both nearshore chl, the tongue of low chl waters visible off the shelf, and the increasing chl towards the Polar



Front region. The gaps in the SeaWiFS record (e.g., 63.5-64.5°S) are due to complete cloud coverage for the entire month. When the measured chl along this transect is compared to the remotely-sensed chl (Fig. 7B), OC2V2 chl again matches low chl concentrations ( $0.1 \text{ mg chl m}^{-3}$ ) and underestimates chl for concentrations greater than  $0.1 \text{ mg chl m}^{-3}$ . The SO-corrected chl matches both the magnitude and general pattern of the measured chl concentrations with a correlation coefficient of 0.9 and a slope approaching unity (not shown).

#### 4.0 Conclusions

As hypothesized, the SeaWiFS OC2V2-derived chl tends to underestimate *in situ* chl by about a factor of 2.5 for concentrations greater than  $0.1 \text{ mg Chl m}^{-3}$ . This difference does not appear to occur from consistent biases in the SeaWiFS retrieval of normalized water leaving radiance. Even though we used monthly-composited SeaWiFS data, we found no consistent offsets between *in situ*  $L_{WN}(\lambda)$  and SeaWiFS-derived  $L_{WN}(\lambda)$  at any wavelength. Moreover, the 490 and 555 nm channels, used in SeaWiFS' OC2V2 chl algorithm, also displayed less variability than the 412 and 443 nm channels. As a result, the inaccuracy of SeaWiFS-derived chl is unlikely to be the result of a radiometric error, but a result of the unique bio-optical properties of this region.

Previous analysis of the bio-optical profiles collected from more than 1000 stations west of the Antarctic Peninsula from 1991 to the present clearly show that OC2V2 will underestimate chl for concentrations greater than  $0.1 \text{ mg Chl m}^{-3}$  [Dierssen and Smith, in press]. Remotely sensed reflectance in the green region of the spectrum (555 nm) was found to be significantly lower than data collected from other regions (i.e., SEABAM dataset), even for high chl concentrations. Preliminary results indicate that green reflectance is due to low

levels of backscattering in these waters. With lower green reflectance per mg of chl, the OC2V2 algorithm will retrieve lower chlorophyll concentrations than expected. In addition, lower chlorophyll-specific absorption can also play a role under bloom conditions when chl concentrations are high. As a result, the polynomial SO algorithm was developed to account for the regional bio-optical differences and correct the SeaWiFS-derived chl to match measured chl concentrations.

When the SO algorithm was applied to SeaWiFS OC2V2-derived chl, SO-adjusted chl explained 70% of the variability in measured chl and followed a slope of unity. A high correlation existed between SeaWiFS and the PAL/LTER *in situ* data even though we compared monthly-composited SeaWiFS images to stations measured under generally cloudy conditions. Moreover, the algorithm was found to be accurate for data collected from the nearshore Coastal and Continental Shelf Zone, and the offshore Permanently Open Ocean Zone and the Polar Front Zone. Studies from other regions of the Southern Ocean suggest that the OC2V2 algorithm may be appropriate for certain types of algal blooms in the Ross Sea [Arrigo *et al.*, 1998]. When compared to the Antarctic Peninsula region, the Ross Sea region is generally characterized by different bloom-forming phytoplankton populations (i.e., *Phaeocystis*) and smaller diatom cell sizes. However, the SO algorithm developed here was found to be accurate not only in the nearshore regions of the Antarctic Peninsula, but also away from the continental shelf and into the Polar Front region of the Drake Passage. Future efforts will be directed towards comparing the finer resolution Local Area Coverage SeaWiFS data to concurrent *in situ* data from the few clear sky passes to further determine the accuracy of SeaWiFS radiance and chl-retrieval.

## 5.0 References

- Arrigo, K.R., D.H. Robinson, D.L. Worthen, B. Schieber, and M.P. Lizotte, Bio-optical properties of the southwestern Ross Sea, *Journal of Geophysical Research*, 193 (C10), 21,683-21,695, 1998.
- Dierssen, H., and R.C. Smith, Bio-optical properties and remote sensing ocean color algorithms for Antarctic Peninsula waters, *Journal of Geophysical Research*, in press.
- Evans, R., Personal Communication, 1999.
- Gordon, H.R., O.B. Brown, and e. al., A semianalytic radiance model of ocean color, *Journal of Geophysical Research*, 93 (D9), 10,909-10,924, 1988.
- Gordon, H.R., and A.Y. Morel, *Remote Assessment of Ocean Color for Interpretation of Satellite Visible Imagery: A Review*, Springer-Verlag, New York, 1983.
- Mitchell, B.G., and O. Holm-Hansen, Bio-optical properties of Antarctic Peninsula waters: differentiation from temperate ocean models, *Deep-Sea Research*, 38 (8/9), 1009-1028, 1991.
- Rossow, W.B., and R.A. Schiffer, ISCCP cloud data products, *Bulletin of the American Meteorological Society*, 72, 2-20, 1991.
- Smith, R.C., K.S. Baker, and P. Dustan, Fluorometer techniques for measurement of oceanic chlorophyll in the support of remote sensing, Visibility Laboratory, Scripps Institution of Oceanography, San Diego, CA, 1981.
- Smith, R.C., K.S. Baker, W.R. Fraser, E.E. Hofmann, D.M. Karl, J.M. Klinck, L.B. Quetin, and etc., The Palmer LTER: A long-term ecological research program at Palmer Station, Antarctica, *Oceanography*, 8 (3), 77-86, 1995.

- Smith, R.C., H.M. Dierssen, and M. Vernet, Phytoplankton biomass and productivity in the Western Antarctic Peninsula Region, in *Foundations for Ecosystem Research West of the Antarctic Peninsula*, edited by R.M. Ross, E.E. Hofmann, and L.B. Quetin, pp. 333-356, AGU Antarctic Research Series, 1996.
- Sullivan, C.W., K.R. Arrigo, C.R. McClain, J.C. Comiso, and J. Firestone, Distributions of phytoplankton blooms in the Southern Ocean. *Science*, 262, 1832-1837, 1993.
- Treguer, P., and G. Jacques, Dynamics of nutrients and phytoplankton, and fluxes of carbon, nitrogen and silicon in the Antarctic Ocean. *Polar Biology*, 12, 149-162, 1992.
- Waters, K.J., and R.C. Smith, Palmer LTER: A sampling grid for the Palmer LTER program. *Antarctic Journal of U.S.*, 27, 236-239, 1992.

## **6.0 Acknowledgements**

This research was supported by NASA Training Grants NGT-30063 (Earth System Science Fellowship) and NGT-40005 (California Space Institute) to H. Dierssen, and NSF Grant OPP90-11927 and NASA Grant NAGW 290-3 to R.C. Smith. We wish to acknowledge Karen Baker for her support in the PAL/LTER data management and all of the individuals from the January 1998 and 1999 cruises who helped collect the chlorophyll and optics data. In addition, we would like to thank Warner Baringer, Angel Li, and Bob Evans from the University of Miami's Rosenstiel School for Marine and Atmospheric Science for their help with the SeaWiFS data. Also, thanks to Brad Seibel for his helpful suggestions on the manuscript.

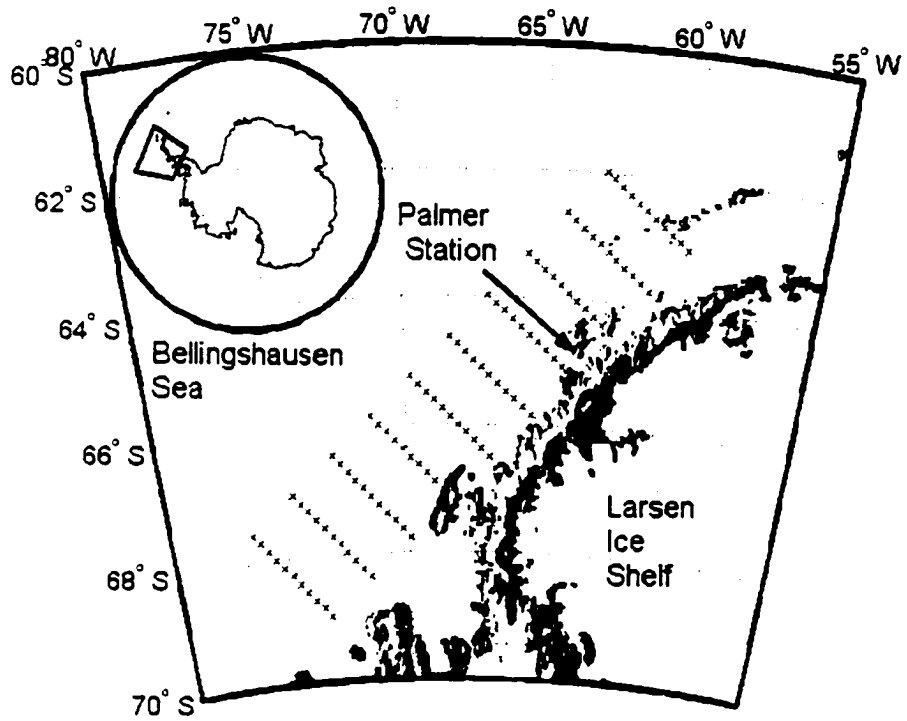


**Figure 1:** Location of the PAL/LTER grid in relation to Palmer Station and the Antarctic Peninsula.

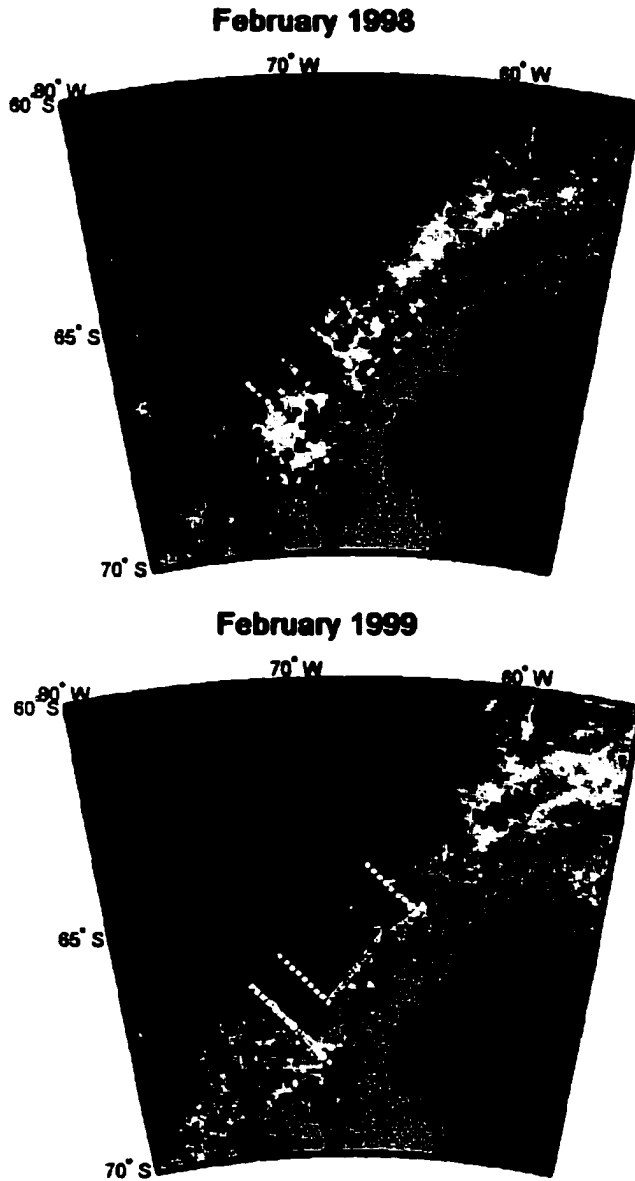


**Figure 2:** SeaWiFS-derived Chl [ $\text{mg Chl m}^{-3}$ ] from February 1998 and 1999 adjusted with SO algorithm (Eq. 1) and the corresponding PAL/LTER stations sampled during that month (white dots). Regions in black were cloud- or ice-covered during every satellite pass during that month.

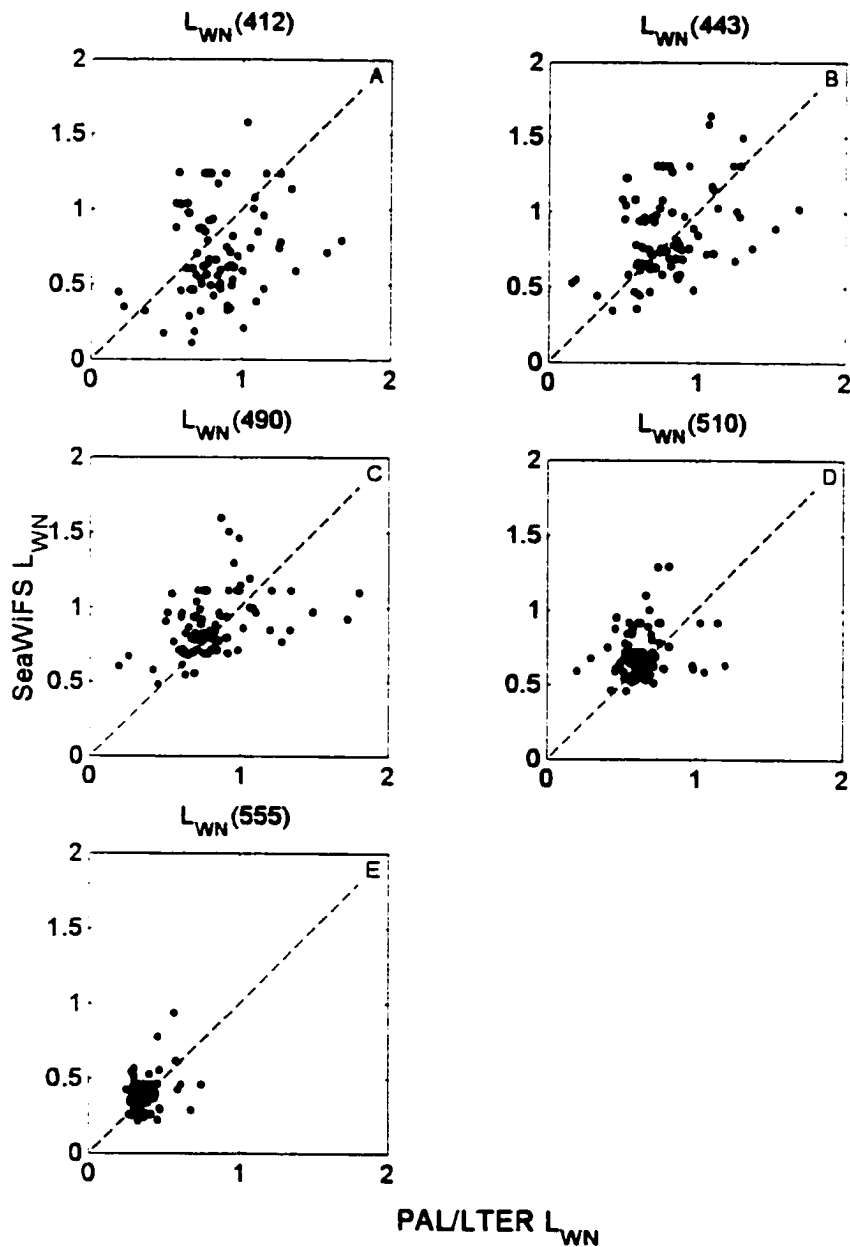


**Figure 3:** Normalized water-leaving radiance,  $L_{WN}(\lambda)$ , measured in conjunction with January/February 1998 and 1999 PAL/LTER cruises compared to corresponding monthly-averaged  $L_{WN}(\lambda)$  derived from the ocean color sensor SeaWiFS for five different wavelengths.



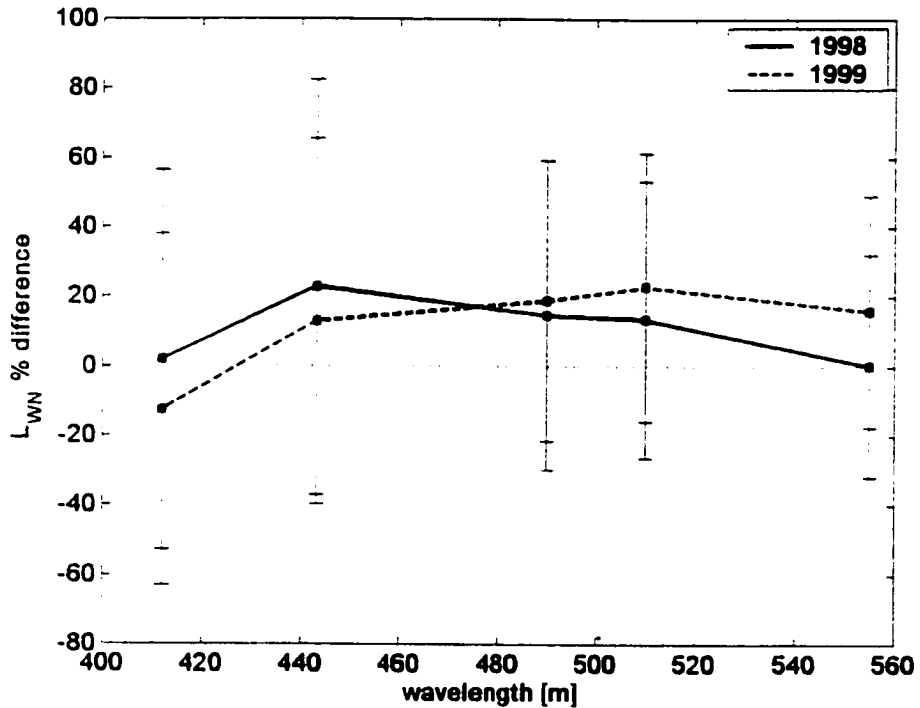
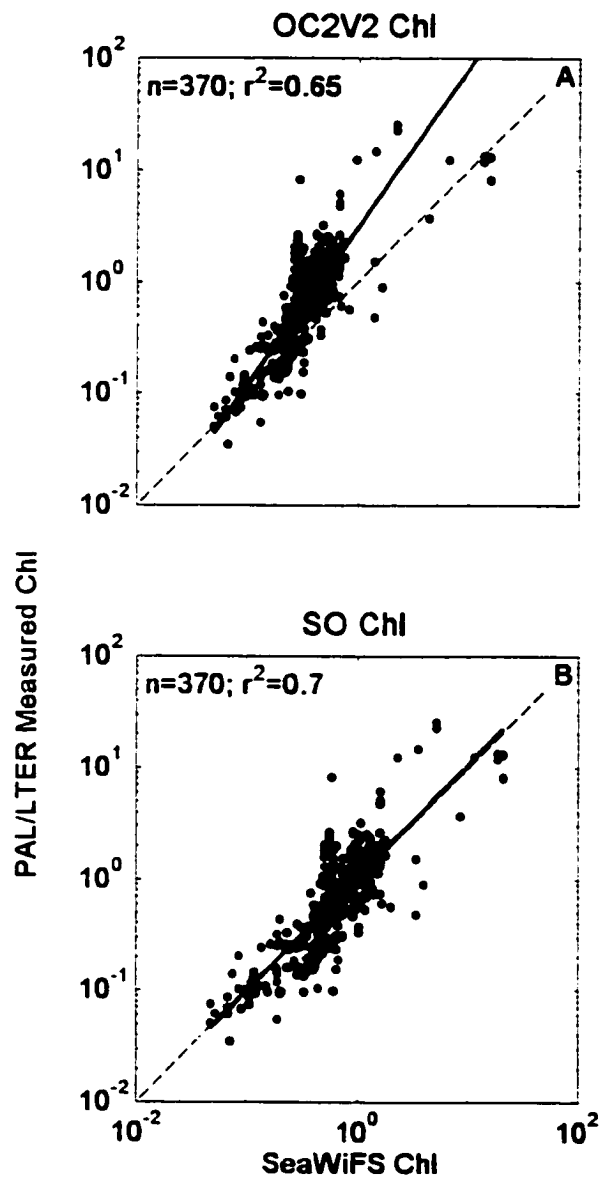
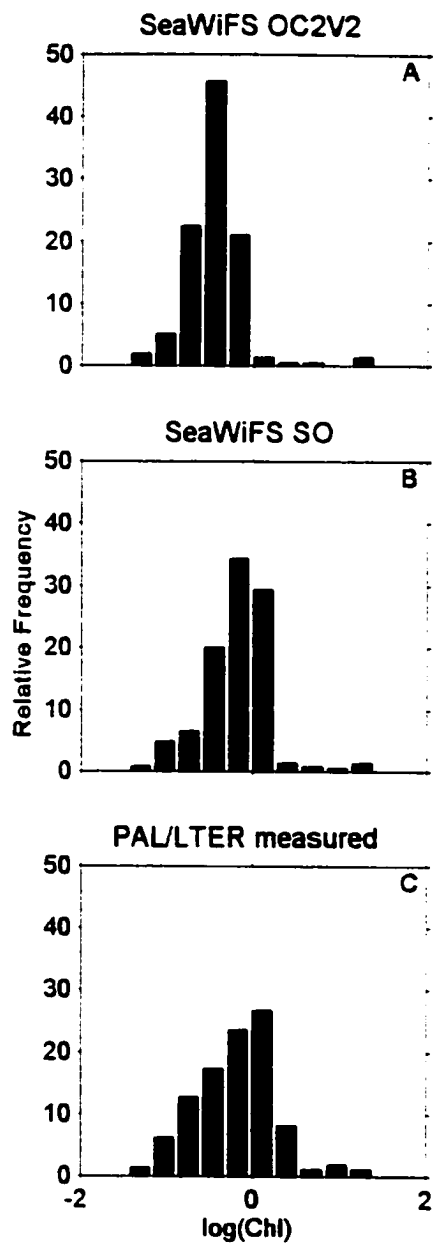


Figure 4: Mean percent difference between the SeaWiFS and PAL/LTER  $L_{WN}(\lambda)$  for January/February 1998 and 1999. Error bars represent one standard deviation from the mean. Values greater than zero indicate the mean percent difference that SeaWiFS  $L_{WN}(\lambda)$  are greater than PAL/LTER  $L_{WN}(\lambda)$ , as shown in Fig. 3.



**Figure 5:** Comparison of SeaWiFS-derived chl [ $\text{mg Chl m}^{-3}$ ] and PAL/LTER measured chl. SeaWiFS chl was processed using: A) OC2V2 algorithm; and B) SO algorithm.



**Figure 6:** Log-normal relative frequency distribution of Chl [mg Chl m<sup>-3</sup>] retrieved with A) OC2V2 algorithm; B) SO algorithm; and C) *In situ*.

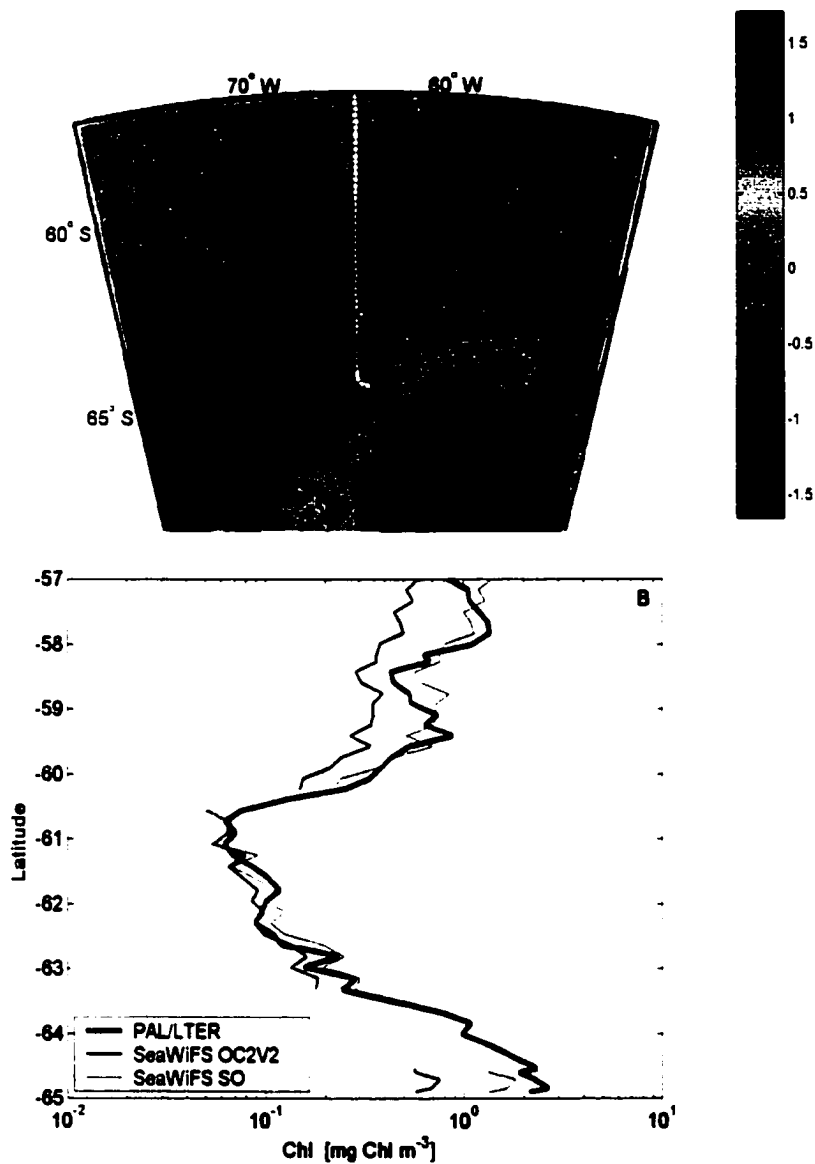


**Figure 7:** A). SeaWiFS-derived Chl [ $\text{mg Chl m}^{-3}$ ] from January 1999 adjusted with SO algorithm across a portion of the Drake Passage between South America and the Antarctic Peninsula. B) Measured surface Chl for the stations shown above compared with SeaWiFS OC2V2 Chl and SO-adjusted SeaWiFS Chl. The SeaWiFS lines are non-contiguous in areas that were cloud covered during all satellite passes for that month.

## Chapter 5

### **Modeling Primary Production from SeaWiFS-derived chlorophyll for waters west of the Antarctic Peninsula and the Southern Ocean**

*H.M. Dierssen and R.C. Smith*

Institute for Computational Earth System Science.

University of California Santa Barbara

Santa Barbara, CA 93106

*M. Vernet*

Scripps Institution of Oceanography

University of California San Diego

La Jolla, CA 92093-0218

## Abstract

Because of the large size, extreme seasonality, and remoteness of the Southern Ocean, collecting sufficient *in situ* data to estimate annual primary production (PP) for the entire basin is impracticable. Therefore, modeling PP from satellite-derived images of chlorophyll (i.e., SeaWiFS-derived Chl) should provide a better understanding of the spatial and temporal variability in this region. Using a simple depth-integrated PP model developed from data collected in conjunction with the Palmer Long Term Ecological Research (PAL/LTER), we estimate PP from SeaWiFS-derived chlorophyll both monthly and interannually for nearshore waters of the Antarctic Peninsula. PP modeled for the coastal waters of the PAL/LTER are compared to approximately weekly measurements of PP. While the PP estimates are relatively consistent for the two seasons with SeaWiFS data (78 and 88 g C m<sup>-2</sup> y<sup>-1</sup> for the 1997-98 and 1998-99 field seasons, respectively), *in situ* PP integrated from November through March can vary by nearly 7-fold (50-350 g C m<sup>-2</sup> y<sup>-1</sup>). When this modeling approach is applied to the entire SO, the PP summed over all months of 1998 is 2.7 Gt y<sup>-1</sup>. Most of this PP comes from the area comprised of the Permanently Open Ocean and Polar Front Zone. Our results are discussed in relation to previously published production estimates that vary by over an order of magnitude (0.6-8.3 Gt y<sup>-1</sup>).

## 1.0 Introduction

Southern Ocean (SO) environments range from the productive coastal regions of the Antarctic Peninsula to the oligotrophic regions of the South Indian Ocean. Estimates of primary production (PP) for the whole SO, however, vary widely from 0.6 to 8.3 Gt C yr<sup>-1</sup> (1 Gt = 10<sup>15</sup> g C) [*El-Sayed*, 1978; *Behrenfeld and Falkowski*, 1997]. Part of this discrepancy is due to the intense seasonal and interannual variability in this region of the world. South of the Antarctic circle, daylength fluctuates from 24 hours of continuous light to constant darkness. Sea ice builds outward from the continent each fall covering an area of approximately 16 million square kilometers, and then retreats back to the continent again in the spring and summer. Clearly, the SO phytoplankton, and the diverse food web that they support, must acclimate to a wide variety of conditions. Using satellites to obtain seasonal images of the entire SO should lead to better estimates of SO PP and an improved understanding of the ecology of the system.

Estimating PP from remotely sensed chlorophyll (Chl) concentrations in the SO involves unique challenges when compared to temperate regions. First, because the SO has no land boundary to its north, different delineations have been used to mark the extent of the SO. Simply normalizing the various SO primary production estimates to cover the same areal extent has rectified much of the differences in these published estimates. Generally two zones of the SO have been defined: the Antarctic zone extending from the continent to the Antarctic Polar Front, and the Subantarctic zone extending northward to the Subtropical Convergence [*Pickard and Emery*, 1990]. However, the extent of the Polar Front separating these water masses extends over a range of latitudes with seasonal and longitudinal changes in width and position. Here, we have

limited our discussion to the Antarctic Zone of the SO and use an approximation of this zone from the continent to 50°S. When comparing estimates of primary production for the SO, we compare estimates from only this region of the SO.

Second, the SO is characterized by highly variable sea ice coverage [Stammerjohn and Smith, 1996]. The continent approximately doubles in size each winter with the growth and decline of sea ice [Gloerson *et al.*, 1992]. The SeaWiFS processing algorithm nulls any pixels with an exceptionally high reflectance, which is indicative of surfaces with high albedos such as clouds and/or ice. When the ocean is covered in sea ice, the underlying ocean color is not visible and PP is assumed to be zero. While primary production can occur within and underneath the sea ice during daylight hours, the magnitude of production is considered to be low relative to the open water systems [Legendre *et al.*, 1992] and is not included in our computations.

Several studies have used multi-year ocean color composites to estimate primary production [Arrigo *et al.*, 1998]. In such cases, only the open water pixels are averaged for a given month. If a pixel was ever ice free during that month, it is assumed to be open water in the multi-year “average” image. The resulting image, therefore, represents the lowest sea ice extent that was ever observed for a given pixel and season. As a result, significant overestimates in average annual production can occur, especially in the spring and fall seasons when sea ice extent is highly variable in time and space. For this study, we use sea ice area that has been determined from satellite-derived passive microwave data for each month individually.

A similar problem revolves around the frequent cloudiness of many regions of the SO. The Antarctic continent is surrounded by subpolar cyclonic pressure systems that cause frequent overcast conditions in the SO [Rossow and Schiffer, 1991]. Neither CZCS nor SeaWiFS can detect ocean color through



cloud cover and any areas underlying a cloud layer are set to null. In order to minimize the area excluded by clouds, we use monthly averages of SeaWiFS data in which the clear sky pixels have been averaged. Even with monthly composites, however, null patches due to clouds still occur in the SeaWiFS data. Without adjustments, these null patches will lead to significant underestimates of PP.

In addition to clouds and ice, chronic darkness also envelops the Antarctic continent in winter months. Even in open water areas north of the Antarctic circle, the levels of light are too low for detection by SeaWiFS in winter months. Satellite images during June and July are generally blank well beyond the sea ice boundaries. While some primary production can occur in these undetectable open water regions, SO waters have been found to have extremely low productivity during the winter [*Brightman and Smith, 1989*]. Therefore, we assume that the contribution of winter primary production is negligible when compared to annual production.

A further challenge to remote sensing of the SO is that the atmospheric corrections used to process SeaWiFS radiances are largely untested for the Antarctic region. In addition, the correction routines assume a plane parallel atmosphere, which can be problematic if solar zenith angles are high. In the Antarctic Peninsula region, for example, the sun reaches a minimum zenith angle of approximately  $40^\circ$  and is around  $50\text{-}60^\circ$  for much of the growing season (November through March). The processing of SeaWiFS imagery can also be challenging in the presence of neighboring high albedo land surfaces, such as glacial fields. Additionally, frequent high winds in the Antarctic can cause formation of whitecaps on the ocean surface. While some correction is made during processing to correct for whitecaps, the presence of large numbers of white peaks can interfere with retrieval of remotely sensed radiances.

Finally, even if water-leaving radiances are accurately retrieved from the satellite, the SeaWiFS general processing algorithm (OC2V2) used to estimate Chl from remotely sensed radiance has been shown to be inaccurate for waters west of the Antarctic Peninsula [*Dierssen and Smith*, in press]. In these waters, SeaWiFS tends to underestimate measured Chl concentrations by roughly a factor of 2.5. Both low pigment-specific absorption coefficients and low backscattering coefficients contribute to this difference [*Dierssen and Smith*, in press].

This contribution compares SeaWiFS OC2V2-derived Chl with roughly concurrent *in situ* Chl measurements made in conjunction with the Palmer Long-Term Ecological Research (PAL/LTER). Using the PP model from Chapter 3, PP is modeled from SeaWiFS Chl both for waters near Palmer Station and for the entire SO. These PP estimates are compared to simulated *in situ* measurements at Palmer Station and to previously published estimates of PP for the SO.

## **2.0 Methods**

In the following section, methods are described for the primary production and biomass data collected as part of the PAL/LTER program. This is followed by a description of the SeaWiFS data and the sea ice data used in this analysis.

### **2.1 PAL/LTER data**

The field data presented in this paper was collected in collaboration with the Palmer Long Term Ecological Research (PAL/LTER) project [*Smith et al.*, 1995]. The location of Palmer Station, Antarctica (64°S, 64°W) is depicted in Fig. 1. Weekly time series of nearshore Chl and bi-weekly primary production was collected from roughly November-March for both the 1997-98 and 1998-99

field seasons. Chl *a* concentrations were estimated using standard fluorometric techniques and subtracting the phaeopigment concentration determined by sample acidification [Smith *et al.*, 1981]. Duplicate productivity samples were estimated by 24-hour simulated *in situ* incubations with <sup>14</sup>C-bicarbonate [Vernet *et al.*, 1996].

In previous work, a standard depth-integrated primary productivity model was developed to fit the relatively uniform chl-normalized production profile of these waters (i.e., high *F* function) and the low photoadaptive variable,  $P_{opt}^B$ , which is characteristic of low-light adapted phytoplankton [Dierssen *et al.*, 2000]. The model formulation is as follows:

$$PP_{eu} = P_{opt}^B D Z_{eu} C_0 F \quad (1A)$$

$$Z_{eu} = 46.8 C_0^{-0.36} \quad (1B)$$

where  $PP_{eu}$ , is daily integrated primary production ( $\text{mg C m}^{-2} \text{d}^{-1}$ ),  $D$  is daylength (h),  $Z_{eu}$  is depth of the euphotic zone (m),  $F$  is equal to 0.64,  $P_{opt}^B$  is  $1.09 \text{ mg C mg Chl}^{-1} \text{h}^{-1}$ , and  $C_0$  is the satellite-derived Chl *a*.

## 2.2 SeaWiFS Data

Monthly SeaWiFS Level-3 Standard Mapped Images of Chl are provided from the NASA Goddard Space Flight Center's Distributed Active Archive Center (Version 2). These images are global-area coverage data that has been averaged over each month using the maximum likelihood estimator mean. The resolution of each pixel in the image is approximately 0.088 degrees latitude and longitude, which translates to roughly a 9.77 km in the north-south direction. These SeaWiFS images have been masked for land regions and for regions of

cloud and ice. The SeaWiFS Chl derived from the OC2V2 algorithm (Version 2) were adjusted with the SO-algorithm [Dierssen and Smith, in press]. The SO-adjusted SeaWiFS Chl was shown to match *in situ* Chl for the Antarctic Peninsula region and offshore waters of the Drake Passage.

### 2.3 Sea Ice Contours

Monthly averaged estimates of the sea ice extent around the SO are used in this analysis. The sea ice edge is considered to be the 15% ice concentration contour derived from the SSMI passive microwave satellite data using the NASA Team algorithm.

## 3.0 Results and Discussion

Section 3.1 compares measurements of *in situ* primary production (PP) with estimates made from SO-adjusted SeaWiFS Chl for waters near Palmer Station. Comparisons are made both on monthly and annual average time scales. In Section 3.2, the same PP model is extrapolated to the entire SO. Modeled estimates of PP for the SO and sectors of the SO are compared to previously published estimates.

### 3.1 Palmer Station Primary Production

As described in previous work, most of the variability (>60%) in primary production (PP) in the PAL/LTER region can be explained by the surface Chl concentration alone [Dierssen *et al.*, 2000]. A simple PP model (Eq. 1) was developed using Chl and ancillary data from the 1994-95 and 1995-96 PAL/LTER field season, but was also tested on historic PP data collected in the region. Fig. 2 further depicts the accuracy of this model by presenting the measured versus modeled depth-integrated PP,  $PP_{eu}$ , for all PAL/LTER data up

through 1997-98 at Palmer Station and for the PAL/LTER grid. As shown, the model is robust and explains around 60% of the variability in the data and, with a nearly 1:1 correspondence, matches the general magnitude of the PP measurements.

Coupled with this simple PP model, the satellite-derived surface Chl can be used to model depth-integrated daily PP for these waters. In Fig. 3, the measured and modeled PP from satellite-derived Chl over the course of two field seasons of SeaWiFS data for nearshore waters at Palmer Station are presented. The first panel (Fig. 3A) shows the variability of *in situ* surface Chl and PP both the 1997-1998 and 1998-99 field seasons. High weekly variability in biomass is evident with Chl ranging from 0.2 – 5 mg Chl m<sup>-3</sup> and PP<sub>eu</sub> ranging from 50-2000 mg C m<sup>-2</sup> d<sup>-1</sup>. Consistent with earlier field seasons [Dierssen *et al.*, 2000], several peaks in biomass are evident each season. For both of these seasons, a moderately large phytoplankton bloom occurred in late December through early January.

While the patterns of Chl and PP<sub>eu</sub> are generally well correlated over the course of the season [Dierssen *et al.*, 2000], two notable exceptions occurred over this time frame. In the Nov-Dec. 1997, PP was fairly high but Chl was low. This was due to the unusual presence of a subsurface Chl maximum which changed the relationship between surface Chl and depth-integrated PP. In contrast, during February 1999, the measurements of Chl were fairly high (3 mg m<sup>-3</sup>) while measurements of PP were low (~100 mg C m<sup>-2</sup> d<sup>-1</sup>). During this time, the phytoplankton were operating at a lower photoadaptive variable  $P_{opt}^B$  than is typical for this region [Dierssen *et al.*, 2000]. Thus,  $P_{opt}^B$  has subregional variability for what seems like short periods of time and small scales.

In order to compare the measured PP with satellite-derived estimates of PP, we must compare data from the same time scale. Unfortunately, due to the frequency of cloud cover in this region, weekly ocean color images of this region are generally not available. In Fig. 3B, we match the average monthly *in situ* Chl with the monthly averaged SeaWiFS Chl data (Version 2) that has been adjusted using the SO algorithm [Dierssen and Smith, in press]. Data shown is from the nearest non-zero pixel to Palmer Station. As shown, the errors between *in situ* and SeaWiFS vary independently by month, with some months having higher or lower estimates of chl. The SeaWiFS images are generally collected from only one or two clear passes a month and will not capture the high weekly variability in biomass. However, the correspondence between the measured and remotely sensed Chl estimates is fairly high when considering that the data has been averaged over a monthly time scale. Over the course of both seasons, SeaWiFS Chl is approximately 3-4% lower on average than the measured *in situ* Chl.

Fig. 3C presents the monthly PP modeled from SeaWiFS Chl (from Fig. 3B) in comparison to the *in situ* measurements of PP. The differences between *in situ* and satellite-derived PP are due to a combination of errors in the satellite retrieval of Chl (from Fig. 3B) and errors in the PP model. As mentioned above, the PP model performs poorly for data collected from the beginning of 1997-98 season and end of the 1998-99 season, when the relationship between Chl and PP was atypical. If we integrate over the course of each season, the resulting annual (November-March) estimates of SeaWiFS modeled PP ( $\text{g C m}^{-2} \text{ y}^{-1}$ ) are 35% lower for 1997-98 and 28% higher for 1998-99 than the *in situ* values.

To place the modeled PP errors in perspective, we compare the annual PP estimates with measurements from previous years when ocean color imagery was not available. Two different techniques were used to measure PP at Palmer

Station. PP was measured using photosynthesis-irradiance curves from 1991-92 through the 1993-94 season [Moline and Prezelin, 1996] and with 24-hour simulated *in situ* for the years thereafter [Dierssen *et al.*, 2000]. Annual PP estimates have been integrated over a 152-day growing season. As shown in Fig. 4, extremely high interannual variability (i.e., 7-fold difference) is evident in waters near Palmer Station. PP varies from a low  $50 \text{ g C m}^{-2} \text{ y}^{-1}$  (1993-94) to a high  $350 \text{ g C m}^{-2} \text{ y}^{-1}$  (1995-96). Although not enough years of data are available to be conclusive, the general trend in PP shown here seems to follow a cycling of low to high productivity. The mean PP estimated for the decade would be  $154 \text{ g C m}^{-2} \text{ y}^{-1}$ .

Additionally, Fig. 4 compares the measured annual PP with results from the PP model (Eq. 1) using both *in situ* Chl and SeaWiFS-derived Chl (when available). The modeled PP matches the general magnitude of the annual PP estimated from *in situ* measurements. The last two seasons of data, where ocean color imagery is available, represent seasons with relatively low Chl and PP. In this context, the errors in monthly and annual PP modeled using SeaWiFS-derived Chl are minor when compared to the high interannual differences in PP. For the last two years, the modeled SeaWiFS PP estimate of  $78$  and  $88 \text{ g C m}^{-2} \text{ y}^{-1}$  for the 1997-98 and 1998-99 seasons, respectively, are close to that modeled with *in situ* Chl and are within 35% of the measured annual PP. Because the last two seasons had lower PP than the decadal average, modeling PP from SeaWiFS Chl for seasons with higher PP would be important to further validate the model.

### 3.2 Southern Ocean Primary Production

The previous section demonstrated that PP in nearshore waters of Palmer Station can be modeled using SeaWiFS-derived Chl and a simple PP model.

Here, we extrapolate these results to the entire SO (South of 50°S) using SeaWiFS Chl and our PP model. Monthly estimates of PP are then summed first over the SO area and then over the entire year to yield an annual estimate of PP representative of the entire SO. Monthly PP was estimated from the SeaWiFS SO-adjusted Chl.

Fig. 5 presents the resulting monthly PP estimated from September 1997 through March 1999. PP is generally high near the shelf, decreases off-shelf, and then increases again at the polar front region. As shown, the most productive regions occur in polynyas around the continent and near the tip of South America. In the 1997-98 season, a large productive polynya opened up in the Larsen Ice Shelf, on the eastern side of the Antarctic Peninsula, which was not visible in the 1998-99 season. While the overall patterns are similar from year to year, significant interannual variability is observed both in the PAL/LTER region and in the SO as a whole.

In addition to Chl concentration, each panel in Fig. 5 also displays the mean sea ice extent for that month estimated from passive microwave satellite data. Generally, the sea ice extent coincides well with the ocean color boundaries on the SeaWiFS images. Beyond the ice extent, however, numerous gaps are still visible in the ocean color images due to persistent cloud cover. On average, clouds cause approximately 20-30% of a monthly-composited satellite image of the SO to be blank for any given month. Without accounting for these large data gaps, total PP for the SO, estimated as the sum of PP from each pixel, would be significantly underestimated. Therefore, we estimated the effective area of the SO that would contribute to primary production irrespective of cloud cover. This is operationally defined as the ocean area from the sea ice extent out to 50° latitude. For each month, the PP estimates were summed to yield an estimate of total PP for the cloud-free portion of the SO. The cloud-free PP was



adjusted by the effective area to produce the effective total PP for each month. This approach assumes that the mean PP rate is representative of PP in the cloud-covered area and that the clouds are randomly distributed with respect to the underlying Chl concentration throughout the SO.

The monthly areal extent and PP estimated from the ocean color data and the effective values adjusted to account for the gaps in the satellite imagery are presented in Table 1. The total effective PP varies from 0 in the winter months, when the SO is dark and covered with sea ice, to nearly 600 Tg C mo<sup>-1</sup> (1 Tg=10<sup>12</sup> g) in January, when days are long and the SO is relatively ice free. For the winter months from May through July, very few pixels contained data and PP was set to 0 (see Fig. 5). The total annual PP (i.e., the sum of the monthly PP estimates from January through December 1998) is estimated to be 2.7 Gt C y<sup>-1</sup> (1 Gt= 10<sup>15</sup> g). According to these calculations, approximately three quarters of the SO PP occurs during the growing season from November through March. If we compare the production from the 1997-98 and 1998-99 field seasons from November to March at Palmer Station, the estimates of the two seasons are quite similar, 2.10 and 2.17 Gt C y<sup>-1</sup>, respectively. The similarity of PP for the last two seasons is also reflected in the results from Palmer Station (see Section 3.1).

To put our estimate of SO PP in perspective, Table 2 is a compilation of previous estimates of primary production for the SO. For each published estimate, we present the total production (Gt C y<sup>-1</sup>), the maximum area used in the analysis, and the resulting annual production per unit area (g C m<sup>-2</sup> y<sup>-1</sup>). The estimates of total PP vary by over an order of magnitude (0.6 to 8.3 Gt C y<sup>-1</sup>) in part due to the different areal extents used to define the SO (delimited by latitudes ranging from 40 to 55°S) and the different methods employed in the analyses. The *in situ* methods extrapolate localized data, primarily obtained

during a single season, over the entire SO and result in estimates of PP that vary by 6-fold ( $16\text{-}100 \text{ g C m}^{-2} \text{ y}^{-1}$ ). Because of the high variability between different zones of the SO (e.g., Coastal and Continental Shelf vs. Polar Front) and between different seasons at one locale, as demonstrated in Section 3.1, large-scale extrapolations from *in situ* data are expected to yield more variable results than methods using satellite data.

Even though satellites should provide a better understanding of the spatial and temporal distributions of biomass throughout the SO, however, PP estimated with satellite-derived Chl from the Coastal Zone Color Scanner (CZCS) are also variable. When normalized over the same areal extent, the variability is reduced and mean PP varies by a factor of two ( $78\text{-}146 \text{ g C m}^{-2} \text{ y}^{-1}$ ). As outlined in the introduction, much of this variability is due to the diverse, often subjective, assumptions inherent in using remotely sensed Antarctic data (i.e., clouds, sea ice, darkness, area estimates, etc.).

In order to understand how PP is distributed throughout the SO, we have divided the SO into two zonal categories. The first covers the portion of the SO that is permanently ice free and includes the biogeochemical provinces dubbed the Permanently Open Ocean Zone (POOZ) and the Polar Front Zone (PFZ) [Treguer and Jacques, 1992] (white area in Fig. 1). The second zone incorporates the area south of the first and includes the Seasonal Ice Zone (SIZ) and the Continental and Coastal Shelf Zone (CCSZ) (lightly shaded region in Fig. 1). The open water area of this zone varies from 0 when sea ice is at its maximum extent to  $16 \times 10^6 \text{ km}^2$  when sea ice is at its minimum. As shown in Table 2, most of the PP occurs within the larger POOZ and PFZ ( $1.8 \text{ Gt C y}^{-1}$ ). The mean annual rate of PP within this zone ( $71 \text{ g C m}^{-2} \text{ y}^{-1}$ ), however, is less than the rate within the more productive CCSZ and SIZ ( $101 \text{ g C m}^{-2} \text{ y}^{-1}$ ). As

expected, both of these values are lower than the mean decadal PP determined for the highly variable and rich nearshore waters of Palmer Station ( $154 \text{ g C m}^{-2} \text{ y}^{-1}$ ). Fig. 6 compares our estimates of monthly PP for these two zones with that determined from mean monthly CZCS data averaged over all months of operation [Arrigo *et al.*, 1998]. As shown, the estimates of PP for the CCSZ and SIZ are comparable, however, the results differ significantly for the POOZ and PFZ. For the pelagic waters of the POOZ and PFZ, the CZCS PP estimates are much higher for all months.

In order to analyze how PP is distributed meridionally throughout the SO, we divided the estimates into five geographical sectors [Zwally *et al.*, 1983]: the South Indian Ocean ( $20\text{-}90^{\circ}\text{E}$ ), Southwestern Pacific ( $90\text{-}160^{\circ}\text{E}$ ), Ross Sea ( $160^{\circ}\text{E}\text{-}130^{\circ}\text{W}$ ), Bellingshausen-Amundsen ( $60\text{-}130^{\circ}\text{W}$ ), Weddell Sea ( $60^{\circ}\text{W}\text{-}20^{\circ}\text{E}$ ). These sectors extend from the continent out to  $50^{\circ}\text{S}$  latitude (see Fig. 1). Of these regions, the area-specific PP in 1998 appears to be highest in the Weddell ( $105 \text{ g C m}^{-2} \text{ yr}^{-1}$ ) followed by the Ross Sea ( $81 \text{ g C m}^{-2} \text{ yr}^{-1}$ ) and the Bellingshausen-Amundsen ( $74 \text{ g C m}^{-2} \text{ yr}^{-1}$ ). Both the South Indian and Southwest Pacific Oceans had rates that were approximately 20% lower than the other sectors (Table 2). This may be due to low concentrations of limiting nutrients, such as silica or iron [Treguer and Jacques, 1992; Jeandel *et al.*, 1998], and the lack of highly productive polynyas.

While the overall SO PP was similar for 1997-98 and 1998-99 (Table 1), a comparison of the seasonal PP for the different sectors reveals significant differences between the two seasons (Table 2). In 1997-98, the Weddell Sea had significantly higher PP than in 1998-99 ( $79$  versus  $67 \text{ g C m}^{-2} \text{ yr}^{-1}$ ). This is largely due to the existence of a large polynya in the Larsen Ice Shelf, which was highly productive in the summer 1997-98 and virtually non-existent in

1998-99 (Fig. 5). In contrast, the Ross Sea had much higher PP in 1998-99 than in 1997-98, which is similarly due to the larger extent of the Ross Ice Shelf polynya in 1998-99 when compared to 1997-98. Consistent with measurements made near Palmer Station, the PP in the Bellingshausen-Amundsen sector remained fairly constant for the two seasons. In general, the Indian, Pacific, and Ross sectors had increasing and the Bellingshausen-Amundsen and Weddell had decreasing PP between 1997-98 and 1998-99 .

#### 4.0 Conclusions

While the Antarctic Zone of the SO makes up approximately 11-12% of the world's oceans in area, the PP determined here ( $2.7 \text{ Gt C y}^{-1}$ ) would account for between 4-6% of the total ocean PP [Longhurst *et al.*, 1995; Antoine *et al.*, 1996; Behrenfeld and Falkowski, 1997]. Our estimate is on the low end of most of the previously published estimates from satellite-derived data (Table 2). However, our approach has many strengths which we feel make this estimate more accurate than previously published estimates:

- 1) We use the latest satellite data from SeaWiFS ocean color sensor that has improved algorithms for atmospheric correction and pigment retrieval from the earlier proof-of-concept CZCS sensor.
- 2) SO-adjusted SeaWiFS Chl has been validated using stations that cross three different biogeographic provinces: the Coastal and Continental Shelf Zone, the Seasonal Ice Zone, and the Polar Front Zone.
- 3) The primary production model explains much of the variability (60-70%) in PP for the Antarctic Peninsula waters. We validate this model by comparing interannual measurements of *in situ* PP at Palmer Station to the satellite-derived estimates.

- 4) Sea ice extent is determined for each month individually using SSMI passive microwave satellite data. These data are used to determine an effective area of SO that includes cloud-covered gaps in the ocean color imagery.

Some possible reasons why our results are lower per unit area than the estimates of PP using CZCS data [Arrigo *et al.*, 1998; Smith *et al.*, 1998] are discussed below. The prior estimates used multi-year composites of CZCS Chl that had been averaged over the lifetime of the sensor (1978-1986). Here, we analyze SeaWiFS data from only one year of data (i.e., 1998). In the nearshore waters of the Antarctic Peninsula, *in situ* data indicate that 1998 may be a relatively low year of PP for this region. Second, by using annually averaged CZCS data, those images represent the lowest sea ice extent that was ever observed during that month. This could cause significant overestimates in average annual production, especially in the spring and fall seasons when sea ice extent is highly variable in time and space. Finally, the biggest differences come from our estimates of PP in the POOZ and PFZ. This could result from differences in the way PP is modeled from Chl. Our PP model uses daylength instead of irradiance and a constant photoadaptive variable  $P_{opt}^B$ . These assumptions can lead to lower PP estimates, especially with increasing irradiance at more northern latitudes. Moreover, models that use temperature-dependent photoadaptive variables could also increase PP estimates in the pelagic areas of the POOZ and PFZ. More seasonal *in situ* data from the POOZ and PFZ would be useful to validate these results.

In contrast, our SO PP estimate, and virtually all other satellite-derived estimates of SO PP, are higher than those estimates made from *in situ* data obtained from the biogeochemical zones of the SO [Holm-Hansen *et al.*, 1977;

*Treguer and Jacques, 1992; Smith et al., 1998*]. The major discrepancy is found in the estimates of PP for the POOZ and PFZ, which make up the bulk of productivity for the SO. Using previously published estimates of PP for the POOZ, Smith et al. (1998) determined that the rate of PP in this zone is  $16 \text{ g C m}^{-2} \text{ y}^{-1}$  compared to the  $60\text{-}70 \text{ g C m}^{-2} \text{ y}^{-1}$  reported here. Their estimate, however, assumed a growing season of only 120 days. When dealing with inshore waters (i.e., Palmer Station) where sea ice is persistent for much of the year, one can reasonably assume that PP is limited to a short growing season (120-152 days). However, confining annual estimates of PP from November to March for SIZ, POOZ, and PFZ waters will underestimate the mean rate of annual PP by at least 20-30% (Table 2).

Additionally, the mean rate of daily PP in the POOZ and PFZ zone is close to that published for the PFZ of  $80 \text{ g C m}^{-2} \text{ d}^{-1}$  [*Treguer and Jacques, 1992*]. Treguer and Jacques (1992) considered the area of the POOZ to be  $16 \times 10^6 \text{ km}^2$ , while the PFZ was only  $3 \times 10^6 \text{ km}^2$ . When analyzing the SeaWiFS images from Fig. 5, however, the oligotrophic regions ( $\leq 0.1 \text{ mg Chl m}^{-3}$ ) appear as small patches distributed in a larger field of higher biomass. In December and January, the largest oligotrophic regions are found in a low biomass tongue off the Antarctic Peninsula and part of the Indian Ocean sector. While eutrophic regions ( $>1 \text{ mg Chl m}^{-3}$ ) make up close to 11% of the SO area, oligotrophic regions account for less than 1% of the area or about  $0.5\text{-}1 \times 10^6 \text{ km}^2$ . Therefore, the POOZ area is much smaller than previously thought, while the area influenced by the more productive PFZ is larger.

The amount of interannual variability that occurs in total SO PP is still relatively unknown. From time series data collected in conjunction with the PAL/LTER program, annual PP near Palmer Station varies by 7-fold depending

on the year of analysis ( $50\text{-}350 \text{ g C m}^{-2} \text{ yr}^{-1}$ ), with a decadal average of  $154 \text{ g C m}^{-2} \text{ yr}^{-1}$ . While there are few similar time series in other regions of the Antarctic, high interannual variability in biomass was not found at the KERFIX station ( $50.7^{\circ}\text{S}$ ,  $68.4^{\circ}\text{E}$ ) in the Indian sector of the SO between 1990 and 1995. This more northern station, located within the POOZ and PFZ zone, is characterized by lower and more consistent Chl concentrations [Jeandel *et al.*, 1998]. Interannual variability in biomass is found to be minimal when compared to the Antarctic Peninsula region. We hypothesize that interannual variability, however, would be greatest in nearshore regions, like the waters surrounding Palmer Station, that are highly influenced by the timing and magnitude of sea ice.

The concentration and duration of sea ice may play an important role in defining the variability of the SO PP. Not only does sea ice determine the open water area available for PP in a given month, high levels of PP occur within polynyas opened up in the sea ice fields. Previous analyses, using annually averaged CZCS data, show the highest PP occurring in the Ross Sea sector, a region where large polynyas form [Arrigo and McClain, 1994; Arrigo *et al.*, 1998]. In contrast, this study determined that the Weddell Sea had the highest PP in 1997-98, in part due to the presence of a large and productive polynya in the Larsen Ice Shelf. While variability in interannual sea ice concentrations is high within the different sectors, the SO as a whole exhibits low interannual sea ice variability [Stammerjohn, 1993]. Clearly, sea ice has a large impact on PP within the CCSZ and SIZ. However, because most of the total PP comes from the ice-free POOZ and PFZ region interannual variability will likely be much lower for the total SO than what is observed within the CCSZ and SIZ zone.

## 5.0 References

- Antoine, D., J.M. Andre, and A. Morel, Oceanic primary production: 2. Estimation at global scale from satellite (coastal zone color scanner) chlorophyll, *Global Biogeochemical Cycles*, 10 (1), 57-69, 1996.
- Arrigo, K., D. Worthen, A. Schnell, and M.P. Lizotte, Primary production in Southern Ocean waters, *Journal of Geophysical Research*, 103 (C8), 15587-15600, 1998.
- Arrigo, K.R., and C.R. McClain, Spring phytoplankton production in the western Ross Sea, *Science*, 266, 261-262, 1994.
- Behrenfeld, M.J., and P.G. Falkowski, Photosynthetic rates derived from satellite-based chlorophyll concentration, *Limnology and Oceanography*, 42 (1), 1-20, 1997.
- Berger, W.H., K. Fischer, C. Lai, and G. Wu, Ocean productivity and organic carbon flux: Part I. overview and maps of primary production and export production, pp. 69, Scripps Institution of Oceanography, San Diego, 1987.
- Brightman, R.I., and W.O. Smith, Photosynthesis-irradiance relationships of Antarctic phytoplankton during austral winter, *Marine Ecology Progress Series*, 53, 143-151, 1989.
- Currie, R.I., Environmental features in the ecology of Antarctic seas, in *Biologie Antarctique*, edited by R. Carrick, M.W. Holdgate, and J. Prevost, pp. 87-94, Hermann, Paris, 1964.
- Dierssen, H., and R.C. Smith, Bio-optical properties and remote sensing ocean color algorithms for Antarctic Peninsula waters, *Journal of Geophysical Research*, in press.



- Dierssen, H.M., R.C. Smith, and M. Vernet, Optimizing models for remotely estimating primary production in Antarctic coastal waters, *Antarctic Science*, 12 (1), 20-32, 2000.
- Holm-Hansen, O., S.Z. El-Sayed, G.A. Franceschini, and R.L. Cuhel, Primary production and the factors controlling phytoplankton growth in the Southern Ocean., in *Scientific Committee for Antarctic Research (SCAR) and the International Union of Biological Sciences*, edited by G.A. Llano, pp. 11-50, Gulf Publishing Co., Washington, D.C., 1977.
- Jeandel, C., D. Ruiz-Pino, E. Gjata, and e. al., KERFIX, a time series station in the Southern Ocean: a presentation, *Journal of Marine Systems*, 17, 555-569, 1998.
- Longhurst, A., S. Sathyendranath, T. Platt, and C. Caverhill, An estimate of global primary productivity in the ocean from satellite radiometer data, *Journal of Plankton Research*, 17 (6), 1245-1271, 1995.
- Moline, M., and B.B. Prezelin, Long-term monitoring and analyses of physical factors regulating variability in coastal Antarctic phytoplankton biomass, in situ productivity and taxonomic composition over subseasonal, seasonal, and interannual time scales, *Marine Ecology Progress Series*, 145 (1-3), 143-160, 1996.
- Rossow, W.B., and R.A. Schiffer, ISCCP cloud data products, *Bulletin of the American Meteorological Society*, 72, 2-20, 1991.
- Ryther, J.H., Geographic variations in productivity, in *The Sea*, edited by M.N. Hill, pp. 347-380, John Wiley & Sons, New York, 1963.
- Smith, R.C., K.S. Baker, M.L. Byers, and S.E. Stammerjohn. Primary productivity of the Palmer Long Term Ecological Research Area and the Southern Ocean. *Journal of Marine Systems*, 17, 245-259, 1998.

- Smith, R.C., K.S. Baker, and P. Dustan, Fluorometer techniques for measurement of oceanic chlorophyll in the support of remote sensing, Visibility Laboratory, Scripps Institution of Oceanography, San Diego, CA, 1981.
- Smith, R.C., K.S. Baker, W.R. Fraser, E.E. Hofmann, D.M. Karl, J.M. Klinck, L.B. Quetin, and etc., The Palmer LTER: A long-term ecological research program at Palmer Station, Antarctica, *Oceanography*, 8 (3), 77-86, 1995.
- Stammerjohn, S., Spatial and temporal variability in Southern Ocean sea ice coverage, M.A. thesis, University of California Santa Barbara, Santa Barbara, CA, 1993.
- Treguer, P., and G. Jacques, Dynamics of nutrients and phytoplankton, and fluxes of carbon, nitrogen and silicon in the Antarctic Ocean, *Polar Biology*, 12, 149-162, 1992.
- Vernet, M., W. Kozlowski, and T. Ruel, Palmer LTER: Temporal variability in primary productivity in Arthur Harbor during the 1994/1995 growth season, *Antarctic Journal of the United States*, 1996.
- Zwally, H.J., J.C. Comiso, C.L. Parkinson, and e. al., Antarctic sea ice, 1973-1976: Satellite passive-microwave observations, National Aeronautics and Space Administration, Washington D.C., 1983.

**Table 1: Southern Ocean Primary Production estimated from SeaWiFS-derived Chlorophyll**

Month	Mean PP <sup>a</sup> mg C m <sup>-2</sup> d <sup>-1</sup>	Cloud-free Area <sup>b</sup> (x 10 <sup>6</sup> km <sup>2</sup> )	Effective Area <sup>c</sup> (x 10 <sup>6</sup> km <sup>2</sup> )	Cloud-free PP <sup>d</sup> (Tg mo <sup>-1</sup> )	Effective PP <sup>e</sup> (Tg mo <sup>-1</sup> )
September 1997	173	15.5	26.1	84	142
October 1997	247	19.2	27.0	150	210
November 1997	377	24.7	28.9	272	318
December 1997	579	29.9	34.9	480	561
January 1998	525	32.7	41.2	457	576
February 1998	377	35.1	42.4	318	384
March 1998	212	33.5	40.5	215	259
April 1998	155	20.1	37.8	94	177
May 1998	144	3.8	34.4	0	0
June 1998	0	0	31.3	0	0
July 1998	138	1.9	28.9	0	0
August 1998	118	9.3	27.0	36	104
September 1998	155	18.1	26.2	88	127
October 1998	256	20.7	26.4	160	204
November 1998	380	22.1	28.6	242	312
December 1998	599	28.0	34.4	455	559
January 1999	545	33.0	40.6	486	597
February 1999	400	33.2	41.9	333	421
March 1999	225	33.4	40.7	229	280
<b>Totals</b>					
Jan. 98-Dec. 98					2.700 <sup>f</sup>
Nov. 97-Mar. 98					2.100
Nov. 98-Mar. 99					2.170

<sup>a</sup> Maximum likelihood estimator mean daily water column primary production estimated south of latitude 50°S for all non-zero pixels. Calculation used monthly composited SO-adjusted SeaWiFS Chl (Eq. 2) and PP model (Eq. 1).

<sup>b</sup> Area of the Southern Ocean that is cloud-free for that ocean color image

<sup>c</sup> Surface area (km<sup>2</sup>) between the monthly ice edge extent and 50°S latitude.

<sup>d</sup> Sum of modeled monthly primary production for all non-zero pixels (1 Tg=10<sup>12</sup> g). PP for May and July are set to zero because these months lack sufficient ocean color data.

<sup>e</sup> Monthly primary production adjusted to cover the effective area of the Southern Ocean.  
Effective PP = Cloud-free PP x Effective Area / Cloud-free Area

<sup>f</sup> Units for the totals are Tg C y<sup>-1</sup>

**Table 2: Comparison of published estimates of Southern Ocean Primary Production**

	PP Gt C y <sup>-1</sup>	Max. Area (x 10 <sup>6</sup> km <sup>2</sup> )	PP g C m <sup>-2</sup> y <sup>-1</sup>
<i>In situ</i>			
Ryther (1963)	3.8	38.1	100
Currie (1964)	1.6	38.1	43
El-Sayed (1968)	3.3		
Holm-Hansen (1977)	0.6	38.1	16
Berger (1987)	5.2		
Trequer (1992)	1.2-1.8	33.9	35-53
Antoine and Morel (1996)	4.0	43.5	92
Smith et al. (1998)	0.7	30.9	23
CCSZ		0.9	140
SIZ		16	21
POOZ		14	20
<i>CZCS</i>			
Longhurst et al. (1995) <sup>a</sup>	5.9	41.1	142
Antoine and Morel (1996) <i>revised</i> <sup>b</sup>	5.9	<del>40.4</del>	<del>146</del>
Behrenfeld and Falkowski (1997)	6.9	76	91
LPCM2			
Behrenfeld and Falkowski (1997)	8.3	76	109
VGPM	<del>4.8</del>	<del>40.4</del>	<del>119</del>
<i>Revised</i> <sup>c</sup>			
Smith et al. (1998)	2.1	27	78
Arrigo et al. (1998)	3.2-4.4	40.4	79-109
<i>SeaWiFS</i>			
<i>This Study</i>	2.7	42.4	73 (57, 59) <sup>c</sup>
<i>Zonal Regions</i>			
CCSZ & SIZ	0.9	0-16	101 (73,79)
POOZ & PFZ	1.8	26	71 (50,52)
<i>Meridional Regions</i>			
S. Indian Ocean	0.42	7.85	54 (41, 45)
S.W. Pacific Ocean	0.42	7.10	59 (39, 43)
Ross Sea	0.70	9.19	76 (56, 66)
Bellingshausen-Amundsen Sea	0.70	8.66	81 (60, 58)
Weddell Sea	0.96	10.11	95 (79, 67)

<sup>a</sup> Sum using the regions defined as ANTA, APLR, and SANT

<sup>b</sup> These estimates were revised using the CZCS pigments of Arrigo et al. 1998

<sup>c</sup> Data in parenthesis is calculated from Nov-March for both the 1997-98 and 1998-99 seasons, respectively.

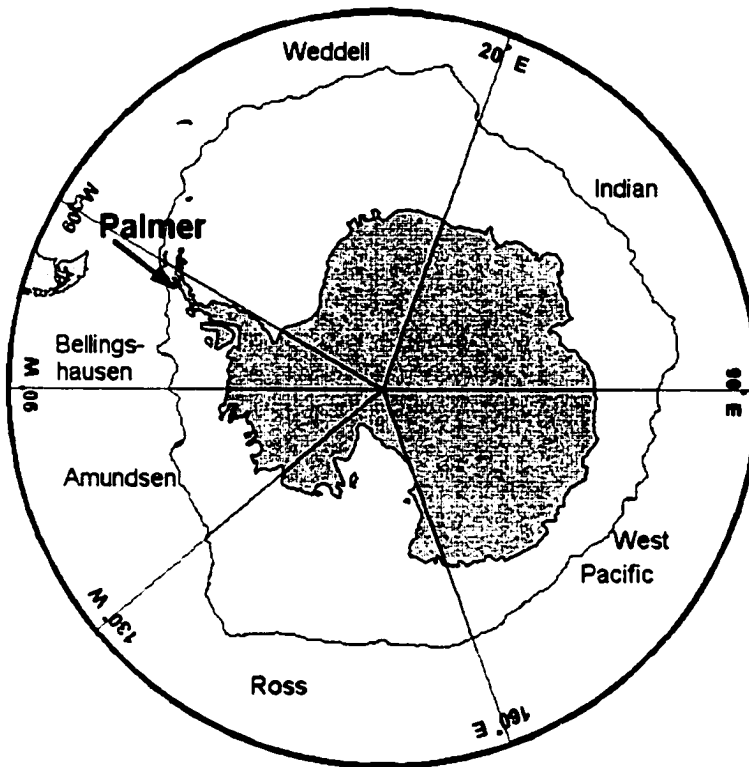


**Figure 1:** Location of Palmer Station and the meridional sectors within the Southern Ocean. Lightly shaded area represents the maximal sea ice extent used to delimit the CCSZ and SIZ zones from the PFZ and POOZ zone (white area).

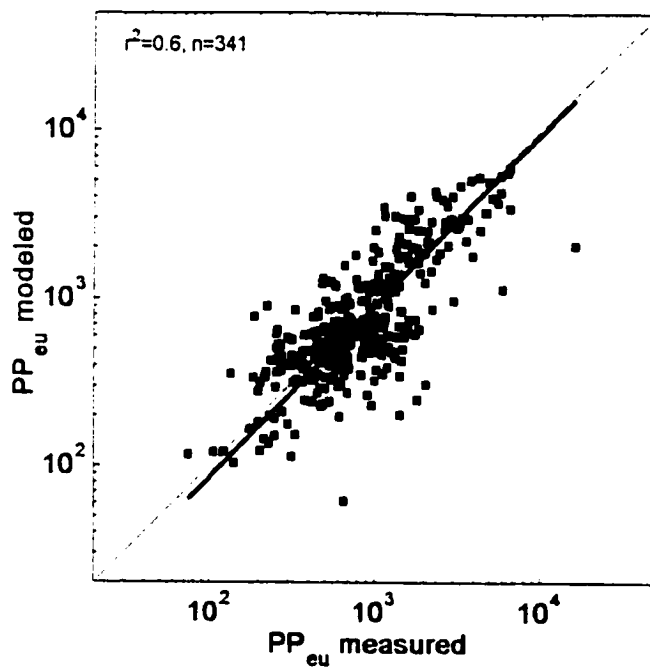


**Figure 2:** Measured water-column primary production [ $\text{mg C m}^{-2} \text{d}^{-1}$ ] versus primary production modeled from measured Chl (Eq. 1) for all PAL/LTER stations from October 1994-March 1998. The model was developed using only a subset of the data (1994-1996).

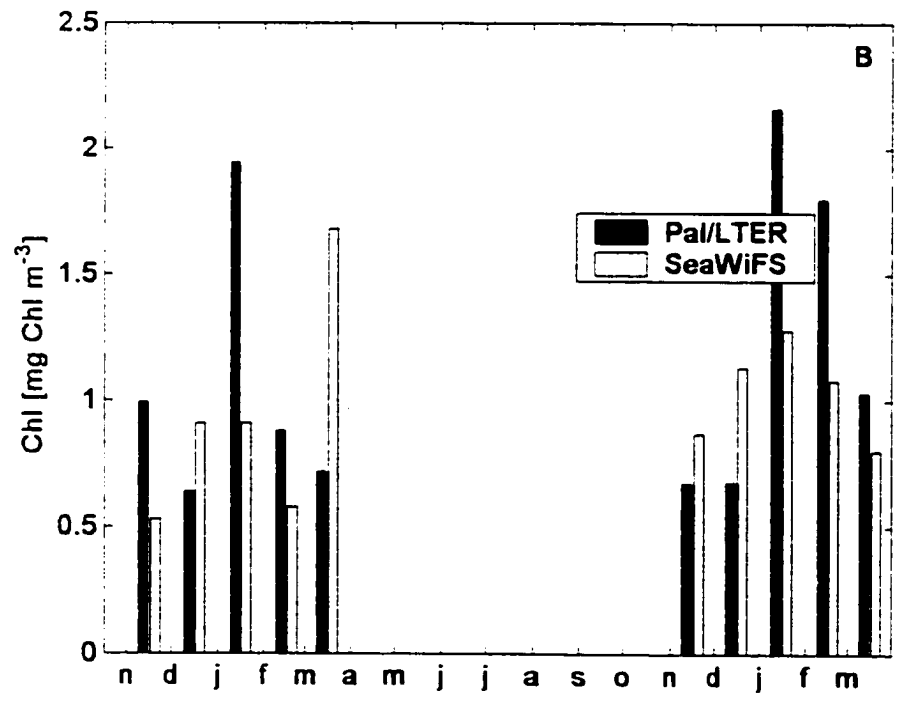
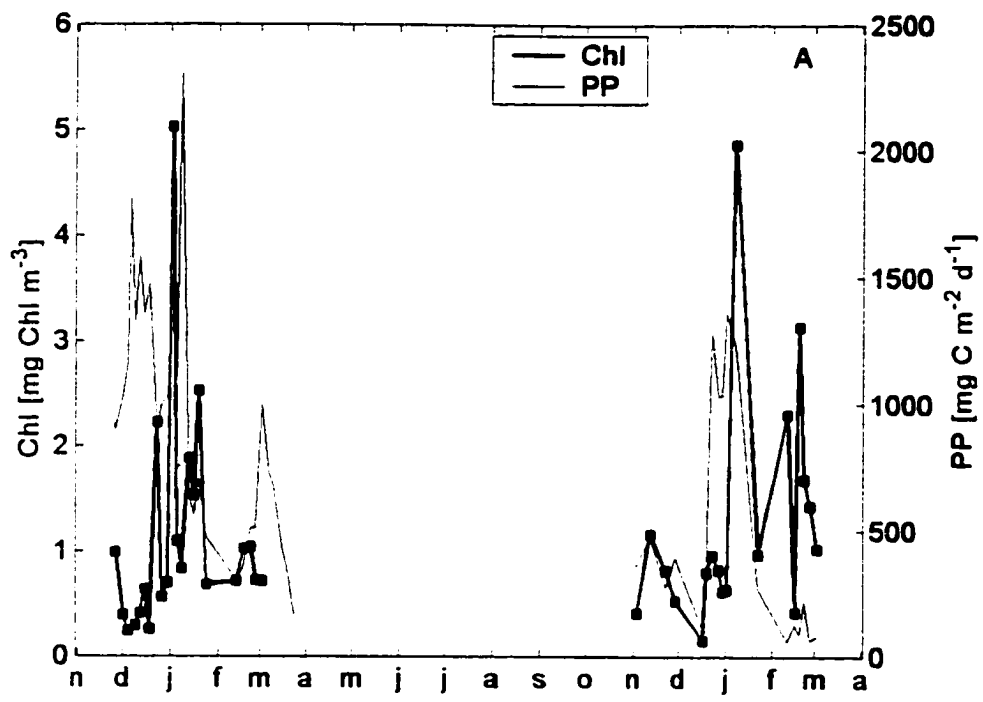
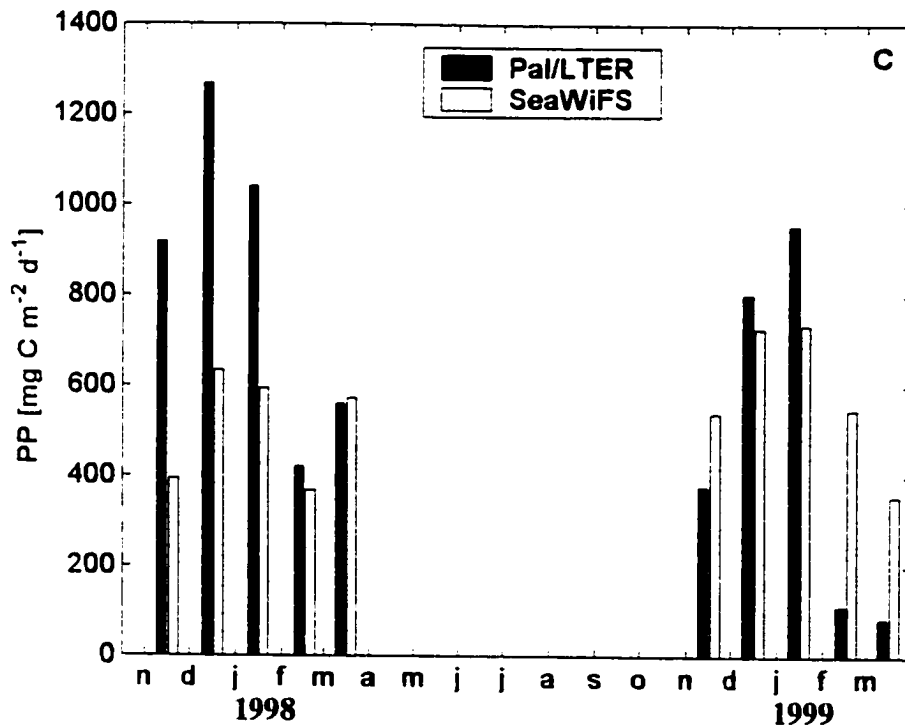
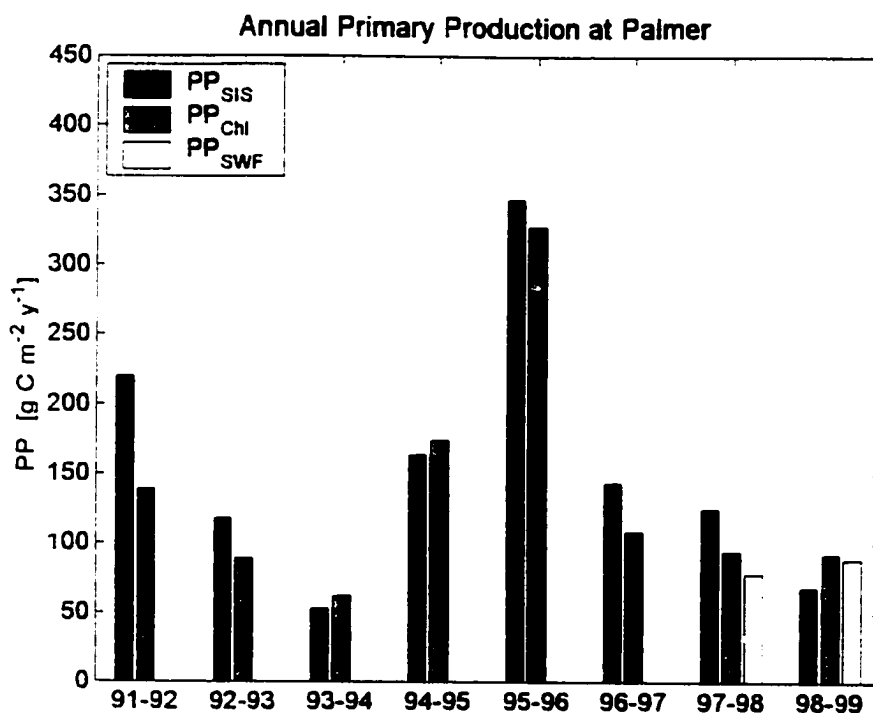


Figure 3A & B



**Figure 3:** A) Measurements of *in situ* Chl and PP at a Palmer nearshore station; B) Monthly averaged *in situ* Chl compared to SO-adjusted SeaWiFS Chl for the nearest non-zero pixel; C) Monthly averaged *in situ* Chl compared to PP modeled from SeaWiFS Chl.





**Figure 4.** Annual primary production [ $\text{g C m}^{-2} \text{ yr}^{-1}$ ] measured nearshore at Palmer Station from 1991-92 season to 1998-99. Annual estimates have been integrated from near-weekly sampling over the growing season from November to March (152 days) at Palmer Station. Gray bars represent daily primary production modeled from measured Chl (Eq. 1) and similarly integrated over the growing season. White bars represent modeled PP from average monthly Chl retrieved from SeaWiFS.

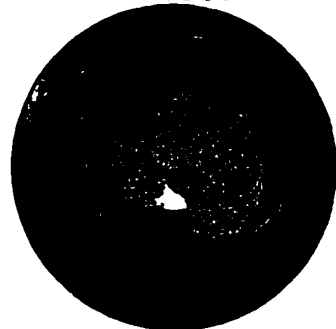
**9/1997**



**10/1997**



**11/1997**



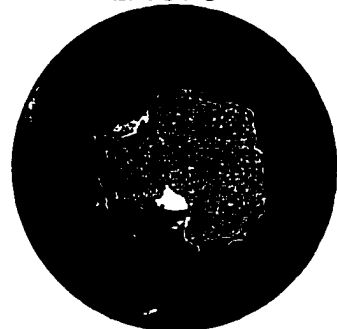
**12/1997**



**1/1998**



**2/1998**



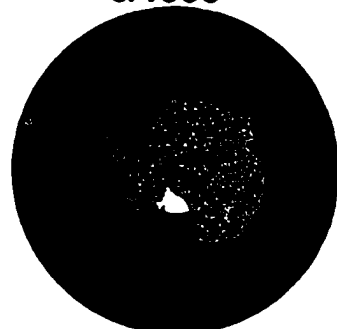
**3/1998**



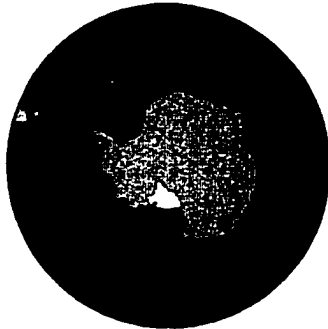
**4/1998**



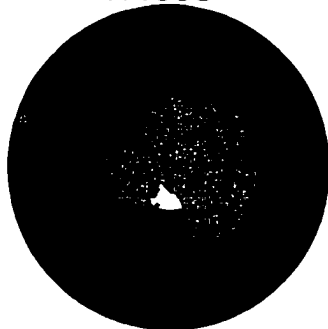
**5/1998**



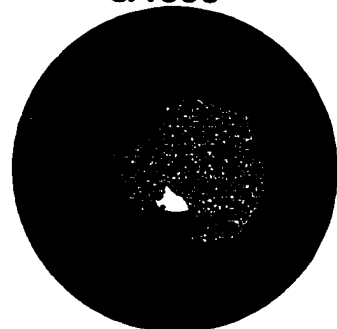
**6/1998**



**7/1998**



**8/1998**



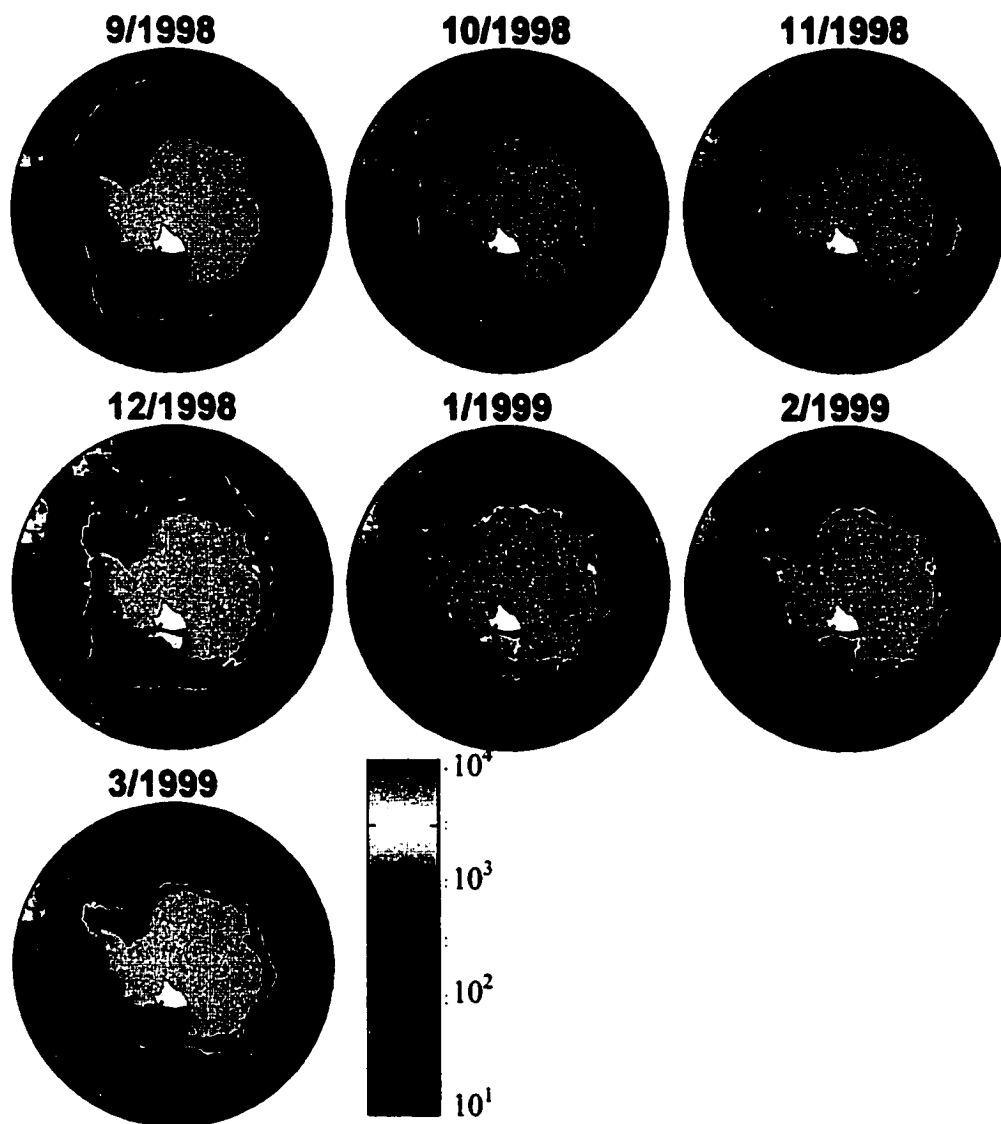


**Figure 5:** Monthly estimates of daily primary production [ $\text{mg C m}^{-2} \text{d}^{-1}$ ] for the Southern Ocean from SO-adjusted SeaWiFS Chl and a depth-integrated primary production model (Eq. 1). White lines represents the sea ice edge as derived from the SSMI passive microwave satellite data.

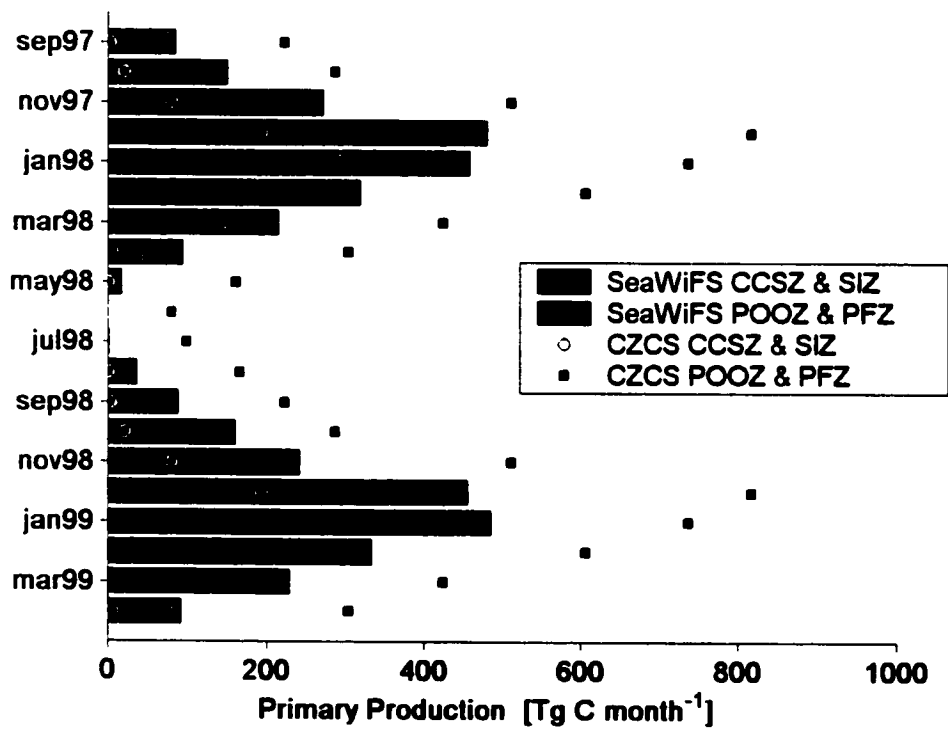


**Figure 6:** Comparison of our monthly PP [Tg C mo<sup>-1</sup>] with estimates made from multi-year composites of CZCS data. Different symbols are provided for subtotals from the SIZ and CCSZ zone versus the POOZ and PFZ zone.

## Chapter 6

### Epilogue

In the first half of my dissertation, I analyze *in situ* optical and biological data collected in conjunction with the Palmer Long Term Ecological Research (PAL/LTER) Project. From this *in situ* data, I develop models for estimating chlorophyll (Chl) from spectral reflectance measurements (Chapter 2) and for estimating primary production (PP) from Chl (Chapter 3). These chapters do not actually use satellite data, but evaluate parameters that can be estimated from a satellite. Both the Chl and PP models are found to be unique from other regions of the world's ocean. In the second half of the dissertation (Chapters 4 and 5), I evaluate how these Chl and PP models perform on real ocean color data collected from the SeaWiFS satellite. Therefore, the validation of the models is performed with data that is independent from the data used in the development of the models. Generally, the satellite-derived Chl adjusted with the SO algorithm from Chapter 2 are found to match the *in situ* Chl concentrations ( $r^2=0.65$ ).

The estimation of PP from satellite-derived Chl is not as accurate as the retrieval of Chl (Chapters 3 and 5). Like all biological processes, PP is highly complex and, as described in Chapter 5, exhibits high interannual variability. Practically every year that we sample along the Antarctic Peninsula, we find different patterns of production. Some years we find extremely high productivity that is driven by episodic blooms of large diatoms. Other years, the

water column has low productivity and is filled with smaller phytoplankton. While Chl is generally greatest at the surface, we occasionally find stations with a deep Chl maxima. The mechanisms underlying this variability are manifold and can include factors such as sea ice forcing, wind mixing, light availability, advection of different water masses, temperature gradients, and the presence of glacial melt. As described in Chapter 3, no simple correlations between these physical factors explained the variability in the phytoplankton's photoadaptive state.

Preparation of this dissertation was challenging in that whenever I found a model that worked well for one set of data, we would collect more data that functioned differently. While the PP model developed in Chapter 3 performed well on data up to 1997, for example, there were periods in 1997-98 and 1998-99 in which the phytoplankton behaved differently and the model performed poorly. I called these periods of time "atypical" compared to the previous years, however, I caution that we are still determining what is "typical" within this extremely variable ecosystem. In general, the greatest variability is found within the area of the Southern Ocean that is covered by sea ice every year, referred to as the Seasonal Ice Zone (SIZ) and Coastal and Continental Shelf Zone (CCSZ). In particular, high interannual variability is found in the Palmer nearshore stations and in open water polynyas within the sea ice.

This dissertation was also limited by the ocean color data that was available. Because this region is one of the cloudiest in the world, I used satellite data that had been composited and averaged over a monthly time frame. Even with using such a large time frame, no data was available for over 30% of the stations that were sampled since the launch of SeaWiFS. In other words, these stations were cloudy during the entire month in which they were sampled. This implies that a monthly composite image from this region is likely only from one or two clear passes during that month. Comparing data collected on a

single day with data composited on a monthly time frame is fairly accurate for most of the large grid PAL/LTER stations that are farther from the coast. In the January/February cruise of 1999, we sampled the grid first in January and repeated sampling at a selection of offshore stations again in February. Only minor differences were found during this time frame. However, at nearshore stations, we find highly weekly variability and episodic blooms that would require satellite sampling at times scales greater than monthly.

As this dissertation is completed (June 2000), the SeaWiFS data is being reprocessed to Version 3. All of the satellite data in this dissertation used Version 2 processing. The new reprocessing will likely not affect the major conclusions of this dissertation, but may have significant implications on data availability. The reprocessing will be accepting satellite passes at greater zenith angles, which should provide more data for comparison purposes. Preliminary results from this reprocessing indicate that many of the high Chl values will be reduced when compared to Version 2. This may have only a minor impact on the polynomial correction algorithm presented in Chapter 2 because the algorithm does not significantly alter the high Chl values.

Extrapolating the results from the PAL/LTER region to the entire Southern Ocean (defined herein as south of 50°S) is fraught with uncertainty. Our Southern Ocean (SO) algorithm developed to retrieve Chl from satellite-derived reflectance (Chapter 2), however, was validated in nearshore productive waters of the CCSZ, in the oligotrophic waters of the Permanently Open Ocean Zone (POOZ), and in waters of the Polar Front Zone (PFZ) (Chapter 4). Hence, we feel more confident in extrapolating this model to regions throughout the SO. However, the PP model was only validated with satellite data from the PAL/LTER region (Chapter 5) and with historic *in situ* data collected in this region (Chapter 3). Validating the PP model with data from the POOZ and PFZ

and with data from other meridional regions of the SO (i.e., Indian Ocean Sector, Ross Sea, etc.) would enhance the confidence of our SO PP estimates.

Finally, several exciting research projects have diverged from topics initiated within this dissertation. In Chapter 2, I hypothesized that the reflectance spectra (particularly in the green) indicated that backscattering was low in these waters. In January 1999, I had the opportunity to measure backscattering using a Hydrosat instrument. Preliminary results indicate that indeed backscattering is low when compared to other regions. These backscattering data and related issues of optical closure are being worked up for publication. In addition, two stations sampled during this cruise had high backscattering but very low Chl. These data came from stations that had meltwater on the surface of the water. Such stations are considered to be Case 2 waters in which ocean color properties are not primarily influenced by the phytoplankton within the water column, but are influenced by the presence of other suspended materials within the water. I am also working on analyzing these and other similar Case 2 stations collected in conjunction with the PAL/LTER program.